Preclinical Models of Dystrophic Cardiomyopathy and Therapies for the Dystrophic Heart

A Dissertation
SUBMITTED TO THE FACULTY OF THE
UNIVERSITY OF MINNESOTA
BY

Tatyana A. Meyers

IN PARTIAL FULFILLMENT OF THE REQUIREMENTS
FOR THE DEGREE OF
DOCTOR OF PHILOSOPHY

Dr. DeWayne Townsend

August 2019

© Tatyana A. Meyers 2019

Acknowledgments

Starting on the path of research as an undergraduate student in the Fall of 2012, I never imagined that I would be submitting a dissertation on the same area of research in the same lab 7 years later. I have been fortunate to have had the range of experiences and the degree of intellectual control over my work that I was afforded during this time. My graduate training has pulled together great influences from many directions, and I have many individuals to acknowledge for that.

First, I would like to thank my advisor, Dr. DeWayne Townsend, for embarking on this crash course in graduate training and mentorship with me as an early assistant professor. This journey has included a large number of projects, countless posters and drafts, and an abundance stimulating scientific debates and discussions, all interwoven with kind and understanding mentorship. I am very grateful for the degree of intellectual freedom that I had to pursue my own incremental successes and failures on the path to my PhD, and I am certain that I learned many important lessons that I would have missed if I was instead meticulously led along this path. With just the right amount of support available within arm's reach, I am very happy with opportunities I've had, the risks I took, and the accomplishments we produced together in this scientific environment.

Secondly, I want to extend my sincere gratitude to my thesis committee, Drs. Dawn Lowe, John Osborn, and James Ervasti. You have all individually helped shape me into the student and scientist that I am today, and I know that I owe my future success in part to your firm and supportive guidance. I have learned a lot from your individual feedback and from our meetings as a group, and have certainly benefitted from the standards that you each set for my work. If I had to go back in time to the point of choosing my committee again with the knowledge that I have now, I would make the same choice without hesitation.

I would also like to thank Jackie Heitzman, who told me that she better be the first person I thank after my adviser and my committee, for her inexhaustible efforts and helpful attitude. Without Jackie's willingness to assist me with thousands of inconvenient mouse injections, drug water changes, and mouse sacrifices, the final result of my efforts would pale in comparison to this body of work in terms of power and scope.

Further, I would like to thank the other members of this academic community that have shaped my graduate school experience. My wonderful and brilliant graduate school

friends, especially Drs. Anthony Vetter and Erika Dahl, have turned this degree pursuit from a grueling process into an awesome social and scientific adventure. The many conversations with my fellow students about science, writing, grad school life, and anything else that matters will always stand out in my mind as highlights of this experience. Other members of the Townsend lab, especially Jackie Heitzman, Lauren Aufdembrink and Aimee Krebsbach, have also fueled this social and collaborative atmosphere, and allowed me to look forward to my time in the lab even when my science would not cooperate.

Finally, I want to thank several other faculty members for leaving me with positive lasting impressions, including Drs. Tim O'Connell, Stephen Katz, and Scott O'Grady, whose influences and teachings were especially formative early on graduate school. Last but far from least, I want to extend my warm gratitude to Jane Barnard for being a wonderful graduate program "mom" who has taken on the arduous task of helping graduate students with any questions and problems they have, big or small, as we try to navigate from start to finish.

Dedication

This dissertation is dedicated to Natalya Hempel.

Mom, your confidence and pride in me have never wavered. You have been my biggest supporter, my most trusted ally, and my rock. Thank you for all that you have done to give me the strength and support to face the most challenging things in life. I could not have done this without you.

Abstract

Muscular dystrophies are a diverse group of genetic diseases characterized by progressive muscle weakness and deterioration with wide variability in severity and affected muscle groups. Some of the more devastating muscular dystrophies result from the absence of components of the dystrophin-glycoprotein complex (DGC). Disruption of the DGC compromises sarcolemmal integrity in striated muscle, leading to increased myocyte injury and death. These forms of muscular dystrophy often feature both skeletal muscle wasting and marked cardiomyopathy. The most common of these muscular dystrophies is Duchenne muscular dystrophy (DMD), caused by mutations in the dystrophin gene that result in the loss of this large membrane-stabilizing protein. DMD features a childhood onset and leads to premature death at ages ranging from the teens into the 30's, often from cardiorespiratory failure. DMD is an X-linked disorder, and is usually inherited from carrier mothers who also face a high risk of cardiomyopathy.

Sarcoglycanopathies are a rarer group of autosomal recessive Limb Girdle muscular dystrophies (LGMD) that arise from mutations in the sarcoglycan genes, sometimes leading to an aggressive Duchenne-like disease course in patients of both sexes. The heterotetrameric sarcoglycan complex is a key component of the DGC, and its loss induces significant myocyte pathology that can trigger childhood disease onset and premature death. Muscles and hearts devoid of the sarcolgycan complex display hallmark dystrophic pathology, including muscle wasting, loss of ambulation, and a high incidence of lethal dilated cardiomyopathy.

The work presented here is driven by efforts to quantify the susceptibility of dystrophic hearts to acute injury caused by increased cardiac workload, and to understand the contribution of angiotensin signaling to dystrophic heart injury. It describes the following key findings: 1) angiotensin receptor blockers (ARBs) can markedly reduce acute injury in dystrophin-null and sarcoglycan-null mouse hearts; 2) female mouse hearts lacking the sarcoglycan complex are significantly protected compared to male hearts, and do not derive the same benefit from ARBs; and 3) mosaic expression of dystrophin in the heart results in elevated vulnerability to injury that is modulated by factors besides dystrophin levels. This work suggests that angiotensin signaling plays an exaggerated role in dystrophic heart injury through mechanisms that may be sex-dependent, and that earlier and more consistent use of angiotensin-blocking therapies has the potential to limit dystrophic cardiomyopathy. Furthermore, it reveals that dystrophic hearts may continue to show significant vulnerability in the context of gene therapies that restore partial dystrophin expression.

Table of Contents

List of Figures

CHAPTER 1: INTRODUCTION

Cardiac Pathophysiology and the Future of Cardiac Therapies in Duchenne Muscular Dystrophy*

1. Overview

Muscular dystrophies are a diverse group of rare genetic diseases characterized by progressive skeletal muscle wasting. Many different molecular mechanisms underlie this loss of healthy muscle tissue, leading to wide variability in severity and affected muscle groups. Some of the more devastating muscular dystrophies are those that develop due to the absence of components of the dystrophin-glycoprotein complex (DGC), resulting in compromised sarcolemmal integrity in skeletal muscle and the heart. These forms of muscular dystrophy feature both skeletal muscle wasting and marked cardiomyopathy. The most common form of muscular dystrophy is Duchenne muscular dystrophy (DMD), which arises due to mutations in the dystrophin gene that result in the complete absence of this large protein that functions in stabilizing the myocyte membrane. Without dystrophin scaffolding the cytoskeleton to the sarcolemma, the mechanical and molecular infrastructure of the cell is significantly compromised. This gives rise to a variety of downstream pathogenic mechanisms, culminating in disease characteristics that include striated muscle degeneration, fibrosis, loss of motor function, and death due to cardiorespiratory failure.

With advancements in life-prolonging symptomatic therapies like ventilatory support, a greater proportion of patients with severe forms of muscular dystrophy survive long enough to develop heart failure, increasing the need for interventions that can ameliorate heart disease in this population [1–3]. In the 21st century, heart failure is a leading cause of death in DMD, with many patients reaching adolescence or adulthood and displaying symptoms of dystrophic heart disease without receiving cardiac therapy [2,4]. To address this issue, the most current guidelines released in 2015 recommend that DMD patients start therapy with ACE inhibitors (ACEIs) or angiotensin receptor blockers (ARBs) by 10 years of age or sooner, based on mounting evidence that early stages of cardiac deterioration may have already begun [5,6].

Currently, there is great excitement in the muscular dystrophy community as new therapeutic approaches are reaching the clinics. While the overall efficacy of these new therapies will be measured in ongoing clinical trials, most of these trials lack detailed

* Under review for publication in the *International Journal of Molecular Sciences*

cardiac end-points, and some of these approaches are known to have relatively poor efficacy in the dystrophic heart. Given the critical role of the heart in the disease process and quality of life, this review will focus on current understanding of cardiac involvement in DMD and detail how current and future therapies may delay or prevent the onset of heart failure in DMD patients.

2. Genetic Basis

One of the earliest recognized features of DMD was its X-linked mode of inheritance, which greatly aided in the identification of the genetic locus that was responsible for the disease. The *DMD* gene is the largest known human gene at 2.4 Mb, producing a 14 Kb mRNA transcript from 79 exons. Several internal promoters and variable splicing give rise to a wide variety of dystrophin isoforms that are expressed in striated and smooth muscle, brain, retina, and kidney, [7]. This vast size and complexity likely contribute to higher probability of a mutation interfering with the gene product. Deletions are the most common type of dystrophin mutation underlying DMD, accounting for over 70% of all mutations and often causing a change in the reading frame that produces a premature stop codon [8,9]. The next most common types of *DMD* mutation are insertions and point mutations, also usually resulting in a premature stop codon and the termination of protein synthesis [8,9]. DMD is most often passed down via the X-chromosome from a mother that has one mutated copy of the gene (carrier) to male offspring, but also has a relatively high rate of *de novo* mutations accounting for roughly 1/3 of all cases [8,9]. Because DMD is an X-linked disease, it affects almost exclusively males, with an incidence of approximately 1 in 5,000 live male births [10,11].

Conversely, mutations that still allow for a truncated dystrophin to be produced and trafficked to the sarcolemma result in the overall milder Becker muscular dystrophy (BMD). With an incidence of about 1 in 18,500 male births, BMD is much rarer than DMD due to its roots in dystrophin mutations that preserve the open reading frame, allowing for a partially functional protein product [9]. BMD displays wide phenotypic variation, ranging from very severe DMD-like disease to very mild muscle weakness. This phenotypic variation depends on the specific regions of dystrophin that are lost as a result of the BMD-causing mutation [12,13]. Accordingly, analysis of the relationship between the underlying mutation and resulting phenotype in BMD has been instrumental in shaping our understanding of dystrophin's structure and the function of its various

domains. In fact, identification of some BMD-causing mutations that produced extensive deletions in the central domain but result in a very mild disease course has led to the development of multiple truncated but functional micro-dystrophins as gene therapy candidates currently in clinical trials.

3. Clinical Manifestation

Duchenne muscular dystrophy was first described in the early 19th century by Italian physicians Gaetano Conte and L. Gioja. In the 1830's, they reported on two brothers displaying progressive muscle weakness in the face of paradoxical hypertrophy, with the older brother dying with an enlarged heart, and the younger eventually losing the ability to move [14]. Brothers afflicted by debilitating muscle deterioration along with hypertrophy in the absence of neurological deficits were again described in 1852 and 1853 by Edward Meryon and William J. Little, respectively [14]. However, the most detailed account was delivered in the 1860's by Guillaume-Benjamin-Amand Duchenne, who provided photos, drawings, and detailed descriptions of 13 of his own patients who shared these characteristics of muscle wasting, progressive muscle weakness accompanied by pseudohypertrophy, and premature death [14].

Initial clinical symptoms tend to be noticed around 3-5 years of age, and typically include apparent muscle weakness and fatigue in the legs and pelvic region, causing an abnormal gait, lordosis, and use of Gowers' maneuver. The gastrocnemius eventually develops pseudohypertrophy, resulting from accumulation of fatty and fibrotic tissue combined with slower atrophy than in the thigh muscles [15]. Elevations in serum levels of creatine kinase (CK), an enzyme typically retained within muscle fibers in healthy tissue, are detectable in newborns with muscular dystrophy at levels around 10-fold higher than in healthy newborns [10]. As children with DMD grow and reach a symptomatic age, serum CK is further elevated to about 50-100 times of the healthy level as myofiber contents leak out of increasingly damaged muscle cells. Since dystrophin also plays a role in the brain and affects cognitive function, cognitive or neuropsychiatric impairment present in roughly 1/3 of all cases [16,17]. Histopathological evaluation of patient muscle biopsies reveals central nucleation indicative of ongoing muscle regeneration, along with fibrosis, myocyte necrosis, fatty accumulation, and immune cell infiltration.

Cardiac functional assessment via echocardiography shows systolic and diastolic dysfunction as the disease progresses. Declines in ejection fraction (EF) to <50% can be seen as early as 9-10 years of age, and ejection fraction may drop as low as 25-30% later in the course of the disease [18]. Cardiac magnetic resonance imaging (CMR) may be used to detect declining myocardial strain as an index of cardiac dysfunction before the onset of measurable ejection fraction deficits [19]. In combination with late gadolinium enhancement (LGE), cardiac MRI can also be used to identify fibrotic scarring in the heart, which appears ahead of cardiac dysfunction [18]. This LGE+ fibrosis tends to be localized sub-epicardially, appearing in some patients even before 10 years of age and in the majority of patients after 15 years of age, and increases in LGE are correlated with age and declining ejection fraction [18,20]. Cardiac troponin (cTn) elevations can be intermittently detected in patient serum, serving as a biomarker of sporadic periods of myocardial destruction [21–23]. Heart rhythm abnormalities are also present in a significant portion of patients, usually in the form of sinus tachycardia, and may be related to myocardial fibrosis in the cardiac conduction system [7].

As the disease progresses, atrophy of posture muscles often leads to scoliosis, and further muscle wasting and contractures result in wheelchair dependence around adolescence. Cardiac dysfunction usually progresses into dilated cardiomyopathy with extensive fibrosis, shown to be present in essentially all patients over 18 years of age, and eventually heart failure sets in [3,24]. Historically, death usually occurred by 20-25 years of age from cardiorespiratory failure, but advancements in respiratory and pharmacological interventions have the capacity to extend lifespans into the 30’s and early 40’s with diligent clinical management [1,25].

4. Pathophysiological Mechanisms of Dystrophic Cardiomyopathy

4.1. Membrane Instability

Membrane fragility has often been viewed as the primary defect in DMD, precipitating multiple secondary pathophysiological mechanisms that lead to myocyte death. In healthy myocytes, rather than distributing diffusely throughout the sarcolemma, dystrophin localizes in a striated pattern that reflects its association with costameres [26]. Costameres are a sub-sarcolemmal network that mechanically couples the extracellular matrix (ECM) to the Z-disc of the sarcomere through the DGC and cytoskeletal γ-actin, with dystrophin playing a central role in this mechanical linkage [27].

Dystrophin's N-terminal region binds filamentous γ-actin and extends to the sarcolemma, where its C-terminus joins with the transmembrane β-dystroglycan. β-dystroglycan's extracellular domain binds to the heavily-glycosylated α-dystroglycan, which in turn links to the ECM through laminin. β-dystroglycan also associates with the transmembrane sarcoglycan complex, which plays its own major role in sarcolemmal stability. This assembly comprises the DGC, and this axis of force transmission and stabilization from the contractile apparatus to the ECM is broken when dystrophin is not expressed. It is worth noting that dystrophin loss precipitates the depletion of the majority of the DGC in skeletal muscle, but cardiac muscle retains most of the other DGC components in the absence of dystrophin [28,29].

Without functional dystrophin, the sarcolemma becomes fragile and displays significant leakiness under increased workload on the myocyte. Serum biomarkers of this increased cellular permeability include elevated levels of CK, the bulk of which is attributable to skeletal muscle, and cTn from the myocardium [21,22,30]. Further preclinical evidence of major membrane disruptions is readily detectable in dystrophic hearts and muscle by Evans Blue dye or endogenous IgG entry into the myocytes, indicating where the sarcolemma was compromised enough to permit influx of serum proteins. These assays reveal markedly higher susceptibility to cardiac and skeletal myocyte injury in dystrophic animals lacking dystrophin compared to healthy controls [31–33].

Studies using genetic models have substantiated a pivotal role for membrane integrity in cardiomyocyte preservation and dystrophic cardiomyopathy. Dysferlin, MG53, and thrombospondin 4 (Thbs4) have been identified as important players in membrane repair and maintenance. Ablation of any of these genes in dystrophin-null or sarcoglycan-null animals has been shown to worsen their cardiac and skeletal muscle pathology [34–38]. In fact, primary dysferlin deficiency is associated with muscular dystrophy in animal models and human patients (Miyoshi Myopathy and LGMD2B) characterized by mild-moderate muscle weakness and infrequent cardiac dysfunction [39]. On the other hand, overexpression or exogenous delivery of MG53 or Thbs4 have been shown to attenuate the severity of myocyte pathology in dystrophic animal models [37,40,41].

In an effort to limit muscular dystrophy and dystrophic cardiomyopathy by patching the sarcolemma, multiple groups have turned to synthetic amphiphilic

copolymers, chiefly poloxamer 188 (P188), as a potential therapy. P188 works to reduce leak in biological membranes by partitioning into the hydrophobic region exposed when the lipid bilayer tears, as demonstrated by molecular simulations [42,43]. Work in cells has yielded convincing evidence of marked reductions in membrane leak following P188 treatment, and dystrophic animal studies with P188 have reinforced the concept of membrane disruption as a major driver of dystrophic pathology [44–47]. Specifically, dystrophic dogs and *mdx* mice showed significant amelioration of various disease indices following P188 treatment, including improved cardiac histopathology and reduced myocyte force drop. Accordingly, a human trial is currently being initiated to test the safety and efficacy of P188 therapy in DMD patients [48].

4.2. Calcium Dysregulation

A major feature of homeostatic disruption that stems from high membrane permeability is the erosion of ion gradients, which contributes to including increased intracellular calcium levels. In addition to passive calcium leak through membrane tears, a number of ion channels and calcium handling proteins may play a role in the elevations in cytosolic calcium concentrations found in dystrophic myocytes. Cardiomyocytes from *mdx* hearts display high diastolic calcium levels, augmented calcium influx in response to stretch, altered calcium transient kinetics, and changes in calcium-handling protein expression, activation, or post-translational modifications [45,49,50].

Aside from passive calcium entry through the leaky membrane, transient receptor potential (TRP) channels and L-type Ca^{2+} channels (LTCC) may be allowing excessive calcium entry into dystrophic cardiomyocytes [51]. TRP channels, including TRPC1, TRPC6, and TRPV2 are thought to participate in the augmented stretch-stimulated cation influx observed in *mdx* cells, and have been shown to be overexpressed and/or hyperactive in dystrophic myocytes [51–54]. Notably, inhibition of TRPC1 and TRPV2 showed a benefit in *mdx* cardiomyocytes at baseline and under osmotic stress by reducing Ca^{2+} accumulation [50,53]. Other studies have shown enhanced calcium influx through the L-type Ca^{2+} channel in cardiomyocytes from mice lacking just dystrophin or both dystrophin and utrophin, and linked this change to delayed inactivation of the LTCC [51,55–57].

Excess diastolic calcium found in dystrophic cardiomyocytes may also come from the sarcoplasmic reticulum (SR) in addition to extracellular sources. Ryanodine receptors (RyR2) and the sarcoplasmic/endoplasmic reticulum calcium ATPase (SERCA2a) are two of the key players that may drive excessive store-operated calcium release in dystrophic cardiomyocytes. In addition to some studies documenting altered channel expression, RyR2 has also been shown to undergo altered phosphorylation and S-nitrosylation in dystrophic hearts, resulting in disrupted channel regulation by calstabin and enhanced release of Ca^{2+} from the SR [58–60]. Accordingly, treatments interfering with RyR phosphorylation or reinforcing its association with calstabin were shown to normalize cytosolic calcium levels, reduce arrhythmogenicity, and improve cardiac pathology in *mdx* hearts [59–62].In a similar vein, some studies have demonstrated SERCA2a activity to be reduced in dystrophic hearts, possibly due to some combination of lower SECRA2a expression and alterations in its regulation by the inhibitory proteins phospholamban and sarcolipin [50,63,64]. Together, the failure of these mechanisms to adequately sequester SR calcium to maintain low diastolic calcium levels may compound upon the problem of high calcium leak across the sarcolemma, resulting in significant myocyte pathology.

Elevated intracellular calcium not only interferes with proper contractile and electrical activity in a myocyte, but also stimulates increased proteolysis, mitochondrial dysfunction, and signaling cascades that promote cell death [65]. Calpains are a family of proteases activated by calcium that have an abundance of cellular targets, including cytoskeletal proteins, receptors, ion channels, and proteins that participate in excitation-contraction coupling [66]. It has been suggested that robust activation of calpain activity could also lead to degradation of non-target proteins, and may even participate in activation of the ubiquitin-proteasome system to drive further proteolysis [67,68]. Recently it was demonstrated that even in healthy mouse hearts, cardiomyocyte injury resulting in endogenous IgG entry into the cell coincides with loss of dystrophin and destruction of the orderly sarcomeric organization of α-actinin within 8 hours after the injury [31]. These outcomes likely reflect the mass action of proteases activated by the calcium influx following major membrane disruption, but similar processes may be underway in dystrophic myocytes that have constant low-grade calcium elevations.

In addition to triggering proteolysis, cytosolic calcium moves through voltage-dependent anion channels and the mitochondrial calcium uniporter complex into the

mitochondria, where it may induce mitochondrial dysfunction that can precipitate cell death [69]. Mitochondrial oxidative metabolism depends upon the maintenance of a negative mitochondrial inner membrane potential that is essential for ATP synthesis. This process that is further stimulated by temporary elevations in mitochondrial matrix calcium that occur during increased workloads in healthy mitochondria [70]. However, excessive calcium loading into the mitochondria may trigger opening of the mitochondrial permeability transition pore (mPTP), depolarizing the mitochondria and interrupting ATP synthesis unless the mitochondrial membrane potential can be restored [71]. Opening of the mPTP leads to mitochondrial swelling, potentially resulting in destruction of the organelle, and can ultimately trigger cell death by depleting cellular ATP content and releasing reactive oxygen species and pro-apoptotic factors from mitochondria into the cytosol [71]. Indeed, *mdx* cardiomyocytes have been shown to have elevated mitochondrial calcium content and mitochondrial swelling, inspiring ongoing efforts to impede mPTP opening or mitochondrial calcium uptake to improve pathology in preclinical dystrophic animal models [56,72,73].

4.3. Reactive Oxygen Species Dysregulation

Dystrophin loss is associated with increased generation of reactive oxygen species (ROS) that contribute to the pathogenesis of DMD. A significant source of ROS production is NADPH oxidase 2 (NOX2), the primary muscle isoform of this membrane-bound superoxide-generating enzyme. *Mdx* mice have been consistently shown to harbor increased NOX2 expression and activity, and NOX2 appears to be responsible for exaggerated stretch-induced ROS production in both skeletal and cardiac myocytes from *mdx* mice [74,75]. This exaggerated increase in NOX2 dependent superoxide production appears to underlie the disorganization of microtubules in skeletal muscle, likely also contributing to the disorganized microtubule array in dystrophic cardimyocytes [76–78]. Upon activation, NOX2 produces extracellular superoxide, which is converted by extracellular superoxide dismutase to the membrane-permeant H_2O_2 [79]. Once inside the myocyte, excess H_2O_2 can cause oxidation of proteins, lipids, carbohydrates, and nucleic acids, precipitating a variety of pathological effects that include deficits in calcium handling, contractility, and cell survival [80,81]. In fact, evidence suggests that NOX2-generated ROS may contribute to SR calcium leak and mitochondrial dysfunction in *mdx* myocytes [51,74–76,81,82].

Accordingly, many studies have demonstrated a protective effect of pharmacological or genetic NOX2 inhibition in *mdx* heart and skeletal muscle, with decreased ROS generation, improved calcium handling, increased myocyte survival, and greater force production among the associated benefits [33,62,74,75,81,82]. NOX2 is also a likely downstream effector of angiotensin II type 1 receptor (AT_1R), which may be activated by the binding of angiotensin II or by stretch to stimulate ROS production via NOX2 [80,83,84]. This relationship could account for some of the reported benefits of angiotensin receptor blockers (ARBs) in dystrophic models, including recent work showing acute protection of *mdx* myocardium when treated with losartan only 1 hour before inducing cardiac injury with isoproterenol [31,85,86].

4.4. Nitric Oxide Dysregulation

In skeletal muscle, there is clear evidence that dystrophin is critical for the localization of neuronal nitric oxide synthase (nNOS) at the membrane of the muscle fiber [81,87]. From this sub-membrane compartment, NO readily diffuses out of the cell, where it signals to neighboring vascular cells to dilate the vasculature, increasing blood flow to actively contracting muscle [88,89]. The presence of this molecular arrangement in the heart is not clearly understood. While dystrophin and nNOS are both expressed in the myocardium, co-immunoprecipitation studies have demonstrated that they do not interact to the same degree as in skeletal muscle [90]. Further, there are many concurrent mechanisms controlling coronary blood flow that may render this nNOS localization less necessary.

Complicating the understanding of cardiac nitric oxide signaling is the fact that all three isoforms of NOS – nNOS, endothelial NOS (eNOS), and inducible NOS (iNOS) – are expressed in the heart. Evidence of NO-related alterations from preclinical studies include declines in nNOS activity and expression, significant increases in iNOS activity and expression, and no reported change in eNOS activity and expression [59,74,91–93]. iNOS is of particular interest in dystrophic hearts and muscle, as its expression is typically high in immune cells, and it is further increased with inflammation, potentially resulting in large contribution of iNOS to NO production in regions of ongoing tissue injury and degeneration [81,94,95]. Furthermore, despite the lack of evidence supporting the interaction of nNOS with dystrophin in the heart, there are indications that mitochondria from dystrophic hearts are associated with nNOS activity that is not

present in wild type hearts [96]. This suggests that nNOS localization is abnormal in dystrophic cardiomyocytes, which, together with the increase in iNOS activity, results in complex effects that alter the NO-dependent physiology of the dystrophic heart. Finally, both skeletal muscle and the heart harbor eNOS, and the regulation of its activity is multifactorial and complex, creating major obstacles to understanding this isoform's contribution to the NO metabolism of dystrophic myocytes [97].

The signaling of nitric oxide is complex, but it can be broadly divided into roughly two branches: one mediated by cyclic guanylyl monophosphate (cGMP), and another via direct covalent modifications. Initially, preclinical work suggested that the cGMP branch of NO signaling may provide significant benefit, as both genetic and pharmacological manipulations of this pathway appeared to partially improve dystrophic cardiac function in mice [98,99]. Based on the promise of these results in the heart and other benefits in skeletal muscle [88,89,100], a clinical trial was initiated to test the effects of inhibiting phosphodiesterase 5 (PDE5), the enzyme partially responsible for the degradation of cGMP, with sildenafil. Surprisingly, this sildenafil trial was terminated due to several DMD patients receiving sildenafil displaying worsening cardiac function [101]. It is not clear if the sildenafil treatment accelerated the dystrophic disease process or simply failed to show a beneficial effect. Importantly, PDE5 inhibition only prolongs the duration of existing NO signaling, thus it is possible that NO synthesis may be too low or mislocalized for sufficient cGMP to be produced in dystrophic cardiomyocytes.

Evidence shows that the dystrophic heart has increased levels of direct covalent modification of cysteine residues in the form of S-nitrosylation (SNO). Proteomics-based approaches demonstrate that *mdx* hearts have globally elevated levels of S-nitrosylation, with modifications of the electron transport chain being particularly prominent [102]. Increased S-nitrosylation of the cardiac ryanodine receptor has been shown to increase its Ca2+ leak, thus potentially contributing to increases in cytosolic Ca2+ and cardiac arrhythmias [59,60]. Furthermore, overexpression of nNOS has been shown to limit fibrosis and improve electrical and contractile properties of the dystrophic heart [103–105]. Together these data describe a very complex role for NO signaling in the dystrophic heart, where it alternates between providing benefit and detriment depending on the particular target or the nature of the study. This complex physiology greatly confounds the use of NO signaling as a therapeutic approach in the dystrophic heart.

4.5. Fibrosis

Fibrosis is one of the earliest clinical features of dystrophic cardiac pathology, making its first appearance in DMD patient hearts before 10 years of age [18,106]. Multiple cell types contribute to the development of fibrosis in the heart, including cardiomyocytes, fibroblasts, endothelial cells, and immune cells. All of these cells can secrete profibrotic cytokines and chemokines in response to stimuli like inflammation, mechanical signals, and signals from neighboring cells. Fibroblasts and cardiomyocytes are also capable of depositing the extracellular matrix components that comprise fibrotic scars. Fibroblasts are an abundant and reactive cell type in the heart, readily transforming into myofibroblasts and increasing their secretion of ECM and cytokines in response to a large number of endocrine, paracrine, and mechanical signals that include transforming growth factor β (TGFβ), ROS, angiotensin, aldosterone, ECM changes, and many others [107,108]. Cardiomyocytes may help drive the fibrotic process not only by dying and leaving a vacancy that must be filled in with ECM, but also by secreting their own signaling molecules and collagen to contribute to the process [109]. Cellular stress and necrotic death among cardiomyocytes likely kick off fibrosis in the dystrophic heart by polluting the surrounding tissue with cytokines, chemokines, and debris that attract neutrophils and macrophages. These cells are phenotypically-diverse, and various contextual factors may contribute to their polarization to promote tissue inflammation or repair through specific paracrine signaling profiles [110]. Furthermore, infiltrating myeloid cells have been shown to harbor aldosterone synthase, thus potentially representing a source of localized aldosterone production and promoting pro-fibrotic gene transcription in mineralocorticoid receptor-expressing fibroblasts and cardiomyocytes [111]. The nature of cardiac fibrosis in DMD is not unique or specific to the dystrophic process, but its start early in the disease course and implications for the rest of the heart make reducing fibrosis a major goal of cardiac-directed therapies for DMD.

The removal of damaged tissue eventually ends with the deposition of a new fibrotic patch, and these lesions appear on CMR with LGE as areas of bright signal that are often distributed in a sub-epicardial pattern on the left-ventricular free wall [18,20,112]. The high consistency of lesion distribution in a mechanically-demanding setting like the heart may indicate that the forces experienced by cardiac cells in this particular region of the heart may be especially injurious, perhaps because of greater cellular dynamics in the epicardium [113]. Aside from the obvious issue of failing to

contribute to the pumping action of the heart, accumulation of fibrosis may present additional challenges. First, it likely accelerates further losses of functional myocardium by shifting the workload demand on the neighboring cardiomyocytes, which will now have to carry out excessive contractile work in a stiff, mechanically burdensome environment. Secondly, the scar may interrupt the tracts of electrical conduction through the heart, potentially giving rise to a variety of arrhythmias. Because the consequences of unmitigated fibrosis can be so dire, a major focus of established cardiac-directed therapies is the amelioration of these processes.

5. Small Molecule Therapies for the Heart

Because of a lack of any potentially curative therapies for dystrophic cardiomyopathy until very recently, these established small molecule-based therapies are aimed at reducing the symptoms and hindering the mechanisms of disease progression in the heart. The four groups of cardiac small molecule approaches listed here are all currently in use in DMD clinical management.

5.1. Angiotensin-Inhibiting Therapies

Inhibition of the renin-angiotensin system has become a cornerstone of cardiac-directed therapeutic efforts in DMD patients, with the goal of ameliorating the adverse remodeling that follows cardiomyocyte loss. Angiotensin II (AngII) and the AngII type 1 receptor (AT_1R) exert many detrimental effects on the heart, including promoting fibrosis, remodeling, ROS production, and cardiomyocyte death [80,83,114–116]. Angiotensin receptor blockers (ARBs) and angiotensin converting enzyme inhibitors (ACEIs) are the two main drug classes used to suppress the deleterious effects of angiotensin in heart failure patients in general and in DMD patients specifically. Current guidelines recommend that DMD patients be placed on either one of these two drugs by age 10 or earlier, influenced by the growing body of work reporting the first signs of ongoing cardiac disease processes around 6-10 years of age [18,19,21,22,106]. ACEIs are an older drug class that is often used as the first line of therapy for general heart failure, and was the first to be used in trials to demonstrate improved cardiac function and survival among DMD patients [117,118]. For these reasons, they have often been named first in guidelines and recommendations regarding management of DMD cardiomyopathy and are more frequently prescribed [5,6,119,120]. ARBs are listed as a secondary option or

an alternative in cases of poor ACEI tolerance, despite the fact that ARBs are not only equally effective when compared directly to ACEIs, they are better tolerated by patients, promoting improved compliance [121–123].

Importantly, recent preclinical work has shown that ARBs may have a unique ability to prevent cardiomyocyte damage during acute bouts of increased workload in the heart. Dystrophic *mdx* mouse hearts displayed 3-fold higher myocardial injury area than wild type hearts after a bolus of the β-adrenergic agonist isoproterenol, but this difference was eliminated by treatment with the ARB losartan [31]. Losartan reduced cardiac damage 2.8-fold in *mdx* hearts without any significant effect on injury in wild type hearts. Surprisingly, neither acute nor chronic ACEI treatment had any effect on the extent of damage in the mouse heart, suggesting that direct blockade of AT_1R may be necessary to achieve the full benefit of anti-angiotensin therapy in the dystrophic heart [120]. One potential explanation could be rooted in the fact that ACE is not strictly necessary for the production of AngII and activation of AT_1R. AngII can be produced through the actions of other peptidases, most notably chymase, thus the inhibition of ACE does not eliminate AngII production [124–126]. Furthermore, AT_1R displays basal activity and can be readily activated further by stretch independently of any ligand, thus potentially giving rise to AngII-independent pathogenic signaling [127,128]. Another compelling explanation for the disparity in benefits of ARBs and ACEIs is the indirect augmentation of cardioprotective AngII type 2 receptor (AT_2R) signaling as a consequence of AT_1R blockade [114,129]. AngII is the main endogenous ligand for both receptors, and the blockade of AT_1R feeds back to increase AngII production, resulting in the redirection of a very robust AngII pool for AT_2R activation [126,129,130].

Further clinical trials with younger patients (<10 years old) will be needed to determine if ARBs have the same unique capacity to preserve cardiomyocytes in the face of ongoing physiological stresses in human dystrophic hearts. Until this work can be carried out, DMD patients should continue to be prescribed either one of these anti-angiotensin drugs at the earliest age that the families and physicians can agree upon in order to protect these vulnerable hearts from the permanent loss of myocardial tissue.

5.2. Beta-Adrenergic Receptor Blockers

Tachycardia is a common characteristic of DMD, reflecting autonomic dysfunction in the dystrophic heart that predisposes it to arrhythmias. Holter monitoring

in DMD patients routinely reveals average heart rates >100 beats per minute, reflecting increased activation of the sympathetic nervous system and increased adrenergic signaling in the heart [6,20,131]. The heart expresses an abundance of β-adrenergic receptors (β-AR) in the pacemaker cells, conduction system, and the rest of the myocardium. Activation of cardiac β-AR drives heart rate elevations and increased contractility by augmenting and accelerating calcium transients in the myocyte, which contributes to arrhythmogenesis [132]. Beta-blockers are regularly used for the treatment of acquired heart failure, where they are often combined with ACEIs and diuretics to improve survival and reduce hospitalization rates [133]. Accordingly, beta-blockers have been considered a candidate for cardiac-directed therapy in DMD with the goal of limiting β-AR effects, although it remains unclear whether these drugs deliver a significant benefit that cannot be achieved without them.

Investigations using beta-blockers in DMD cardiomyopathy have turned up mixed results, with some studies demonstrating a clear benefit while others show little effect of β-AR blockade on outcomes [131,134,135]. Although some DMD patient studies indicate that beta-blockers preserve cardiac function and survival beyond the effects of ACEIs alone, a recent trial revealed no difference between treatment groups receiving ACEIs alone versus ACEIs with beta-blockers when the ACEI dose was adjusted according to the severity of cardiac dysfunction [131,134,135]. These inconclusive results have contributed to variable and often delayed initiation of beta-blocker use in DMD.

Because beta-blockers are a second-line therapy in DMD, a major obstacle to successfully determining their capacity for benefitting the dystrophic heart may lie in the delayed initiation of therapy and combined use of beta-blockers with other drugs. Indeed, it seems most common in clinical practice to start beta-blockers once tachycardia or other arrhythmias become detectable, which may be well after the onset of early cardiac disease processes [6]. Because ACEIs and ARBs continue to be the first line of therapy, it is unlikely that studies investigating the effects of beta-blockers alone on the natural course of the disease will be possible [5]. However, sustained efforts should be made to evaluate outcomes in patients receiving early intervention with beta-blockers compared to those receiving similarly early therapy without beta-blockers in order to identify any significant benefits specific to beta-blocker use.

5.3. Mineralocorticoid Receptor Antagonists

Mineralocorticoid receptor (MR) activation by aldosterone can contribute to cardiac pathology by promoting cardiomyocyte death, hypertrophy, and fibrosis in DMD cardiomyopathy and other types of heart failure [136]. For this reason, MR antagonists like eplerenone and spironolactone are a part of the standard approach for managing heart failure with low EF, and are occasionally incorporated into treatment for DMD cardiomyopathy [7]. The potential importance of aldosterone signaling is underscored by reports that myeloid cells infiltrating the site of heart and muscle injury in dystrophic mice express aldosterone synthase, serving as a local source of paracrine aldosterone signaling that may exacerbate the injury and the adverse remodeling that follows it [111]. MR signaling may also play a larger role in DMD due to the ability of corticosteroids like prednisolone, which are used to preserve muscle function in DMD patients, to activate MR in addition to their target receptor [137]. It is worth noting that spironolactone is slightly more potent, but has lower selectivity for MR over androgen receptor, resulting in higher potential for side effects associated with androgen imbalance, whereas eplerenone is less likely to interfere with androgen receptor.

Preclinical work using mouse models of DMD cardiomyopathy has shown a protective effect of the combination of spironolactone and ACEI in dystrophic muscles and hearts that was attenuated in the group treated later in life, again reinforcing the importance of proactive initiation of therapy [112,138]. Clinical trials went on to demonstrate that patients with DMD and preserved ejection fraction already receiving treatment with an ACEI or ARB showed modest but significant improvements in myocardial strain, ejection fraction, and chamber dilation with eplerenone treatment, compared to those without eplerenone [136]. The open label extension in patients using eplerenone with ACEI or ARB showed that myocardial circumferential strain was preserved over a period of 36 months [139]. The recent discovery of vamorolone, an MR antagonist that is equally potent to eplerenone and also mirrors the anti-inflammatory benefits of corticosteroids, may represent a critical step toward the inclusion of this MR antagonist as a standard and proactive therapy for DMD cardiomyopathy [137].

5.4. Corticosteroids

Currently, a daily regimen with a corticosteroid like prednisone or deflazacort is the earliest and most widely used DMD therapy, based on the ability of steroids to

reduce inflammation and prolong strength and ambulation in DMD patients with [7,51,140]. Because steroids are unequivocally beneficial in ameliorating the natural course of DMD in skeletal muscle, therapy is often initiated fairly proactively around 2-5 years of age, making corticosteroids the earliest pharmacological influence on the dystrophic heart [9]. The use of these drugs is not without controversy, with the primary obstacle rooted in challenging systemic side effects, which arise from the classic transcriptional effects of glucocorticoid receptor and include reduced bone density, increased adiposity, and increased muscle catabolism [141]. However, some additional concerns stem from preclinical studies providing evidence that steroids may worsen the progression of DMD in the mouse heart [138,142]. Nevertheless, DMD patient studies are largely in agreement that steroids are likely to be protective in the dystrophic heart, with possible benefits including improved survival, preserved ventricular function, and even reductions in fibrosis [143–148]. Perhaps the most telling is the observation that increased survival among the steroid-treated cohort of one study was largely reflective of a striking reduction in heart failure deaths [143].

Vamorolone, the novel drug that recapitulates the anti-inflammatory actions of glucocorticoids and the anti-remodeling effects of MR antagonists, may deliver the same benefits derived from corticosteroid use with minimized side effects [137,149]. It represents a new class of steroids called dissociative steroids, which serve the function of activating glucocorticoid receptor for signaling transduction, but do not result in its binding to glucocorticoid response elements (GRE) and activation of GRE-dependent transcription [141]. It remains to be seen if Vamorolone may replace glucocorticoids and/or MR antagonists in the clinic, but it has already demonstrated efficacy in preclinical studies using dystrophic mice, and is currently being tested in DMD patient trials [137,149,150].

6. Gene-Targeted Therapies

In recent years, potentially curative approaches for DMD have begun to take shape. Unlike the small molecule treatments, these gene-targeted therapies are designed with the goal to induce expression of a functional gene product that will reestablish normal myocyte physiology. Since these therapies aim to repair the original defect in the cell by restoring functional dystrophin expression, their success is less dependent upon making the correct assumptions regarding the exact mechanisms

driving the cellular dysfunction in the absence of dystrophin. However, the high complexity of these gene-targeted systems results in great challenges to achieving efficient and lasting correction. Because of the large variety of mutations that cause DMD, many of these approaches need to be tailored to suit subgroups of patients based on the location of their disease-causing mutation.

An additional challenge lies in the difficulty of assessing the cardiac effects of these approaches, because their efficacy will depend absolutely upon the whole-body efficiency of transduction and dystrophin restoration. Ideally, corrective therapies should be initiated as early in life as possible, both to achieve maximal preservation of healthy muscle tissue and to facilitate dosing. Since the heart cannot be routinely biopsied to check the efficiency of dystrophin re-expression, clinicians will depend on more sensitive measures like myocardial strain to evaluate patient hearts at early time points in the natural course of the disease. Achieving sufficient therapeutic efficacy in the heart will be of the utmost importance, because correcting skeletal muscle without effectively addressing the cardiomyopathy may result in increased demand on the fragile myocardium, accelerating the progression of heart failure. Even if high efficiency of these therapies is achieved in skeletal muscle, the phenotypic outcome in DMD patients may resemble the disease characteristics of Becker muscular dystrophy or X-linked dilated cardiomyopathy (XLCM) due to the reduced expression and/or truncation of dystrophin. Patients with BMD and XLCM often have sufficient dystrophin expression to display mild skeletal muscle pathology, but BMD has a high risk of heart failure, and XLCM patients succumb to heart failure between 10-20 years of age [7,151–154]. To minimize the risk of this outcome, careful ongoing cardiac monitoring and therapy will be necessary to characterize the cardiac effects of these therapies and successfully manage all aspects of DMD patient health in the context of partial dystrophin replacement. Thus, even DMD patients who undergo treatments with good efficacy in the heart will likely continue to require careful cardiac monitoring and be good candidates for small molecule-based cardiac therapies to limit the effects of improved skeletal muscle function on the dystrophic heart.

6.1. Stop Codon Readthrough

Roughly 10% of DMD patients have a nonsense mutation that replaces a regular amino acid triplet with a premature stop codon and causes the ribosome to terminate

translation, failing to synthesize the remainder of the protein [8]. The principle of stop codon read-through, also referred to as nonsense suppression, is simply to induce the ribosome to continue translating the mRNA through the premature stop codon and the rest of the transcript. This concept was initially demonstrated using the aminoglycoside antibiotic gentamicin, but due to the toxicity of gentamicin, ataluren (Translarna) was developed as a safer alternative serving the same purpose. The drug works by binding to the ribosome itself and mildly disrupting its ability to recognize the premature stop codon, enabling the occasional addition of an amino acid in its place, followed by the synthesis of the remainder of the gene [155]. This mechanism appears to be fairly specific to premature stop codons, without enabling readthrough of regular stop codons, and effectively enables partial dystrophin expression in skeletal muscle [155,156].

Based on preclinical efficacy, ataluren advanced to clinical trials and was approved for the treatment of DMD in Europe, although it is still under investigation for efficacy in the US. Unfortunately, very little evidence exists to inform the question whether ataluren displays any degree of efficiency or delivers a benefit in the heart. Preclinical work suggests that ataluren can induce a modest increase in diffuse dystrophin expression in the *mdx* mouse heart [156]. Results in human patients are more ambiguous, showing no measurable effect on cardiac function in a small cohort of non-ambulatory DMD patients, although the cardiac function remained stable during the treatment period of 20-24 months [157]. Additional work will need to be performed to better understand the effects of ataluren in the heart and the clinical relevance of these observations.

6.2. Antisense-Mediated Exon Skipping

Deletions are the most common type of *DMD* mutation, with many of them causing dystrophin loss due to the disruption of the open reading frame. When the open reading frame is shifted, it often results in a downstream premature stop codon that terminates translation, so the premise of exon skipping is to sacrifice one exon to restore the open reading frame of the rest of the gene. To accomplish this, antisense oligonucleotides (AON) are designed to bind to the premature mRNA at the splice acceptor site of the mutated exon to obscure the splice site. This causes the spliceosome to move on to the next available splice acceptor site, resulting in the omission of the mutated exon from the final mRNA transcript. Multiple AONs can be

used to skip adjacent exons in cases where the removal of multiple exons is required to restore the reading frame. The ultimate goal of this approach is the synthesis of a truncated dystrophin protein that harbors a deletion but retains most of its functionality. Over half of all *DMD* mutations and up to 80% of deletions are amenable to exon skipping therapy, but since each therapy must be tailored to the mutation region, each successfully-developed AON will only rescue a fraction of those mutations [8]. Preclinical studies demonstrated the strong potential of AON to reestablish dystrophin expression in skeletal muscles, but raised concerns about efficacy in the heart based on work showing negligible effects in cardiac muscle [158,159]. Upon probing the underlying cause of this discrepancy, it was found that these AON therapies, often delivered in the form of a phosphorodiamidate morpholino oligomer (PMO), were more likely to be trapped in endosomes in cardiomyocytes than skeletal muscle [160]. Subsequent preclinical work demonstrated that optimizing the dose and modifying the delivery system could solve this problem in the heart, showing improved cardiac muscle dystrophin restoration with these approaches in dystrophic mice and dogs [161,162]. Currently, conjugation of PMOs to peptides that enhances cell permeability is an active area of development, with preclinical studies demonstrating considerable expression of dystrophin in the hearts of *mdx* mice and dystrophic dogs treated with high doses of these peptide-conjugated PMO (PPMO) therapies [162–164].

At this time, one exon-skipping therapeutic is FDA approved, and several more are in development to target the exons that represent the highest proportions of deletions amenable to exon-skipping. Eteplirsen is a PMO from Sarepta Therapeutics that induces the skipping of *DMD* exon 51, which may target up to 14% of all mutations. It received FDA approval in 2016 amid controversy, with modest but positive results based on clinical trials and patient experiences despite surprisingly modest effects on dystrophin re-expression in patient biopsies [165,166]. However, tissue penetration and longevity of PMOs has remained an ongoing concern, and no evidence exists of significant eteplirsen uptake or benefits in the heart [51,167]. To address these shortcomings, other delivery systems for AON are currently being investigated to identify the modifications that can optimize cellular penetration and systemic safety, with a big focus on PPMOs [160]. Additionally, multiple other exon-skipping AONs are being actively developed, with PMOs targeting exons 45 and 53 already in clinical trials. Because these agents only work at the level of premature RNA and have limited

longevity in the cell, it will be important to set appropriate guidelines for dosing frequency to reflect sufficient efficacy in the heart in order to minimize the risk of XLCM-like heart failure.

6.3. Micro-dystrophin Viral Gene Therapy

Viral gene therapy has long been considered the potential key to curing genetic diseases, based on its theoretical capability to completely replace the missing gene product. For this reason, viral gene replacement therapy is the only approach currently in development for clinical use that offers hope for all DMD patients regardless of the underlying dystrophin mutation, and is the only available therapy for patients with mutations that span critically important regions of dystrophin. There is a long history of evidence from animal and human studies identifying both the great promise and the significant challenges of viral gene therapy, but the field has made major strides toward clinical applications in recent years. The broad lessons learned from this vast body of work are: 1) viral gene therapy is feasible and can even be efficiently systemically delivered; 2) only adeno-associated virus (AAV) is currently safe enough to use as a gene therapy vehicle in human patients; and 3) the safety and efficiency of viral gene therapy depend upon many factors that are unique to particular species and also the individual biology of the patient.

In addition to the general limitations of viral gene delivery, the pursuit of a DMD gene therapy faces the additional obstacles of gene size, as the full coding *DMD* gene sequence exceeds the packaging capacity of AAV by over 2-fold. Because the 11 kb cDNA cannot be delivered by an AAV with a 4-5 kb capacity, great effort has been directed at optimally miniaturizing the *DMD* gene by reducing it to its most vital components, producing the candidate micro-dystrophin constructs currently under investigation [168]. Preclinical pursuit of over 30 of these micro-genes largely followed the lessons learned from mildly-affected BMD patients with extensive *DMD* sequence deletions, preserving the actin-binding N-terminus and the DGC-binding cysteine-rich domain, but sacrificing large sections of the central rod domain that spans between them [169]. While most of the preclinical work with AAV-delivered micro-dystrophins has focused on skeletal muscle, strong evidence of the cardiac benefits of systemic treatment includes marked reductions in histopathology and improvements in function, supporting their advancement into clinical trials [29,170,171].

Three different micro-dystrophins are currently under investigation in human DMD patient trials of AAV-mediated micro-dystrophin therapy. The composition of the micro-dystrophin constructs in these trials is relatively similar, however the micro-dystrophin vector from Pfizer uses a skeletal muscle promoter that does not drive any expression in the heart [172]. The other two micro-dystrophin AAV trials, spearheaded by Sarepta Therapeutics and Solid Biosciences, are using vectors driven by different promoters that induce expression in both skeletal and cardiac muscle, delivered by a different AAV serotype, and injected at different doses, significantly complicating any comparison between these two trials [169]. Nonetheless, both the MHCK7 promoter in Sarepta's AAV construct and the CK8 promoter in Solid's AAV construct have been shown to drive robust cardiac expression of micro-dystrophins used in preclinical studies [173,174].

It is still too soon to know if human cardiac function will be preserved by these micro-dystrophin treatments, but it is possible that these initial trials may reveal the need for higher doses to effectively transduce the majority of the post-mitotic myocardium, and these higher doses may be accompanied by significant side-effects [169]. While some preclinical literature supports the notion that transduction of half of the heart may be sufficient to reap the full benefits, it is difficult to extrapolate confidently from mice to human patients in light of the vastly different body sizes, lifespans, and phenotype severity [32]. Furthermore, AAV-delivered plasmids are not expected to last forever, so repeated dosing (along with immunosuppressive measures like plasmapheresis) may be needed if reductions in the therapeutic effect are detected [175,176]. Finally, even if it becomes possible to achieve complete cardiac transduction and lasting expression of these *DMD* micro-genes, the treated patient population will still be at a similar risk for developing cardiomyopathy as BMD and XLCM patients due to the extensive truncation of the gene. These limitations on the maximal theoretical efficacy of AAV gene therapy for DMD may result in the continued need for additional small molecule-based management of cardiomyopathy in the setting of an otherwise BMD-like phenotype.

6.4. CRISPR-Cas9 Gene Editing

CRISPR-Cas9 is a highly versatile genome-editing approach that was found at the root of a bacterial self-defense system against viral infection and gave rise to a promising new strategy for correcting genetic diseases. This system is based simply

upon a single guide RNA (sgRNA) molecule that recognizes a genomic sequence and flags down an endonuclease to create a double-stranded break in the DNA at specific recognition sites. In bacteria, both the Cas9 endonuclease and the guide RNAs are encoded by genomic sequences, the latter of which is made up of clustered regularly-interspaced short palindromic repeats (CRISPR), but in eukaryotic applications, the sgRNA and Cas9 gene must be delivered exogenously. In non-proliferating cells like skeletal muscle fibers and cardiomyocytes, CRISPR-Cas9 editing can be used to excise a duplication or out-of-frame exon, disrupt a splice site to induce exon skipping, edit a nucleotide in a nonsense mutation, or reframe an exon with a base insertion or deletion that accompanies non-homologous end-joining repair [177,178]. Because the editing occurs at the genomic level and myocyte nuclei will not divide further, this approach represents the potential to treat DMD by reinstating dystrophin expression through a single administration of the therapeutic agent.

Since the CRISPR-Cas9 treatment strategy depends upon the systemic delivery and expression of foreign genes, this therapeutic approach has often made use of AAV-mediated gene delivery in preclinical work to achieve sufficient transduction in vivo, with promising outcomes from a large number of separate studies [178]. Using either a single vector or two separate vectors to encode the sgRNA and the Cas9 sequences with a cardiac-expressing promoter, several studies have demonstrated significant restoration of cardiac dystrophin expression and improvement in cardiac pathology in different mouse and dog models of DMD [179–182]. Importantly, the correction was shown to persist long-term in mice, supporting the notion of permanent gene repair with this genomic editing strategy [183–185].

Despite significant promise, this approach is not without its own setbacks. AAV-mediated gene delivery will always face the challenge of possible immunogenicity, and the delivery of a foreign gene exacerbates the issue with the potential of eliciting an immune response to the bacterial protein. Careful screening and immunosuppressive measures will be required to ensure patient safety and effective transduction, although long term studies in preclinical models suggest immune response against Cas9 does not limit the therapeutic efficacy [179,186]. Furthermore, the possibility of off-target mutagenesis with CRISPR-Cas9 is a cause for concern that has previously been substantiated in human cells, and recent studies have identified dozens of off-target mutations throughout the mouse genome following 8 weeks of CRISPR-Cas9

expression [185,187]. While most of these off-target mutations are found in introns, many are in exons, indicating a need for additional preclinical work to investigate the rate of accumulation and the physiological significance of these mutations. The risk of off-target editing can be managed by optimizing both the guide RNAs and the Cas9 endonucleases to minimize non-specific activity and improve fidelity [178,188]. Finally, as with AON-mediated exon skipping, some of the patients undergoing CRISPR-Cas9-mediated exon skipping therapy may still find themselves with a BMD-like risk of cardiomyopathy. Additional preclinical studies with longer post-treatment monitoring in dog and/or non-human primate DMD models will be required to confirm the safety and efficacy of this genome-editing therapy, but current results inspire optimism about the possibility of CRISPR-Cas9 treatment reaching clinical trials.

7. Conclusions

Just over 30 years since the discovery of the protein dystrophin, and nearly two centuries after the first descriptions of the devastating disease precipitated by its loss, efforts to understand and correct the underlying pathology of DMD are advancing by leaps and bounds. The preceding decades have been marked by careful mechanistic studies aiming to tease part the molecular processes derailed by dystrophin loss, providing extensive insights into the cellular dysfunction driving the progressive deterioration and premature death seen in patients. These insights helped to form the foundation for devising symptomatic interventions and small molecule treatment strategies to prolong and improve the lives of DMD patients. Now, the tireless and innovative efforts of the neuromuscular disease research community have started to open the door for potentially curative approaches that may allow individuals with DMD-causing mutations to live out their adult lives with manageable health.

This turning point in the development of DMD therapies marks the beginning of a new mission to map the shifting landscape of cardiac health and disease in patients that undergo these cutting-edge treatments. This will require continued improvements in cardiac diagnostic and treatment strategies used in the clinics and in preclinical studies that will build upon recent breakthroughs. Deletions are the most common mutation type underlying DMD, but even at their highest theoretical efficiency, these corrective approaches cannot restore missing portions of the *DMD* gene sequence. For this reason, even patients that are successfully treated with the next generation of gene-

targeted therapies will likely continue to benefit from regular monitoring or treatment by a cardiologist. Ensuring that the vulnerable hearts of DMD patients receive careful consideration should remain a major priority in the management of this deadly disease as new questions and possibilities continue to arise from current and future discoveries.

CHAPTER 2

ACUTE AT_1R BLOCKADE PREVENTS ISOPROTERENOL-INDUCED INJURY IN *MDX* HEARTS

Tatyana A. Meyers[1], Jackie A. Heitzman[1], Aimee M. Krebsbach[1,2], Lauren M. Aufdembrink[1], Robert Hughes[1], Alessandro Bartolomucci[1], DeWayne Townsend[1,2]

[1] Department of Integrative Biology and Physiology, University of Minnesota Medical School, Minneapolis, MN, USA
[2] Lillehei Heart Institute, University of Minnesota Medical School, Minneapolis, MN, USA

Published in:

Journal of Molecular and Cellular Cardiology. 2019, *128*, 51–61.
DOI: 10.1016/j.yjmcc.2019.01.013

J.A.H. provided essential support with animal handling, drug delivery, tissue harvesting, colony management, and protocol adherence. A.M.K., L.M.A., and R.H. contributed extensive troubleshooting efforts and technical assistance that enabled the completion of histological staining and analysis. A.M.K. researched the physical basis of light polarization and birefringence. A.B. supplied β-adrenergic receptor knockout mice for use as controls. D.T. developed the automated analysis of immune cell microscope images, and performed the cTnI analysis.

Summary

Duchenne muscular dystrophy (DMD) is an X-linked disease characterized by skeletal muscle degeneration and a significant cardiomyopathy secondary to cardiomyocyte damage and myocardial loss. The molecular basis of DMD lies in the absence of the protein dystrophin, which plays critical roles in mechanical membrane integrity and protein localization at the sarcolemma. A popular mouse model of DMD is the *mdx* mouse, which lacks dystrophin and displays mild cardiac and skeletal pathology that can be exacerbated to advance the disease state. In clinical and pre-clinical studies of DMD, angiotensin signaling pathways have emerged as therapeutic targets due to their adverse influence on muscle remodeling and oxidative stress. Here we aim to establish a physiologically relevant cardiac injury model in the *mdx* mouse, and determine whether acute blockade of the angiotensin II type 1 receptor (AT_1R) may be utilized for prevention of dystrophic injury.

In the present study, a single IP injection of isoproterenol (Iso, 10 mg/kg) was used to induce cardiac stress and injury in *mdx* and wild type (*C57Bl/10*) mice. Mice were euthanized 8 hours, 30 hours, 1 week, or 1 month following the injection, and hearts were harvested for injury evaluation. At 8 and 30 hours post-injury, *mdx* hearts showed 2.2-fold greater serum cTnI content and 3-fold more extensive injury than wild type hearts. Analysis of hearts 1 week and 1 month after injury revealed significantly higher fibrosis in *mdx* hearts, with a more robust and longer-lasting immune response compared to wild type hearts. In the 30-hour group, losartan treatment initiated 1 hour before Iso injection protected dystrophic hearts from cardiac damage, reducing *mdx* acute injury area by 2.8-fold, without any significant effect on injury in wild type hearts. However, both wild type and dystrophic hearts showed a 2-fold reduction in the magnitude of the macrophage response to injury 30 hours after Iso with losartan.

This work demonstrates that acute blockade of AT_1R has the potential for robust injury prevention in a model of Iso-induced dystrophic heart injury. In addition to selectively limiting dystrophic cardiac damage, blocking AT_1R may serve to limit the inflammatory nature of the immune response injury in all hearts. Our findings strongly suggest that earlier adoption of angiotensin receptor blockers in DMD patients could limit myocardial damage and subsequent cardiomyopathy.

1. Introduction

Muscular dystrophies are a genetically diverse group of rare muscle wasting diseases that often involve the heart, resulting in clinically significant cardiomyopathy [3,5,6,148,189]. Duchenne muscular dystrophy (DMD) is the most common form, having an X-linked inheritance pattern with an incidence of roughly 1 in every 3,500-5,000 boys [5,11]. The molecular basis of DMD lies in the loss of the protein dystrophin, which normally plays a critical role in maintaining the membrane integrity of muscle cells by serving as a molecular link between the cytoskeleton and the extracellular matrix and a signaling scaffold at the sarcolemma [52,190–193]. Dystrophin loss results in myocyte necrosis, replacement of myocytes with extensive fibrosis, and eventual loss of muscle mass [194,195]. Clinically, DMD is characterized by rapidly progressing skeletal muscle wasting, loss of ambulation and other motor functions, respiratory insufficiency, and pronounced heart disease [5,6,196]. As improvements in symptomatic respiratory therapies have prolonged patient life spans, heart failure is becoming a more common cause of premature death in patients with muscular dystrophy [1–3].

The *mdx* mouse is a commonly-used preclinical model of DMD, having a spontaneous mutation in the DMD locus that results in the absence of dystrophin [190,197,198]. In young adulthood, its disease is mild, but investigators have successfully used aged mice, exogenous stressors, or additional genetic manipulations to advance the disease state [5,29,32,112,199–203]. Multiple studies aimed at modulating the *mdx* phenotype have pointed to angiotensin-related signaling pathways and oxidative stress as important factors in both the skeletal and cardiac phenotype of dystrophic mice [111,203–207]. Importantly, drugs including ACE inhibitors (ACEi), angiotensin receptor blockers (ARBs), and antioxidants have shown a significant benefit for dystrophic mice and human patients [86,112,123,131,208–211]. Current recommendations guide clinicians to consider initiating ACEi or ARB therapy at the age of 10 in Duchenne patients even without cardiac symptoms. This recommendation is grounded in the thought that these drugs help primarily by minimizing adverse remodeling following cardiomyocyte loss [5,6]. However, if these drugs are able to limit cardiomyocyte loss, initiation at the age of 10 may be too late, as patients may already be losing myocardium well before this point [3,212–214].

Our group and others have used adrenergic agonists like isoproterenol (Iso) and dobutamine to stress *mdx* hearts to better recapitulate the severity of the human cardiac

pathology [29,32,45,77]. Iso is a selective agonist of all β-adrenergic receptor isoforms that drives a sharp increase in heart rate and cardiac contractility [215], producing a sufficiently high workload to damage membranes of susceptible cardiomyocytes. This model has advantages over further genetic manipulation or aging by reducing confounding factors and allowing for more direct comparisons to other literature featuring adult *mdx* mice. Additionally, this adrenergic stress model may be particularly relevant to the perioperative stresses faced by Duchenne patients, whose treatment course may include procedures requiring anesthesia, such as scoliosis correction or fracture repair, that may result in bouts of elevated cardiac stress [6,216].

In the present study, we evaluate the cardiac consequences of a single bolus of Iso in the *mdx* mouse, and combine this Iso-mediated cardiac insult with acute losartan treatment to evaluate the potential benefits of ARB therapy for cardiomyocyte survival. These data reveal an interaction between workload-induced cardiac injury and exacerbation of this injury downstream of angiotensin II type 1 receptor (AT_1R) in dystrophic hearts, showing a significant reduction in acute myocardial damage with ARB treatment at the time of Iso-induced cardiac stress. The potential cardiac protection and good overall tolerability suggest that early initiation of ARB therapy may provide a readily available means to slow the onset of dystrophic cardiomyopathy.

2. Methods

2.1. Animals

The wild type control strain *C57BL/10SnJ* (C10) and the dystrophic strain *C57BL/10ScSn-Dmd^{mdx}/J* (*mdx*) were bred and maintained at the University of Minnesota from breed stock obtained from Jackson Laboratories. To limit genetic drift in this colony, breed stock were purchased from Jackson Laboratories every 5-6 generations. All mice were 4-6 months of age at the time of experiments and were housed in static (non-ventilated) cages with a 12-hour light-dark cycle. As DMD is a disease predominantly affecting males, only male mice were used in these studies. All animal procedures were approved by the University of Minnesota Institutional Animal Care and Use Committee and performed in compliance with all relevant laws and regulations.

2.2. Isoproterenol studies

(-)-Isoproterenol hydrochloride (Iso; Sigma #I6504) was dissolved in saline and sterile filtered into a foil-wrapped red-top glass vial prior to injection. The sterile Iso solution was stored at 4˚C for no more than 3 days, and any solution developing discoloration indicative of degradation was discarded. Mice received a single IP bolus injection of 10 mg/kg Iso in volumes of 40-70 µl adjusted for body weight. Hearts were harvested at timepoints of 8 hours, 30 hours, 1 week, and 1 month after the injection (Fig. 2.1A).

2.3. Serum cTnI measurements

For a subset of mice, blood was collected from the facial vein of isoflurane-anesthetized mice 1 week prior to the Iso injection for the baseline serum cTnI measurement, and again 8 hours following the Iso injection. The collected blood was allowed to clot on ice, then spun to separate the serum, which was then stored at -80˚C until analysis. Serum cardiac troponin I content (cTnI) was measured via a cTnI test kit on the Stratus CS Stat fluorometric analyzer (Siemens Healthcare).

2.4. Losartan studies

An additional subset of mice was assigned to receive losartan 1 hour prior to and alongside Iso, terminating at the 30-hour timepoint. Losartan solution was made on the day prior to Iso injections from a crushed generic losartan tablet (100mg) dissolved in saline to a final concentration of 6 mg/ml, and sterile filtered. Doses were calculated based on mouse body weights, the injection schedule, and the pharmacokinetics of losartan as well as its primary active metabolite EXP3174 [217,218]. At the start of the light cycle on the day of the study (7am), the mice received a loading dose in the form of a 60 mg/kg losartan bolus injection, followed a single 10mg/kg Iso injection 1 hour later (8am), and a 20 mg/kg losartan booster 6 hours after the first bolus (1pm). At the end of the light cycle, the mice received another bolus of 60 mg/kg losartan to span the dark cycle (7pm). At the end of the dark cycle, they received a final booster of 20 mg/kg losartan (7am), and hearts were harvested 7 hours later (30 hours from the Iso bolus). This dosing regimen was based on the half-lives of losartan and its major active metabolite, and intended to minimize the troughs in drug serum levels after the loading dose without disruptions to the dark cycle.

2.5. Histopathology

Fresh excised hearts were rinsed in PBS and cut in half along the transverse plane. The apical half was placed into OCT medium inside a block mold, and the OCT block was frozen in liquid nitrogen-cooled isopentane. Heart block sections were cut to 7 microns and placed on plus slides to be stained. Slides used for dystrophin and actinin staining were fixed in cold acetone for 10 minutes before rehydration and staining, while all other immunofluorescent staining was performed on unfixed slides. The following antibodies and reagents were used for IF staining: goat serum for blocking (Jackson ImmunoResearch # 005-000-121, 10%), rabbit actinin polyclonal antibody (Novus #NBP1-32462, 1:150), rabbit dystrophin polyclonal antibody (Abcam #ab15277, 1:150), rat AlexaFluor 488 anti-mouse CD68 antibody – clone FA-11 (Biolegend, 1:150), rat AlexaFluor 647 anti-mouse CD45 antibody – clone 30-F11 (Biolegend, 1:100), goat anti-mouse IgG (H+L) secondary antibody (Invitrogen #R37121, 1:200), goat anti-rabbit IgG (H+L) secondary antibody (Invitrogen #A-11008, 1:200), WGA AlexaFluor conjugate (ThermoFisher, 5µg/ml), and ProLong Gold Antifade Mountant with DAPI (ThermoFisher). All immunofluorescence incubation steps were carried out at room temperature for 1 hour, separated by three 5-minute washes in fresh PBS.

The following reagents were used for Sirius Red Fast Green (SRFG) staining: 1.2% picric acid solution (Ricca #R5860000), Direct Red 80 (Sigma #365548), Fast Green FCF (Sigma #F7252), Formula 83 clearing solvent (CBG Biotech F83), and organic mounting medium (CBG Biotech MM83). Prior to SRFG staining via a modified protocol based on previously described methods [200], slides were fixed for 3 hours in cold acetone, then rehydrated in 70% ethanol followed by tap water. The tissue was then stained for 25 minutes in SRFG dye solution of picric acid, 0.1% Direct Red 80, and 0.1% Fast Green FCF, followed by washes in tap water and dehydration in 70% ethanol, 100% ethanol, and Formula 83.

2.6. Microscopy

All imaging was performed in NIS Elements software on a Nikon Eclipse Ni-E upright epifluorescent microscope with motorized stage and filter wheel. For cell infiltration and acute lesion studies, whole heart montages were collected as a stack of three to four fluorescent channels at a resolution of 0.92 µm/pixel. For fibrosis studies,

SRFG-stained sections were collected as brightfield montages at a resolution of 0.85 μm/pixel. For assessment of birefringence, images with a resolution of 0.17 μm/pixel were collected using orthogonally oriented polarized filters flanking the slide. Dystrophin and actinin IF close-up images were collected at a resolution of 0.23 μm/pixel, and deconvolved via the automatic 2D deconvolution package in NIS Elements.

2.7. Image analysis

All images were analyzed under deidentified names in a blinded fashion in Fiji using custom macros and scripts [219]. IgG analysis was carried out using 1180×944 μm (1280×1024 pixels) non-overlapping frames taken from whole montages to minimize complications arising from variations in brightness across the whole heart section. IgG lesion area was determined by thresholding the IgG image for total lesion area (indicated by bright IgG-positive signal) and dividing that by total heart section area (provided by tissue autofluorescence).

Fibrosis analysis of SRFG-stained sections was carried out on entire heart montages using the color threshold function in Fiji. Areas containing collagen, which takes up Sirius Red dye, were identified by measuring the pixel area corresponding to a red hue. The fibrotic area was then divided by total heart pixel area, corresponding to any hue and saturation that exceeds the neutral background.

Birefringence analysis was carried out using 2360×1770 μm (2560×1920 pixels) frames imaged using brightfield, and matching frames imaged with orthogonally oriented polarized filters flanking the slide. Total birefringent area was calculated as the number of pixels corresponding to a signal that exceeds the brightness of the surrounding myocardium. The birefringent area was divided by the total red area from the matched brightfield image to calculate the percent birefringence of each fibrotic lesion.

Cell infiltration analysis workflow began with a blinded scrubbing of IF montage images in which artifacts were removed, including blood within the ventricles or large vessels, non-specific aggregates of dye, and areas in which the tissue was folded. Lesion-positive regions and total muscle area were determined by thresholding the entire montage, followed by a manual removal or addition of misidentified areas. Cell-specific thresholds were set to identify cell-positive regions, which were then compared to the lesion areas. Any cell-positive region containing a shared pixel with a lesion was considered a lesion-positive cell region. Results represent the percentage of cell-positive

pixels relative to the total number of heart pixels. All data analysis scripts were performed in Fiji and R.

2.8. Statistics

Statistical analyses were performed using Prism 7 (GraphPad Software) and R [220]. Statistical comparisons were made using one-way ANOVA or two-way ANOVA where appropriate, with Sidak multiple comparison post-hoc test to identify specific differences between relevant groups. All column and line graphs display the mean ± standard error.

3. Results

3.1. A single dose of isoproterenol causes acute myocardial injury that is significantly exacerbated in dystrophic hearts.

Within hours of injection of a single dose of isoproterenol (Iso), areas of acute myocardial injury could be identified by staining for myocyte infiltration of endogenous IgG. The accumulation of intracellular IgG is only expected to occur in myocytes whose membranes have been sufficiently disrupted to become permeable to large molecules like serum proteins. Quantification of acute myocardial damage revealed that injured myocyte area is already prominent as early 8 hours, with a peak at 30 hours after Iso administration. This acute injury is completely removed 1 week after the Iso injection (Fig. 2.1B). A significant difference was found between healthy and dystrophic hearts at the 30-hour timepoint, with *mdx* hearts showing 3-fold greater injury than that seen in wild type hearts (18.9±2.8% versus 6.3±1.7%, respectively).

Examination of entire heart montages revealed that in dystrophic hearts, these acute lesions were large and scattered throughout the whole heart section. In contrast, acute injury in wild type hearts manifested as smaller lesions that were concentrated in the endocardium (Fig. 2.1C). This hints that the Iso-induced injury in C10 hearts may result from perfusion-demand mismatching, with relative hypoperfusion of the endocardium during Iso-induced increases if cardiac workload resulting in myocardial injury. This mechanism is likely also active in the dystrophic heart, but large swaths of injured myocardium are also found throughout the rest of the heart, suggesting an additional mechanism of injury is at play. Mice with genetic ablation of all β-adrenergic receptors showed no functional or histological response to the dose of Iso used in these studies (data not shown), confirming the β-adrenergic receptor specificity of Iso action.

3.2. Isoproterenol-induced sarcolemmal injury triggers cardiomyocyte destruction.

Closer inspection of the regions of acute injury revealed multiple signs of myocyte degeneration at 8 hours after Iso injection. In intact myocytes, sarcomeric α-actinin was localized in a pattern of orderly striations, but within IgG^+ myocytes it displayed a marked disruption of this striated pattern (Fig. 2.2A). Signs of myocyte breakdown are not limited to the degradation of the contractile apparatus, as dystrophin staining at the membrane was also largely lost in injured wild type myocytes (Fig. 2.2B). The loss of normal sarcomeric patterning and sub-membrane protein localization suggests that these damaged myocytes are undergoing widespread proteolysis. No qualitative differences in the myocyte degradation process were found between injured areas in wild type and dystrophic hearts at 8 or 30 hours after Iso administration.

Serum cardiac troponin (cTn) content is an index of cardiomyocyte integrity, and elevated cTnI and cTnT levels have been documented in boys with DMD [21–23,30]. Untreated adult dystrophic mice showed no detectable ongoing basal cardiac injury, as indicated by little to no IgG^+ cardiac myocytes and negligible levels of serum cTnI that are not different from those observed in wild type mice. Corroborating the histological evidence of cardiomyocyte breakdown, serum levels of cTnI were found to be dramatically increased 8 hours after Iso administration in both *mdx* and C10 hearts. Serum collected from *mdx* mice 8 hours after the induction of Iso-induced injury showed 2.2-fold greater cTnI concentration than wild type mouse serum (Fig. 2.2C), consistent with the greater acute myocardial injury present in dystrophic hearts (Fig. 2.1B).

3.3. Fibrotic replacement of Iso-induced cardiac injury is dynamic.

Many, if not all, of the acutely damaged cardiomyocytes were removed following injury, resulting in their replacement with fibrotic lesions by 1 week after Iso administration. At timepoints of 1 week and 1 month following Iso-induced injury, dystrophic hearts displayed over 2-fold larger fibrosis area relative to wild type hearts (Fig. 2.3A), consistent with the elevated acute injury observed in *mdx* hearts at earlier timepoints. Replacement fibrosis area was highest 1 week following Iso administration in hearts from both strains, and closely reflected the peak acute injury area measured at 30 hours (Fig. 2.1B). Interestingly, 1 month after Iso-induced injury, total fibrotic lesion area was lower relative to its peak at 1 week after injury (Fig. 2.3A).

This curious observation of fibrotic area reduction between 1 week and 1 month following Iso administration could be explained by lesion contraction over this time period rather than by removal of deposited matrix. Collagen bundles display birefringence, the optical property that causes transmitted light to become polarized [221]. Collagen's orderly triple-helical structure underlies its inherent birefringence, which becomes more pronounced as the density of collagen fibers increases. Sirius Red staining further enhances this property due to the alignment of the dye molecule along the collagen strands [221–223]. Birefringence can be assessed microscopically by using two orthogonally-oriented polarized filters, referred to as the polarizer and the analyzer, flanking the sample [200]. Polarized light passing through the first filter (polarizer) and non-birefringent material will be blocked by the second filter (analyzer). However, a birefringent material will polarize the light further as it traverses, allowing some of it to pass through the analyzer and be detected by the camera. The wavelength and intensity of the light passing through the analyzer can provide information about the relative amount and organization of the birefringent material in the sample. For example, a diffuse patch of collagen fibers that are oriented in many directions results in a small amount of green or yellow polarized light. In contrast, a patch of densely-bundled and organized collagen strands would result in bright orange or red light, with structural collagen (e.g. tendons) serving as an excellent example of the latter [222–225]. Upon measuring the polarized light passing through prominent lesions of 1-week and 1-month *mdx* hearts, the older lesions were found to display a significantly greater birefringent area relative to the total area stained by Sirius Red (Fig. 2.3C). Accordingly, representative images show that the polarized light exiting 1-month-old lesions appears noticeably brighter with prominent areas of red and orange color (Fig. 2.3D), supporting the notion that tighter bundling of collagen over time is likely responsible for the modestly reduced area seen in older lesions.

3.4. Iso-induced injury triggers extensive immune cell infiltration in dystrophic hearts.

Infiltrating immune cells were labeled by antibody staining for CD45, a cell marker expressed by all leukocytes [226,227], and CD68, a phagocytic marker that is generally utilized as a differentiated macrophage marker [207,228–230]. Both of these immune cell markers showed a robust response to Iso-induced damage in *mdx* hearts, but this response was significantly attenuated and truncated in C10 hearts (Fig. 2.4 A

and D). Immune cell infiltration appeared to be delayed relative to the appearance of cardiac injury, with no response evident at 8 hours after Iso administration. In dystrophic hearts, an upsurge in immune infiltration could first be noted at 30 hours, with similarly robust immune cell presence lingering for at least 1 week following injury. In wild type hearts, a smaller increase in immune cells was apparent at 30 hours, and began to regress toward baseline levels 1 week post-injury. The prevalence of these immune cell markers dropped off to near-baseline levels 1 month post-injury in hearts from both strains.

In addition to different amplitudes of the peak response, immune infiltration also displayed different distribution in *mdx* and wild type hearts. $CD45^+$ leukocytes and $CD68^+$ macrophages were diffusely scattered throughout all of the hearts at baseline, and remained so up to 8 hours after injury. In dystrophic hearts, 30 hours and 1 week after injury both immune cell markers displayed robust expansion predominantly in regions of damage, evidenced by the majority of the cells clustering in lesion areas (Fig. 2.4 B and E). Although wild type hearts showed significant immune expansion in lesion areas at the 30-hour timepoint, some augmentation of non-lesion immune cells was also observed. At least 50% or more of the immune cells continued to occupy non-lesion areas of wild type hearts at all timepoints, possibly due to the more diffuse nature of C10 cardiac injury.

3.5. Acute AT_1R blockade dramatically reduces dystrophic Iso-induced injury and modulates the immune response in the heart.

Angiotensin II (AngII) type 1 receptor (AT_1R) is expressed in many cell types, serving as a major mediator of AngII effects, including pro-fibrotic gene program activation and increased ROS production [80,83,84,231,232] (Fig. 2.5A). These outcomes can be attenuated by blocking activation of AT_1R with an angiotensin receptor blocker (ARB) like losartan. The anti-remodeling effects of ARBs are well-documented in long-term studies [194,233,234], but much less is known about the potential acute benefits of AT_1R blockade for the dystrophic heart. To shed more light on this question, *mdx* and wild type mice were treated with a brief course of intraperitoneal injections of losartan starting 1 hour before the bolus of Iso and spanning the period of 30 hours after Iso (Fig. 2.5A). Acute losartan treatment dramatically protected dystrophic hearts from cardiac damage following Iso injection, cutting *mdx* IgG^+ injury area by 2.8-fold (Fig.

2.5B). Conversely, AT_1R blockade showed no significant effect on wild type cardiac damage, resulting in comparable Iso-induced injury area in wild type and dystrophic hearts with acute losartan treatment. Interestingly, losartan did not change the distribution of lesions in dystrophic hearts, with *mdx* lesions remaining larger and localized more epicardially than C10 lesions (Fig. 2.5C).

The $CD45^+$ leukocyte response in 30-hour post-Iso hearts reflected the same trends as acute injury area. While C10 hearts showed no significant reduction in $CD45^+$ area with losartan, *mdx* hearts showed a 38% reduction in the prevalence of CD45 after losartan treatment, resulting in CD45 levels that are not different from those observed in wild type hearts (Fig. 2.5D). Interestingly, $CD68^+$ macrophages showed a different trend, with a significant 53% reduction in total $CD68^+$ area in C10 hearts treated with losartan, despite no change in total injury area or total leukocyte infiltration (Fig. 2.5E). Dystrophic hearts also showed a trend toward a proportionately larger CD68 decline with losartan, with 56% lower CD68 compared to only 38% reduction in CD45. These declines in $CD68^+$ area appeared to manifest in both lesion and non-lesion areas in hearts of both strains, suggesting that the overall immune profile of these mice may have shifted as a consequence of AT_1R blockade (Fig. 2.5E). Representative images, highlighting lesion-positive areas in hearts of both strains, demonstrate the visibly reduced prominence of $CD68^+$ cellular infiltrates in losartan-treated groups (Fig. 2.5F).

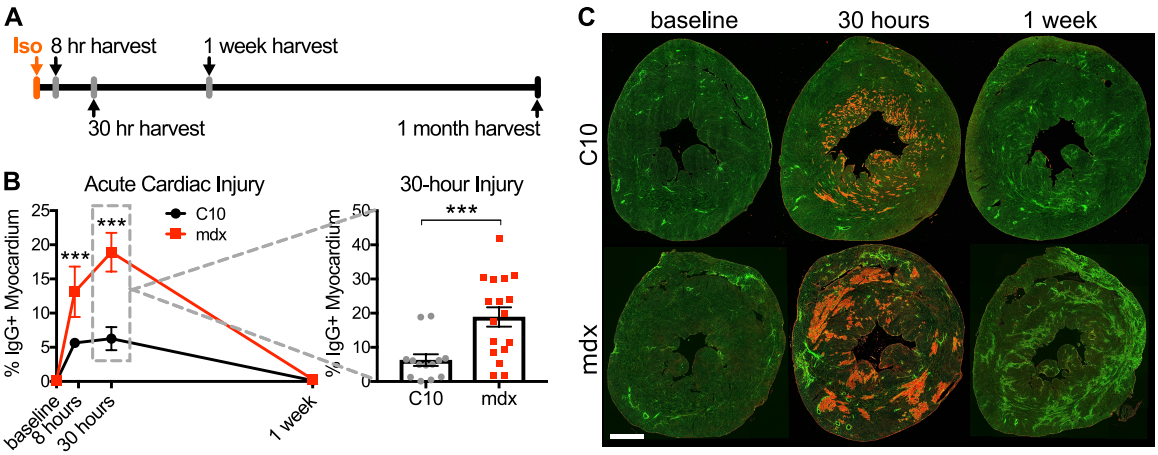

Figure 2.1: *Effects of a single dose of isoproterenol on healthy and dystrophic hearts.*

(A) After one bolus injection of 10 mg/kg isoproterenol (Iso), mice were sacrificed at timepoints of 8 hours, 30 hours, 1 week, or 1 month. **(B)** *Left:* Acute Iso-induced injury, measured by IgG incorporation, was prevalent as early as 8 hours, with a peak at 30 hours. Evidence of acute injury was totally removed by 1 week. (*** indicates $p<0.001$ vs. baseline; interaction $p=0.01$; n = 6-17 mice per group). *Right:* Wild type (C10) hearts displayed a peak acute injury area of only 6±2%, while *mdx* peak injury was 3-fold higher at 19±3%. (*** indicates $p<0.001$). **(C)** Representative images of data shown in panel B. Whole hearts are shown with WGA (green) marking the total tissue area and IgG (red) indicating areas of acute myocyte injury. Scale bar = 1mm.

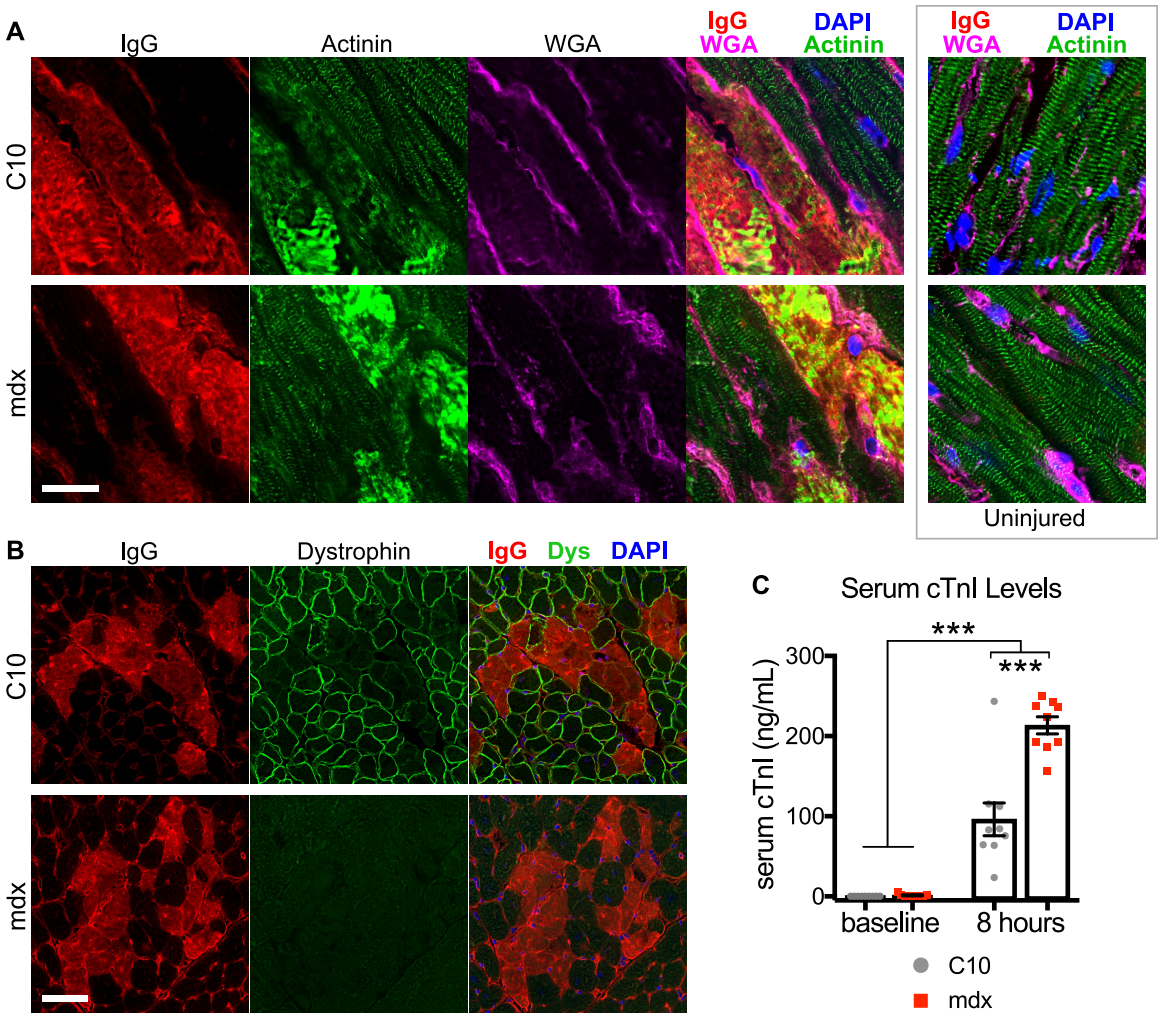

Figure 2.2: Sarcolemmal injury triggers cardiomyocyte destruction as early as 8 hrs after Iso.

(A) In both wild type (C10) and dystrophic hearts, uptake of IgG into injured myocytes corresponds with profound disruption of sarcomere structure as early as 8 hours following a bolus of Iso, compared to uninjured cardiomyocyte sarcomeres (right). Sarcomeres were visualized by α-actinin staining (green), myocyte injury was marked by endogenous IgG uptake (red), and extracellular matrix was visualized by WGA staining (magenta). Scale bar = 20 μm. **(B)** In wild type mouse hearts, myocytes that had taken up IgG also lost dystrophin at the sarcolemma, evidenced by absence of dystrophin staining (green). As expected, *mdx* hearts did not exhibit dystrophin staining. Scale bar = 50 μm. **(C)** Cardiac troponin I (cTnI) concentration was measured in serum collected from wild type and *mdx* mice as an index of myocardial damage. Dystrophic mice showed significantly higher serum levels of cTnI 8 hours after Iso. (*** indicates $p<0.001$; $n \geq 8$ mice per group).

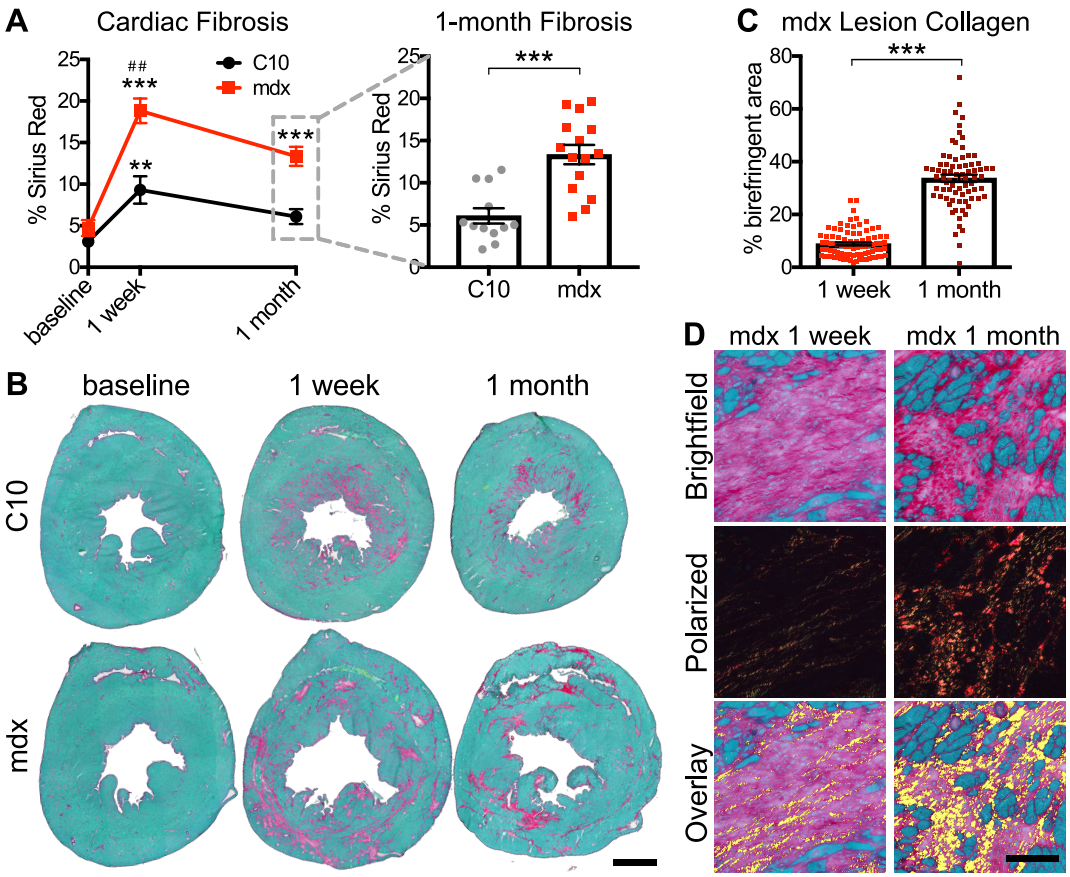

Figure 2.3: Fibrotic replacement of Iso-induced cardiac injury is dynamic.

(A) *Left:* In wild type and dystrophic hearts, the area of fibrosis was the highest 1 week after Iso-induced injury, and declined by 1 month (** indicates p=0.009 vs. baseline, *** indicates p<0.001 vs. baseline, ## indicates p=0.003 vs. 1 month; interaction p=0.02; n = 8-15 mice per group). *Right:* One month after injury, *mdx* hearts displayed significantly larger fibrotic area (13±1%) than control hearts (6±1%) (*** indicates p<0.001). **(B)** Representative montages of data displayed in panel A. Whole hearts are shown with Fast Green-stained myocardium and Sirius Red-stained fibrosis. Scale bar = 1mm. **(C)** One month after Iso-induced injury, fibrotic lesions in *mdx* hearts displayed dramatically increased birefringent area relative to 1-week lesions, suggesting that replacement fibrosis contracts during maturation. (*** indicates p<0.001, n = 76-86 lesions from 14 mice per group). **(D)** Representative images of data displayed in panel C. Matched brightfield, cross-polarized, and overlay images of *mdx* hearts show the change in the birefringence of 1-week and 1-month-old lesions; areas of birefringence are denoted in yellow on overlay images. Scale bar = 100 μm.

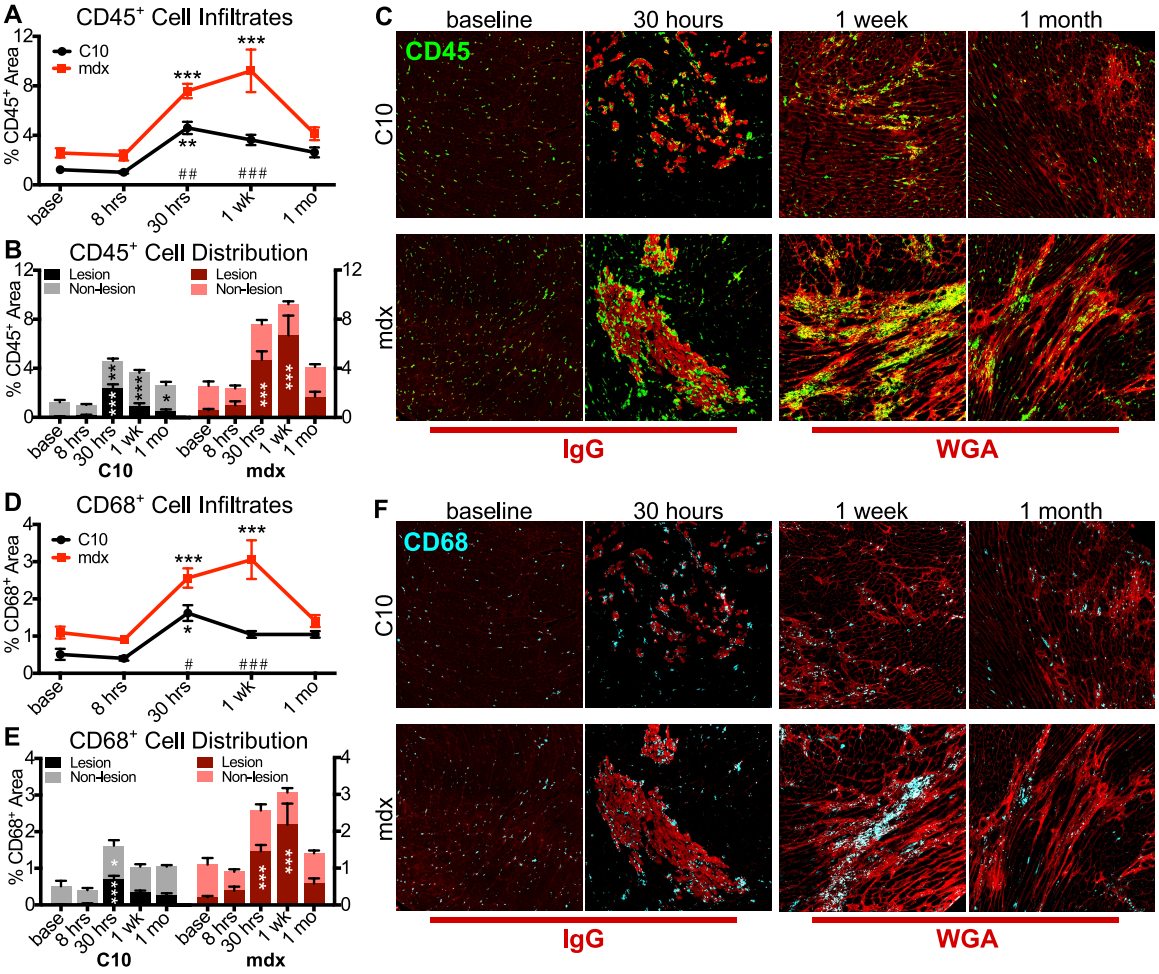

Figure 2.4: Iso-induced injury triggered a significantly greater immune cell response in dystrophic hearts.

(A) $CD45^+$ cell area was dramatically increased in *mdx* hearts 30 hours and 1 week after Iso administration, with a return toward baseline at 1 month after injury. Wild type (C10) hearts followed a similar pattern, with lower overall levels of infiltration and a faster return toward baseline levels (*** indicates $p<0.001$, ** indicates $p=0.008$ vs. baseline; ### indicates $p<0.001$, ## indicates $p=0.004$ difference between strains at the same timepoint; interaction $p=0.02$; n = 5-11 mice per group). **(B)** The expansion of the $CD45^+$ cell population occurred primarily in lesioned areas of the heart, where the $CD45^+$ area significantly increased compared to baseline in dystrophic hearts (*** indicates $p<0.001$, ** indicates $p=0.008$, * indicates $p<0.05$ vs. baseline). **(C)** Representative images for data shown in panels A and B. Cardiac lesions are represented by endogenous IgG uptake (red, baseline and 30 hours) and WGA accumulation (red, 1 week and 1 month). $CD45^+$

cells are shown in green. Each panel is 1 mm^2. **(D)** $CD68^+$ immune infiltrates were significantly increased in dystrophic hearts 30 hours and 1 week after Iso administration, with a return toward baseline by 1 month post-injury. Wild type hearts displayed a smaller and shorter-lived surge in cardiac $CD68^+$ cells, with a significant increase observed only at 30 hours after Iso injection (*** indicates $p<0.001$, * indicates $p=0.02$ vs. baseline; ### indicates $p<0.001$, # indicates $p=0.01$ difference between strains at the same timepoint; interaction $p=0.02$; n = 4-12 mice per group). **(E)** $CD68^+$ cell expansion occurs primarily in lesioned areas of the heart, where their numbers are significantly greater compared to baseline. Only wild type hearts showed any expansion of non-lesion $CD68^+$ cell numbers at 30 hours after Iso injection (*** indicates $p<0.001$ vs. baseline, * indicates $p=0.02$ vs. baseline). **(F)** Representative images for data shown in panels D and E, with $CD68^+$ cells shown in cyan. Each panel is 1 mm^2.

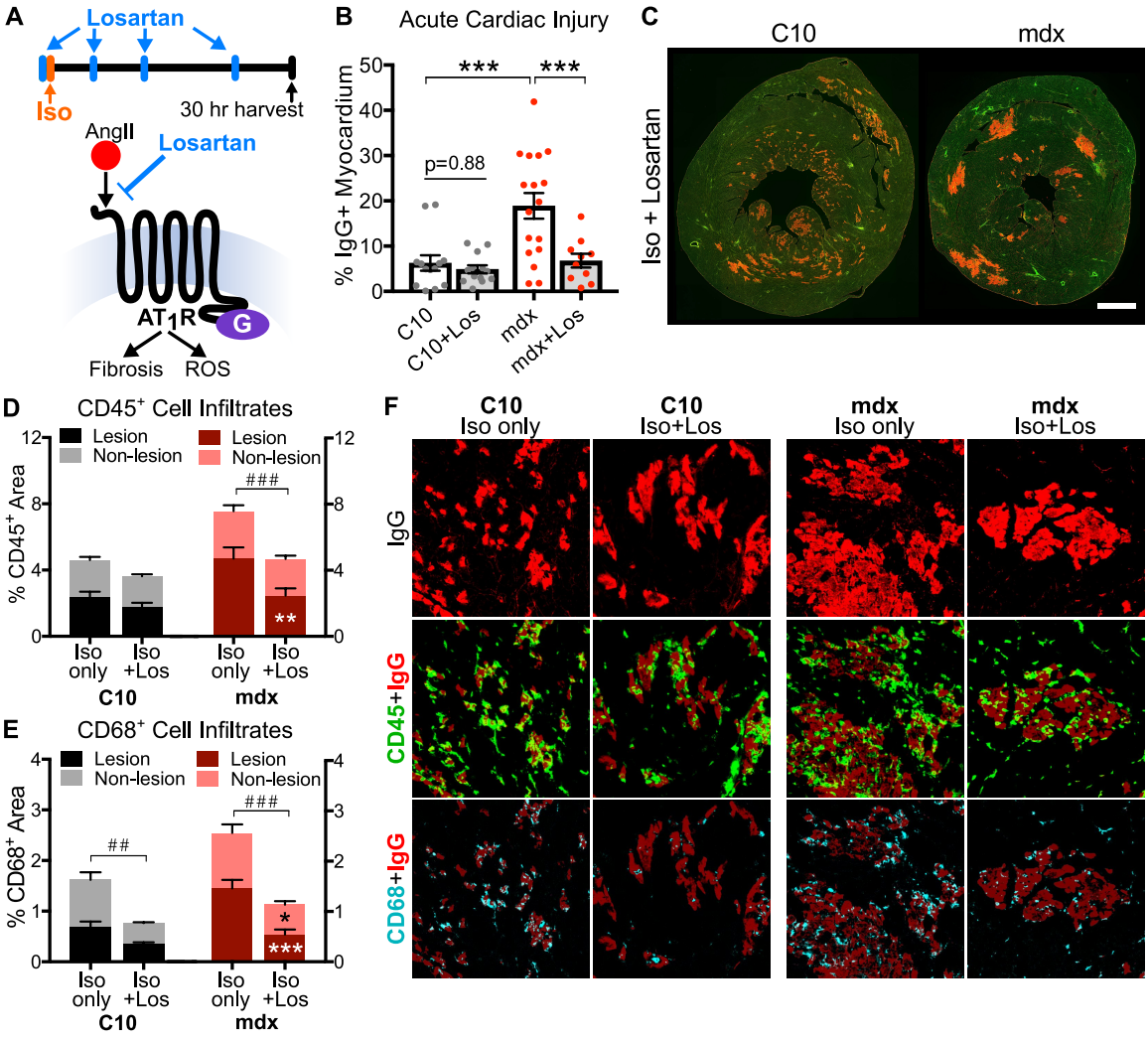

Figure 2.5: Acute losartan administration dramatically reduces Iso-induced injury in dystrophic hearts.

(A) Angiotensin II type 1 receptors (AT_1R) are G protein-coupled receptors that can be activated by angiotensin II (Ang II) and blocked by losartan. *Top:* Mice were treated with bolus injections of losartan (blue) 1 hour prior to Iso administration (orange), and at regular intervals over 30 hours following Iso injection. **(B)** 30 hours after Iso, losartan treatment caused no significant change in wild type (C10) cardiac injury, resulting in similarly low levels of acute Iso-induced injury in wild type and dystrophic hearts with losartan treatment. Untreated C10 and *mdx* data originally presented in Fig. 1B, shown here for comparison. (*** indicates $p<0.001$; interaction $p=0.02$; n = 10-17 mice per group). **(C)** Representative images of data shown in panel B. Whole hearts are shown with WGA

(green) marking the total tissue area and IgG (red) indicating areas of acute myocyte injury. Scale bar = 1mm. **(D and E)** $CD45^+$ and $CD68^+$ areas with and without losartan in wild type and *mdx* hearts, in both lesion and non-lesion areas. (*** indicates $p<0.001$, ** indicates $p<0.01$, * indicates $p=0.03$ vs. same domain without losartan; ### indicates $p<0.001$, ## indicates $p<0.01$ difference in total immune area; n = 9-13 mice per group). **(F)** Representative images for data shown in panels D and E, with $CD45^+$ cells shown in green and $CD68^+$ cells shown in cyan. Cardiac lesions are indicated by endogenous IgG uptake (red). Each panel is 0.25 mm^2.

4. Discussion

Dystrophic cardiomyopathy is a progressive disorder in which the accumulation of lesions results in extensive fibrosis and global cardiac dysfunction. One major goal of the present study is to characterize myocardial injury in the dystrophic heart and the response to this injury over time. The cardiac injury protocol detailed here, resulting in a scattered distribution of myocardial lesions sustained secondary to increased workload on the heart, represents a physiologically relevant approach for modeling the injury that a dystrophic patient's heart might sustain during surgical procedures or other severely stressful events. This applicability is underscored by reports of elevated cardiac troponin I in DMD and Becker muscular dystrophy (BMD) patient serum [21,30], aligning with our observation of elevated cTnI in the serum of *mdx* mice following Iso-induced cardiac damage. Isoproterenol's well-characterized actions, ease of handling, and specificity for β-adrenergic receptors result in a simple and reproducible adrenergic stress model that can provide a reliable basis for evaluation of cardiac therapies. In addition to its utility in evaluating acute injury prevention as demonstrated here, this Iso-based injury model also provides quantifiable readouts for therapies that may target fibrosis or immune infiltration, broadening its applicability.

Another major goal of this work is to investigate whether intervention with angiotensin receptor blockers (ARBs) at the time of injury may help limit myocardial damage during the early necrotic phase, rather than only mitigating the cardiac remodeling during the later fibrotic period. ARBs may exert their action through multiple mechanisms downstream of angiotensin II type 1 receptor (AT_1R), a G-protein coupled receptor (GPCR) found widely expressed in many tissues, including cardiomyocytes and non-myocyte cardiac cells [114]. One pathway classically linked to AT_1R activation in the heart is the upregulation of genes associated with adverse remodeling, most notably TGF-β [108,232,235], a cytokine known to worsen dystrophic processes [236,237]. The inhibition of this pro-fibrotic and pro-hypertrophic gene program is often discussed as the main benefit of ARBs as a cardiac therapy. However, mounting evidence suggests that more acute effects of AT_1R activation include increased production of reactive oxygen species (ROS) by NADPH oxidase, a key mediator of angiotensin II's effects in many tissues [80,83]. Current literature features multiple reports of excessive NADPH oxidase-mediated superoxide production contributing to cardiac and skeletal muscle injury in *mdx* mice [33,74,81,207,238], indicating that early treatment with ARBs is a promising

approach for limiting dystrophic injury. Here we show that Iso-induced cardiac injury can be reduced 3-fold in dystrophic hearts by acute losartan treatment initiated 1 hour prior to adrenergic stress and maintained during the 30-hour period that followed it. This rapid protective effect strongly implicates an immediate signaling-based mechanism of action rather than transcriptional effects. Importantly, Iso-induced cardiac injury in wild type mice did not reflect any losartan benefit, suggesting that the mechanism of myocardial injury targeted by losartan's actions is uniquely exaggerated in dystrophic hearts. This notion is further supported by the different distributions of cardiac lesions in dystrophic and wild type hearts, even in the context of a strong reduction in dystrophic injury area. Wild type hearts display a peppering of small lesions clustered in endocardial regions, while *mdx* hearts show larger patches of damaged myocardium, which seem distributed at random throughout the walls of the heart. These *mdx* lesions become smaller and less frequent in losartan-treated hearts, but the distribution remains constant.

Our results, along with existing literature, support a model wherein ROS-mediated exacerbation of initial myocyte injury is a key driver of the accumulation of dystrophic heart damage. Oxidative stress induces a wide variety of pathological processes in the cell, including sarcolemmal damage, and has been thoroughly implicated in worsening cell survival [81,239]. NADPH oxidase, an effector of AT_1R signaling and an important source of reactive oxygen species within the heart, has been shown to have increased expression and activity in dystrophic muscle, and can be further activated in a stretch-dependent manner [75,82]. The approaches of specific inhibition of NADPH oxidase or general scavenging of ROS via N-acetylcysteine have been shown to improve both the skeletal muscle and cardiac phenotypes in dystrophic mice [33,74,81,207,240]. Together, these data suggest that AT_1R inhibition may benefit DMD patients by limiting the amplification of myocardial injury secondary to excessive ROS production in the dystrophic heart.

This work raises important questions regarding the mechanism of losartan action. The first question regards the significance of the altered immune response to cardiac injury, represented by the change in relative prevalence of macrophages. Wild type hearts showed a 53% reduction in $CD68^+$ area with losartan treatment, despite showing no significant changes in acute injury area or total $CD45^+$ leukocyte infiltration. A similar trend in relative proportions of immune cell markers can be observed in *mdx* hearts, where losartan treatment resulted in a 38% reduction in $CD45^+$ leukocytes, but a larger

56% reduction in $CD68^+$ cells. CD68 is a surface marker that is expressed to some degree by nearly all differentiated macrophages [229,230]. Similar reductions in CD68 content have been demonstrated in models of atherosclerosis and diabetic nephropathy treated with losartan [241,242]. Furthermore, it has been shown that macrophage AT_1R activation plays an important role in macrophage polarization toward the more pro-inflammatory M1 form and increased ROS production via macrophage NADPH oxidase [239,243,244]. If the immune response to cardiac damage is modified by losartan to become less inflammatory, then it's possible that both dystrophic and healthy hearts could derive delayed benefits from losartan in the form of more effective post-injury healing and less adverse remodeling.

Another important question is the relative benefit of ARB therapy compared to the broadly acting ACE inhibitors, which are currently more often prescribed to treat DMD patients despite showing lower tolerability [209,233]. Despite targeting similar physiological pathways, these two approaches have divergent effects on endogenous angiotensin signaling. ACE is a critical step in the enzymatic process that convert angiotensin I (AngI) to a variety of biologically active angiotensin peptides, including angiotensin II (AngII) and angiotensin (1-7). AngII may bind to both AT_1R and AT_2R, while angiotensin (1-7) binds to Mas receptor (MasR), triggering physiologically distinct downstream responses [245–247]. Importantly, signaling through AT_2R and MasR is considered to be protective, and is often characterized in terms of opposing the adverse pro-fibrotic and pro-inflammatory effects of AT_1R. ACE inhibition results in a large pool of uncleaved AngI, which, through the actions of non-ACE peptidases, may partially spill over into greater production of angiotensin (1-7) and greater MasR activation [126]. On the other hand, AT_1R blockade may leave large pools of both AngII and AngI [130], with much of the AngII presumably being displaced to signal more through AT_2R when AT_1R is inaccessible. Furthermore, ACE inhibition has been shown to alter the availability of bradykinin, another peptide associated with cardiac protection, by blocking its breakdown to inactive metabolites, whereas ARBs leave it unaffected [248,249]. Despite these differences, little work has been done to directly compare these two treatment approaches, and clinical trials in dystrophic patients have demonstrate that ARBs or ACEi have similar effects on the preservation of cardiac function when initiated after the onset of cardiac pathology [123].

Preclinical work has made only limited contributions to shedding light on this matter. Previous work using a 6-month or 2-year course of oral losartan demonstrated reductions in muscle fibrosis and cardiac remodeling, significantly preserved cardiac function, and markedly improved survival in losartan-treated *mdx* mice [85,250]. Comparable treatment courses with ACEi have not been documented in dystrophic mice. Studies using young, unstressed dystrophic mice with treatment periods of 2-4 months show mixed results, with most studies demonstrating little to no cardiac benefit compared to the natural disease course [138,142,251]. The short duration, lack of challenge, and co-administration of other drugs complicate the interpretation of the benefit of ACEi in dystrophic mice. The robust prevention of cardiac injury by AT_1R blockade presented here suggests that additional preclinical studies and patient trials should investigate the relative efficacy of ARB-based versus ACEi-based therapeutic approaches in limiting cardiac dysfunction when initiated prior to clinically evident cardiac disease.

Current best practice recommendations suggest that anti-angiotensin therapy should be initiated in DMD patients by the age of 10 [5,6]. This recommendation is based on a trial of the ACEi perindopril, in which the group of patients that initiated therapy at 10.7 ± 1.2 years of age demonstrated better cardiac function 5 years later and higher 10-year survival than the group that started therapy at 13.6 ± 1.2 years of age [117,118]. This clinical trial underscores the importance of early initiation of therapy. However, the observation that global cardiac dysfunction can be detected in patients at the age of 10 indicates that the loss of myocardium likely begins much earlier [3,212]. A significant concern with early initiation of cardiac therapy in the pediatric patient population is that potential side effects may significantly impact quality of life. The issue of tolerability has been studied in over 250,000 heart failure patients, demonstrating that ACEi and ARBs are equally effective, but ARBs are significantly better tolerated [121,122]. The new discovery of a striking benefit for acute myocardial injury shown here, coupled with limited side effects, strongly supports inclusion of ARBs among the first interventions to limit cardiomyopathy in DMD patients, well before the onset of global cardiac dysfunction. The earliest age at which any cardiac damage can be identified remains unclear, but it is clear that once myocardial damage occurs, that myocardium is lost forever.

The studies presented here provide a new, readily reproducible model of inducing cardiac injury in a genetic model of DMD. This approach provides an excellent platform for the study of myocardial injury responses, and offers significant potential for the pre-clinical assessment of therapies directed at dystrophic cardiomyopathy. The nature of the progression of dystrophic cardiomyopathy is unclear, but recent evidence suggests that DMD patients experience periods of significant cardiac damage resulting in elevations in serum markers of cardiac injury [3,212–214]. These episodic periods of cardiac injury are closely mirrored by the Iso-induced injury model used in these studies. The heart disease associated with DMD is of growing clinical importance, however many of the new therapeutic approaches have limited efficacy in the heart. Using this new model system, we demonstrate the acute protective capability of losartan pre-treatment in limiting the extent of new cardiac injury. This raises the important possibility that AT_1R blockade may not only result in favorable cardiac remodeling, but may limit the accumulation of injury in the first place. If true, early ARB therapy could significantly delay the onset of cardiac dysfunction in DMD patients, extending survival and improving their quality of life.

5. Acknowledgments

The β-adrenergic receptor knockout mice were provided by Dr. B.B. Lowell, Beth Israel Deaconess Medical Center. The authors thank Dr. Anthony Vetter (University of Minnesota) for assistance with preparation of the manuscript.

This work was supported by the National Institutes of Health (R01 HL114832 and K08HL102066 to DT, F31HL139093 to TAM), the Muscular Dystrophy Association (Grant 351960 to DT), stipends from the Lillehei Heart Institute and the Greg Marzolf Jr. Foundation to AK, and the University of Minnesota.

CHAPTER 3

ACUTE MYOCARDIAL INJURY IN *MDX* HEARTS AMELIORATED BY ARB BUT NOT ACE INHIBITOR TREATMENT

Tatyana A. Meyers[1], Jackie A. Heitzman[1], DeWayne Townsend[1,2,3]

[1] Department of Integrative Biology and Physiology, University of Minnesota Medical School, Minneapolis, MN, USA

[2] Paul and Sheila Wellstone Muscular Dystrophy Center, University of Minnesota Medical School, Minneapolis, MN, USA

[3] Lillehei Heart Institute, University of Minnesota Medical School, Minneapolis, MN, USA

Submitted to:

Neuromuscular Disorders, July 2019

J.A.H. provided essential support with animal handling, drug delivery, tissue harvesting, colony management, and protocol adherence.

D.T. obtained and refined the DMD patient ACEI and ARB data presented in Figure 3.

Summary

Duchenne muscular dystrophy (DMD) is a devastating muscle disease that afflicts males due to the loss of the protein dystrophin, resulting in muscle deterioration and cardiomyopathy. Dystrophin's absence causes increased membrane fragility, myocyte death, and tissue remodeling. Inhibition of angiotensin signaling with ACE inhibitors or angiotensin receptor blockers (ARBs) is a mainstay of DMD therapy, with clinical guidelines recommending starting one of these therapies by the age of 10 to address cardiomyopathy.

Using the *mdx* mouse model of DMD, we previously showed that isoproterenol causes extensive damage in dystrophic hearts, and treatment with the ARB losartan starting only 1 hour before isoproterenol dramatically reduced this myocardial injury. In the present study, we probed whether ACE inhibitors, which are more frequently prescribed, can deliver similar protection. Surprisingly, lisinopril treatment initiated 1 hour before isoproterenol failed to demonstrate any effect on injury in *mdx* hearts. Further, with a 2-week pretreatment, only losartan significantly lowered *mdx* cardiac injury, without any benefit associated with lisinopril treatment. These results confirm the ability of ARBs, but not ACE inhibitors, to prevent acute injury in mouse hearts, and prompt the question whether ARBs should be more frequently used for DMD cardiomyopathy because of these potential protective actions.

1. Introduction

Duchenne muscular dystrophy (DMD) is a devastating muscle wasting disease that results in the loss of skeletal muscle function and development of cardiomyopathy. This X-linked disease occurs almost exclusively in males at a rate of roughly 1:5000 live male births [10,11]. The absence of the protein dystrophin leads to increased sarcolemmal fragility and dysregulation of signaling processes associated with proper dystrophin localization, triggering myocyte necrosis and replacement with fibrosis. DMD is lethal in young adulthood, with death typically occurring from respiratory or heart failure. In recent decades, advancements in symptomatic respiratory therapies have resulted in prolonged patient lifespans, leading to higher rates of advanced heart disease among individuals with DMD [1].

The cardiomyopathy of DMD is a progressive disorder, with the earliest signs of disease processes appearing before the age of 10, and extensive myocardial fibrosis and contractile deficits marking the end stage of the disease [11,18,22,106]. Attempts to slow the progression of heart disease in patients with DMD include the recommendation that chronic treatment with ACE inhibitors (ACEIs) or angiotensin receptors blockers (ARBs) be initiated by 10 years of age or earlier, with the goal of mitigating fibrosis and adverse remodeling that follows cardiomyocyte loss in the dystrophic heart [5,6]. Both drugs aim to limit the deleterious processes associated with angiotensin II (AngII) signaling in the heart and muscle, which include increased production of reactive oxygen species (ROS), profibrotic gene transcription, and myocyte death [80,83,84,231]. ACEIs interfere in these processes upstream of AngII, hindering its production by blocking the ability of angiotensin-converting enzyme (ACE) to cleave angiotensin I into AngII. Conversely, ARBs limit the effects of AngII after it is formed by blocking activation of angiotensin II type 1 receptor (AT_1R), a key mediator of many of AngII's harmful effects. Several early clinical trials demonstrated improved cardiac function in DMD patients using ACEIs, paving the way for ACEIs being viewed as the top candidate for heart failure therapy [117,118]. Additional trials went on to show that ARBs were just as effective as ACEIs when used in patients whose cardiac health has begun to decline, and that ARBs are better tolerated by patients, but ACEIs continue to be used more widely in clinical management of DMD [121,123,233].

Recently, our group used the *mdx* mouse model of DMD to demonstrate that a single bolus injection of the β-adrenergic receptor agonist isoproterenol (Iso) results in

acute damage to 18.9±0.3% of the *mdx* myocardium, relative to 6.3±2% injury in wild type mice [31]. This experimental model of increased cardiac workload aims to approximate the bouts of stress experienced by DMD patient hearts during surgical procedures [216], with the subsequent injury likely resulting from the exacerbation of the ongoing disease mechanisms of the dystrophic heart [30,252]. Importantly, we reported that dystrophic *mdx* mice acutely treated with the ARB losartan shortly before this injurious stimulus show a striking degree of protection from myocardial injury. High-dose losartan treatment initiated only 1 hour prior to the bolus of Iso resulted in a 2.8-fold reduction in *mdx* myocardial injury, seemingly preventing the accumulation of myocyte damage in the dystrophic heart [31]. Interestingly, acute losartan did not have a significant effect on Iso-induced damage in wild type hearts, resulting in similarly low injury area in *mdx* and healthy hearts (6.8±2% vs. 4.9±1%, respectively) [31]. This demonstrated that dystrophic hearts are uniquely vulnerable to AT_1R-based exacerbation of myocardial injury via a mechanism that plays a negligible role in healthy hearts.

This discovery of losartan's ability to prevent dystrophic heart injury has prompted the question whether ACEIs would exert a similar effect. While it is well-documented that both classes of drugs are effective at limiting the fibrosis and remodeling that follow injury, the preservation of functional dystrophic myocardium is of utmost importance in the management of cardiac disease in patients with DMD. To determine the effectiveness of ACEIs in preserving dystrophic myocardium, here we present our previously published Iso-induced injury protocol with the ACEI lisinopril. Our new findings demonstrate that neither acute nor chronic treatment with lisinopril shows the protective capacity to limit Iso-induced myocardial loss in dystrophic hearts that is present with ARB treatment.

2. Methods

2.1. Animals

The wild type control strain *C57BL/10SnJ* (C10) and the dystrophic strain *C57BL/10ScSn-Dmd^{mdx}/J* (*mdx*) were bred and maintained at the University of Minnesota from breeding stock obtained from Jackson Laboratories. All mice were 4-6 months of age at the time of experiments. Since DMD almost exclusively affects males, male mice were used in these studies. All animal procedures were approved by the

University of Minnesota Institutional Animal Care and Use Committee, and were performed in compliance with all relevant laws and regulations.

2.2. Isoproterenol studies

(-)-Isoproterenol hydrochloride (Iso; Sigma #I6504) was dissolved in saline to a concentration of 6 mg/ml and sterile-filtered prior to injection. The sterile Iso solution was stored protected from light at 4˚C for up to 3 days, and discarded at the first sign discoloration indicative of degradation. Mice received a single intraperitoneal bolus injection of 10 mg/kg Iso in a volume of 40-70 µl, and hearts were harvested 30 hours after the Iso injection, as previously described [31].

2.3. Acute lisinopril study

A subset of mice received acute lisinopril treatment starting 1 hour prior to Iso and continuing after Iso, terminating at the 30-hour timepoint. Lisinopril powder (Cayman Chemical #16833) was dissolved in sterile saline on the evening prior to Iso injections to a concentration of 12 mg/ml, and stored protected from light at 4˚C. At the start of the light cycle (7 am) on the day of the study, the mice received a 20 mg/kg loading dose of lisinopril via IP injection in a volume of 40-70 µl, followed by a 10mg/kg Iso injection 1 hour later. At the end of the light cycle (7 pm), the mice received another bolus of 20 mg/kg lisinopril to span the dark cycle. At the end of the dark cycle, they received a final dose of 20 mg/kg lisinopril, and hearts were harvested 7 hours later (30 hours after the Iso bolus). This dosing regimen was based on the serum half-life of lisinopril, and designed to minimize troughs in drug serum levels. Littermate *mdx* and wild type mice were distributed evenly between the groups receiving Iso with lisinopril or Iso only.

2.4. Lisinopril and losartan pretreatment studies

To account for the possibility that additional protective effects may be revealed with pretreatment, an additional subset of mice was assigned to drink either lisinopril or losartan dissolved in water for 2 weeks prior to Iso-induced injury. Lisinopril was given at a concentration of 264 mg/L in 1% dextrose water with an average consumed dose of 40 mg/kg daily [253]. Losartan was given at a concentration of 600 mg/L in 3% dextrose, with an average consumed dose of 80 mg/kg daily [138]. The 2-fold difference in doses of losartan and lisinopril is reflective of the similar 2- to 3-fold difference in doses of

these drugs in human clinical applications. Drug-containing water was replaced 3 times per week, and each mouse was weighed before and during the pretreatment at weekly intervals [253].

The physical discomfort experienced by mice following Iso administration can disrupt their water and food intake for up to 24 hours, so the mode of drug delivery was switched from the drinking water to IP injections to ensure that therapeutic levels are maintained during that time. At the start of the light cycle on the 15th day after the start of pretreatment, mice received fresh tap water and a single a single 10mg/kg Iso IP injection. For the next 30 hours, the mice pretreated with lisinopril received the same booster injections of lisinopril as described in section 2.3 above, and mice pretreated with losartan received booster injections as described previously [31]. Mice were sacrificed and hearts were harvested 30 hours after the Iso injection.

2.5. Histopathology

Histopathology studies were carried out as previously described [31]. Briefly, fresh excised hearts were cut in half along the transverse plane and placed into OCT medium to be frozen in liquid nitrogen-cooled isopentane. Heart sections were cut to 7 μm, and the slides were stored at -80˚C before staining. All staining was performed on unfixed tissue. The following reagents were used for IF staining: goat serum for blocking (Jackson ImmunoResearch # 005-000-121, 10%), goat anti-mouse IgG (H+L) secondary antibody (Invitrogen #R37121, 1:200), WGA AlexaFluor conjugate (ThermoFisher, 5μg/ml), and ProLong Gold Antifade Mountant with DAPI (ThermoFisher). After blocking, staining was performed as a single step at room temperature for 1 hour, flanked by three 5-minute washes in PBS.

Only hearts from mice that survived the initial 24 hours were analyzed for injury area, due to the difficulty of quantifying the poorly-defined early IgG-positive injury present in hearts that succumb earlier in the time course. To ensure that this approach would not skew results, we confirmed that the mortality rates of 20-37% among *mdx* mice and 5-14% among wild type mice did not differ significantly between treatments.

2.6. Microscopy and image analysis

All imaging was performed in NIS Elements software on a Nikon Eclipse Ni-E upright epifluorescent microscope with motorized stage and filter wheel. Whole heart

montages were collected as a stack of three fluorescent channels at a resolution of 0.92 μm/pixel. IgG-positive injury area was determined using Fiji by subtracting the WGA channel (staining extracellular matrix) from the IgG channel to better distinguish intra-myocyte IgG signal [219]. This lesion area was then quantified by thresholding the resulting IgG image for total lesion area, and normalizing it to total heart section area.

2.7. Patient anti-angiotensin drug information

Electronic medical records from patients diagnosed with Duchenne muscular dystrophy at the University of Minnesota were surveyed for prescriptions of either ACEIs or ARBs. In total, we examined the records of 95 DMD patients seen from 2009-2019. The 30 patient records that did not specifically mention an ACE inhibitor or an ARB were excluded from the analysis. Several patients had received both ACEIs and ARBs, and in these cases they were classified by the most recent prescribed class of medication. No patients were receiving both drug classes at the same time. Collection and analysis of these data were performed in accordance with an IRB-approved protocol.

2.8. Statistics

Statistical tests were performed using Prism 7 (GraphPad Software). Preclinical study statistical comparisons were made using two-way ANOVA with Sidak post-hoc test. Ages from patient data were compared using the non-parametric Mann-Whitney test. All graphs display the mean ± standard error.

3. Results

3.1. Acute treatment with lisinopril has no effect on Iso-induced cardiac injury area.

Acute ACE inhibition with lisinopril initiated 1 hour prior to the bolus of Iso failed to decrease IgG+ cardiac injury area in both *mdx* hearts and wild type hearts (Fig. 3.1). As previously shown, *mdx* hearts stressed with a 10 mg/kg bolus of Iso displayed very high injury compared to wild type hearts (20.2±2% vs. 5.3±2%), and this difference persisted with ACE inhibition (16.2±2% vs. 6.4±2%) (Fig. 3.1 B and C). This result stands in stark contrast to our earlier published findings demonstrating that acute losartan treatment has a robust capacity for myocardial injury reduction in dystrophic hearts [31].

3.2. *Pretreatment with losartan, but not with lisinopril, significantly reduces Iso-induced injury in* mdx *hearts.*

To address the possibility that lisinopril may require a period of pretreatment to exert a protective effect, *mdx* and C10 mice were placed on a 2-week course with either lisinopril or losartan delivered in their drinking water before repeating the bolus injection protocol (Fig. 3.2A). In agreement with our earlier work, losartan pretreatment exerted a significant protective effect in dystrophic hearts, reducing *mdx* cardiac injury to 12.2±3% without any effect in C10 hearts (5.7±1% injury area) (Fig. 3.2 B and C). In contrast, pretreatment with lisinopril still did not reveal any protective effect on myocardial damage in mouse hearts. *Mdx* mice pretreated with lisinopril and injected with a bolus of Iso showed 20.9±2% IgG-positive cardiac injury, and C10 mice in the same treatment group showed 5.4±2% cardiac injury (Fig. 3.2 B and C).

3.3. *Patient records show that few patients with DMD receive ARB-based therapies.*

According to electronic records from patients with DMD seen in the years between 2009-2019 at the University of Minnesota, the majority of patients whose records mention an anti-angiotensin drug are receiving ACE inhibitors. Among the records that indicated the use of one of these drug classes, 72% of patients were on ACEIs while only 28% were taking ARB drugs (Fig. 3.3). The ACE inhibitor group included several patients that had begun the treatment before the age of 10, but all patients in the ARB treatment group were above the age of 10. Interestingly, only 38% (18/47) of patients in the ACEI-treated group but 72% (13/18) of the patients receiving ARBs were also being treated with beta blockers. This may be related to the fact that patients receiving ARBs were on average significantly older than those receiving ACEI, and thus more likely to be in more advanced stages of cardiac dysfunction (Fig. 3.3). Out of 95 patient records listing a diagnosis of DMD, 30 lacked any mention of ACE inhibitors or ARBs, and were thus excluded from the analysis.

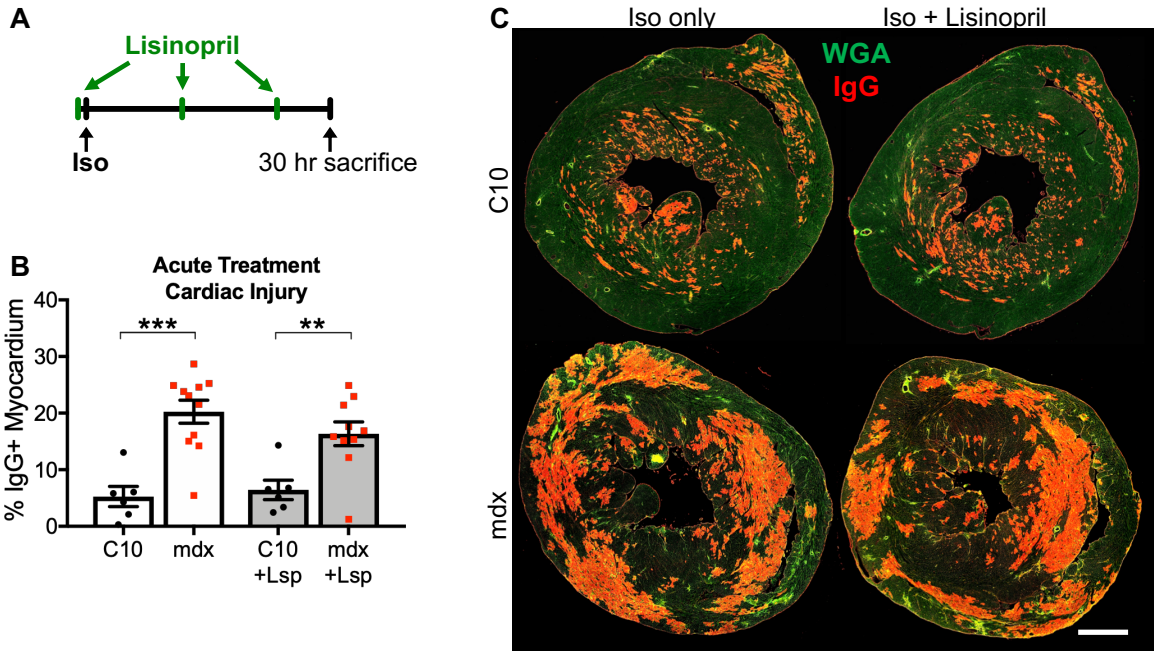

Figure 3.1: Acute ACE inhibition is insufficient to protect the heart from Iso-induced injury.

(A) The ACE inhibitor lisinopril was given as a 20 mg/kg IP injection 1 hour prior to a 10 mg/kg bolus injection of isoproterenol (Iso). Booster injections of lisinopril were given twice at 12-hour increments to maintain drug serum levels. **(B)** Dystrophic (*mdx*) hearts displayed 3.8-fold higher myocardial injury than wild type (C10) hearts 30 hours post-Iso. Acute treatment with lisinopril (Lsp) did not significantly change Iso-induced injury area in either group (*** $p<0.001$, ** $p= 0.003$; C10 n=6 per group; *mdx* n=10-11 per group). **(C)** Representative images of data in panel B. Whole heart transverse sections are shown with WGA (green) marking the tissue area and IgG (red) indicating areas of myocardial injury. Scale bar = 1 mm.

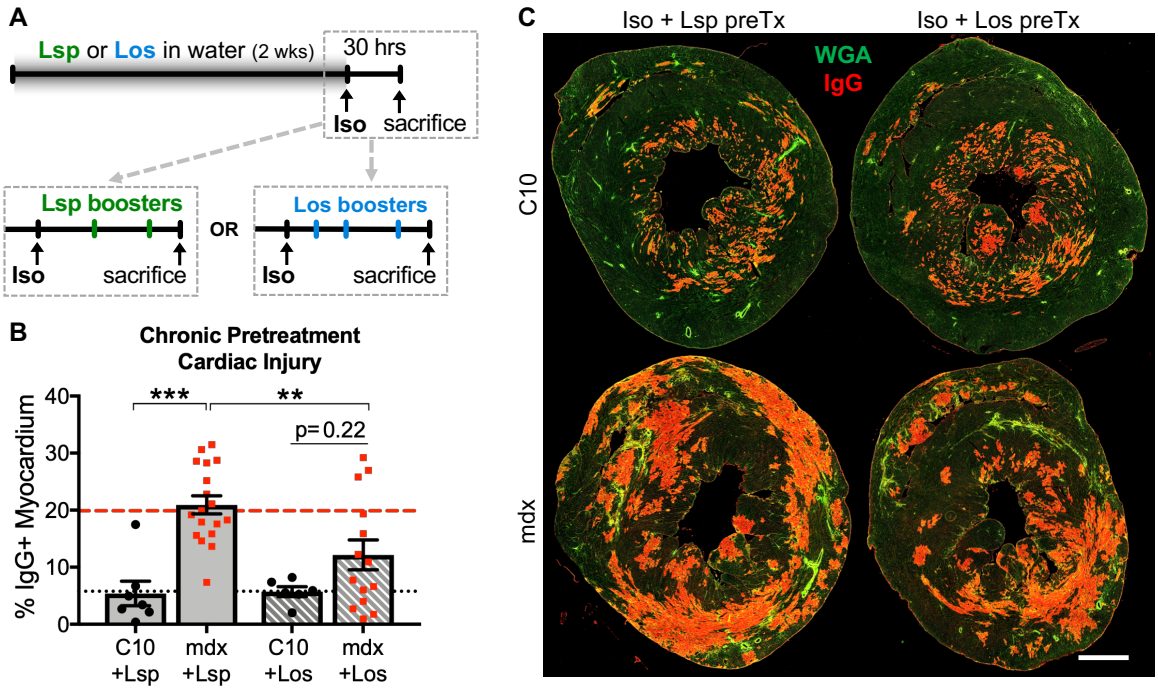

Figure 3.2: Pretreatment with losartan, but not lisinopril, protects mdx *hearts from acute myocyte injury.*

(A) To investigate and compare potential chronic benefits of lisinopril (Lsp) and losartan (Los), each drug was given as a pretreatment in drinking water for 2 weeks before resuming the injection-based 30-hour protocol. **(B)** Losartan pretreatment significantly lowered Iso-induced IgG+ injury in *mdx* hearts, but did not alter the injury outcome in C10 hearts. Lisinopril pretreatment failed to show an effect in either group. Red dashed line indicates injury level of Iso-only *mdx* hearts, and black dotted line indicates injury in Iso-only C10 hearts, as shown in Fig. 1. (*** $p<0.001$, ** $p=0.004$; C10 n=6-7 per group; *mdx* n=14-18 per group). **(C)** Representative images of data in panel B. Whole heart transverse sections are shown with WGA (green) marking the tissue area and IgG (red) indicating areas of myocardial injury. Scale bar = 1 mm.

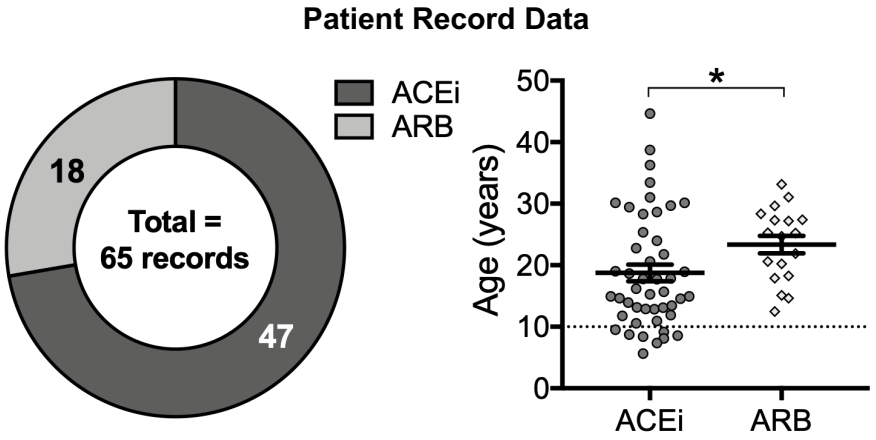

Figure 3.3: Patient records show that fewer patients with DMD receive treatment with ARBs than ACE inhibitors.

Left: Of 65 records belonging to patients diagnosed with DMD that mentioned an anti-angiotensin drug, 72% (47/65) indicated the use of an ACEi, and 28% (18/65) indicated the use of an ARB. *Right:* The dotted line at 10 years of age corresponds to the 2015 guideline to initiate treatment with an ACEi or ARB at or before 10 years of age. Only the ACEi group includes patients who are younger than 10 years of age, and the group of patients receiving ARBs is older on average than the group receiving ACEi (*p=0.02).

4. Discussion

Cardiomyopathy is a major feature of DMD that afflicts essentially all patients over 18 years of age, becoming a leading cause of death in this era of life-prolonging symptomatic respiratory therapies [1,3,7]. The earliest signs of cardiac pathology appear in childhood, with transient elevations in serum levels of cardiac troponins and early cardiac fibrosis detected in patients as young as 6 years of age [18,19,21,22,106]. These observations indicate that the destruction of healthy myocardium is ongoing well before the onset of global cardiac dysfunction manifesting in reduced ejection fraction [19,106]. Therefore, clinical approaches that preserve the myocardium by preventing this early degeneration are critically important for the successful management of dystrophic cardiomyopathy. This evidence of early cardiac degeneration has resulted in the updating of earlier recommendations, that cardiac treatment be initiated in response to detectable deficits in function, with the current guidelines that all DMD patients without contraindications should start on ACE inhibitors or ARBs by 10 years of age or earlier [5,20]. Currently, most DMD patients receiving an anti-angiotensin therapy are on ACEIs, which are considered to be a first-line therapy for heart failure in general and are named first by the guidelines for managing dystrophic cardiomyopathy [5,6,254]. ARBs are often mentioned as an alternative to ACEIs or the next step for those who are poorly tolerant of ACEI side effects, although clinical trials have not shown any differences in efficacy between the two drugs in DMD [121,123].

This study and our previous work demonstrated that losartan treatment significantly lowered myocardial injury following Iso-induced cardiac stress in the *mdx* mouse heart. This injury-preventing effect is only evident in the dystrophic hearts, without significant reduction in wild type cardiac damage after losartan treatment. This observation suggests that an angiotensin-related mechanism that is uniquely exaggerated in the dystrophic process is driving the accumulation of myocardial injury in the dystrophic heart. This finding raised many questions regarding the potential ability of ACE inhibitors to deliver similar protection, prompting the work presented here. Surprisingly, we found a lack of benefit associated with lisinopril treatment before the onset of Iso-induced myocardial injury, regardless of the treatment being initiated 1 hour or 2 weeks before injury. These results indicate that ARBs have a unique protective action in the dystrophic heart that is not recapitulated by ACEI treatment.

Since ACE inhibitors and ARBs exert their respective actions at different points within the renin-angiotensin system, it may be expected that these drug classes would have similar beneficial effects. Indisputably, both drugs do provide significant benefits in the dystrophic heart, as indicated by multiple clinicals trials supporting their efficacy. However, the path from angiotensin I to AngII and AT_1R activation is complex and multifaceted, opening the door for some divergence in the effects and benefits of these two drug classes that could explain the differences reported here. One possibility is that some combination of ACE-independent production of AngII by other peptidases and stretch-dependent activation of AT_1R by the mechanical forces induced by increased cardiac workload results in substantial AT_1R signaling even in the presence of ACEIs [124–128]. If the maximum benefit of anti-angiotensin therapies to cardiomyocytes lies in blocking AT_1R activation, then the indirect inhibition provided by ACEIs may be insufficient to protect cardiomyocytes from damage in light of these alternative activating mechanisms.

Another possible explanation is that ARB and ACEI treatments trigger distinct homeostatic responses that result in different secondary effects on the production and metabolism of angiotensin peptides. One unique secondary effect that may contribute to the distinctive ability of ARBs to prevent cardiomyocyte injury may lie in enhanced activation of angiotensin II type 2 receptor (AT_2R) as a compensatory consequence of AT_1R antagonism. When AT_1R is blocked, homeostatic mechanisms feed back to increase circulating levels of AngII, and all of this displaced AngII can serve as a ligand for AT_2R activation, which has been shown to mediate cardioprotective effects of angiotensin peptides [126,129]. Conversely, the distinct secondary effects induced by ACEIs include increases in angiotensin (1-7) and bradykinin, both of which have documented cardioprotective actions that may play a role in the demonstrated clinical efficacy of ACEIs. Angiotensin (1-7) may be produced at higher rates by non-ACE peptidases secondary to the accumulation of angiotensin I that follows ACEI treatment, and may also be removed at a slower rate because its degradation is normally mediated by ACE, resulting in its accumulation with ACE inhibition [126,130]. Angiotensin (1-7) is the endogenous ligand for the Mas receptor, and like AT_2R, Mas receptor activation causes a variety of protective effects that oppose the actions of AT_1R, including reducing inflammation, reducing oxidative stress, and increasing vasodilation [245,255,256]. Bradykinin, the ligand for BK receptors, is another substrate for degradation by ACE that

accumulates during ACE inhibition and may bear protective effects. However, while bradykinin is indeed linked to beneficial effects on inflammation, NO signaling, and pain, it is also a major contributor to the poorer tolerance of ACEIs, triggering a cough that prompts many patients to discontinue ACEI use [248]. Together, the joint effects of these protective mechanisms may drive the documented ACEI benefits of preventing remodeling and preserving function in the surviving myocardium. However, the inability of ACEIs to prevent myocardial damage in the Iso-induced injury model used here suggests that its protective mechanisms may be insufficient to overcome the acute effects of ACE-independent AT_1R activation.

The work presented here has some important limitations that should be addressed in future studies. First, the molecular effects of ACEI and ARB that are described above participate in overlapping physiological pathways, thus it is not possible to estimate the magnitude of their respective contributions to the overall protection derived from the use of these drugs in a whole animal model. Further work should make use of more selectively targeted agonists and antagonists to investigate the distinct mechanisms that contribute to ACEI and ARB cardiac effects, including AT_1R modulation, AT_2R activation, and Ang 1-7 signaling, to better understand the protective pathways in the dystrophic heart. Furthermore, the studies described here have used the mildly-affected *mdx* mouse, so additional work will be needed to determine if these protective actions of ARBs are present in more severe or earlier-onset disease models. It is possible that a different approach to evaluating cardiac or skeletal muscle vulnerability in a dystrophic animal model would reveal a different relationship between the benefits of ACEI and ARB treatments.

Despite these limitations, the existence of the novel and specific protective influence of ARBs that we have described may carry major implications for clinical management of dystrophic cardiomyopathy. Not only does the injury-limiting capacity of ARBs support earlier initiation of anti-angiotensin therapies to precede the beginning of cardiac deterioration, but it also calls for a more thorough comparison of potential benefits between ARB and ACEI treatments. To date, clinical trials comparing ACEIs and ARBs have been performed in DMD patients old enough to have established cardiac injury, and records matching a DMD diagnosis from the University of Minnesota show a trend toward older patients in the ARB treatment group than the ACEi group. Based on these limitations, the lack of evidence supporting a significant benefit of ARBs

over ACEIs may reflect the possibility that the additional ARB benefits described here are less evident in hearts with significant pre-existing myocardial damage. Additional clinical trials that enroll patients with DMD at a sufficiently young age to benefit from the potential protective actions of ARBs will be necessary to compare the therapeutic potential of ARBs and ACEIs in these fragile hearts. Data from our center show that the small proportion of patients currently receiving ARB treatment may already be too old to benefit maximally from early myocardial preservation by ARBs, so any comparisons based on data from patients who started their ARB treatment after the onset of cardiomyopathic symptoms should be made very cautiously.

In summary, we have presented data demonstrating that ARB treatment has a unique capacity to save cardiomyocytes from injury rather than just mitigating remodeling after their loss. These results support a shift in clinical practice toward using ARBs as a first-line therapy before 10 years of age for any child diagnosed with DMD, considering the certainty that virtually all of them will develop cardiomyopathy by their late teens. ARBs are safe, relatively well-tolerated, and readily available drugs that may hold the key to significant improvements in prognosis and quality of life for these patients, only requiring some adjustments to their clinical application.

5. Acknowledgments

The authors would like to thank Dr. Peter Karachunski and Dr. James Ervasti for helpful comments regarding the manuscript. This work was supported by the National Institutes of Health (R01 HL114832 and K08HL102066 to DT, F31HL139093 to TAM) and the Muscular Dystrophy Association (Grant 351960 to DT). The patient data collection was supported by National Institutes of Health's National Center for Advancing Translational Sciences, grant UL1TR002494.

CHAPTER 4

DMD CARRIER MODEL WITH MOSAIC DYSTROPHIN EXPRESSION IN THE HEART REVEALS COMPLEX CARDIAC VULNERABILITY TO ISOPROTERENOL-INDUCED INJURY

Tatyana A. Meyers[1], Jackie A. Heitzman[1], DeWayne Townsend[1,2,3]

[1] Department of Integrative Biology and Physiology, University of Minnesota Medical School, Minneapolis, MN, USA

[2] Paul and Sheila Wellstone Muscular Dystrophy Center, University of Minnesota Medical School, Minneapolis, MN, USA

[3] Lillehei Heart Institute, University of Minnesota Medical School, Minneapolis, MN, USA

J.A.H. provided essential support with animal handling, drug delivery, tissue harvesting, colony management, and protocol adherence.

Summary

Duchenne muscular dystrophy (DMD) is a devastating neuromuscular disease that causes progressive muscle wasting and cardiomyopathy. This X-linked disease results from mutations in the dystrophin gene and primarily affects males, with most cases being passed via the X-chromosome from a mother who carries the mutation. The loss of dystrophin causes widespread cellular pathology that leads to the loss of healthy myocytes, thus great effort has been invested in gene-targeted therapies that may restore dystrophin expression in striated muscle. Preclinical studies show that some of these approaches result in a mosaic pattern of dystrophin-expressing and dystrophin-null myocardium, raising the question of what extent of dystrophin restoration is sufficient to rescue the heart from DMD-related pathology. Female carrier hearts can provide insights into this question, due to their mosaic dystrophin expression pattern resulting from random X-inactivation.

In the present study, a mouse model of DMD carriers was used to model myocardial injury resulting from isoproterenol-induced stress in hearts partially expressing dystrophin. Carrier mice were derived either from dystrophic mothers or dystrophic fathers breeding with a wild type mate. Our results revealed that, despite expressing ~57% dystrophin, Carrier hearts are significantly susceptible to acute cardiomyocyte injury induced by one or repeated high doses of isoproterenol. Importantly, Carrier survival after cardiac injury depended on their parental genotypes, as only Carrier mice derived from dystrophic mothers showed mortality. These findings indicate that dystrophin expression in just over half of the heart may still leave the heart with marked vulnerability to injury. Additionally, the differential survival observed in mice expressing the same dystrophin levels underscores a need for better understanding of the impact of other factors, including epigenetic, developmental, and environmental influences, on this vulnerability in the dystrophic heart.

1. Introduction

Duchenne muscular dystrophy (DMD) is a progressive muscle wasting disease that involves the heart, resulting in clinically significant cardiomyopathy [3,5,6,148,189]. The *DMD* gene locus on the X-chromosome encodes the protein dystrophin, which plays a critical role in healthy muscle cells by bolstering membrane integrity and serving as a signaling scaffold [52,190–193]. The loss of dystrophin leads to myocyte necrosis, fibrosis, skeletal muscle wasting, and cardiomyopathy, culminating in premature death from cardiorespiratory failure. Due to its X-linked origin, DMD occurs almost exclusively in males at a rate of roughly 1:5000, and in the majority of cases, it is passed down from a mother that carries one mutated copy of the gene [8,10,11]. Virtually all patients with DMD over 18 years of age display overt clinical signs of cardiomyopathy, including cardiac fibrosis, ventricular dilation, and reduced contractile function [3,24]. The devastating cardiac pathology caused by DMD has been recognized since its earliest descriptions, including an 1836 report by Conte and Gioja about two brothers who had progressive debilitating muscle weakness, and the oldest of whom evidently suffered from cardiomyopathy at the time of death [3,14]. The natural history of the disease often terminated with death from cardiorespiratory failure in the late teens or early 20's. With advancements in symptomatic respiratory therapies and pharmacological management, DMD patient lifespans have extended into the 30's or early 40's, magnifying the incidence of heart failure in this patient population [1,25].

In recent years, a variety of potential new therapies aiming to enable dystrophin expression in dystrophic muscle have emerged from preclinical work, with a few of them now entering the clinical arena. Some of these therapeutic strategies, like antisense oligonucleotide-mediated exon skipping and CRISPR-Cas9 gene editing, can restore the expression of the endogenous *DMD* gene [161,162,179,180,182]. Conversely, micro-dystrophin gene therapy aims to replace the endogenous gene with a highly truncated but functional substitute that has been scaled down to its essential components [29,170,171]. These potential therapies hold great promise, and they have all been shown to induce dystrophin expression in both the skeletal muscle and the heart in preclinical studies. However, successful cardiomyocyte transduction continues to be a major obstacle to their cardiac efficiency. In preclinical work, these approaches have often displayed a mosaic pattern of transduction in the heart, with clusters of

cardiomyocytes that still lack dystrophin adjacent to those that now express it [161,164,180,183,257].

This mosaic dystrophin expression pattern is reminiscent of that seen in DMD carrier hearts, who harbor one intact copy of the *DMD* gene and one disease-causing copy that carries a mutation resulting in the loss of dystrophin. Because of the requirement for two X-chromosomes for carrier status, DMD carriers are genetically female. Due to X-inactivation around the mid-gestational point in embryonic development, female cell nuclei have near-exclusive gene expression from a single X-chromosome [258]. This genetic composition results in a nearly uniform distribution of dystrophin-positive myofibers in skeletal muscle, since each fiber is comprised of many independent nuclei that contribute to the overall expression profile of the cell. In contrast, each cardiomyocyte develops with a single nucleus, and any nuclear division that occurs after X-inactivation maintains the X-inactivation status of the original nucleus [259]. For this reason, the expression profile of any given cardiomyocyte generally depends on only one X-chromosome, giving rise to the mosaic pattern of positive and negative dystrophin expression in DMD carrier hearts.

In animal models, DMD carrier hearts have been shown to have roughly 50% dystrophin-positive cardiomyocytes [32]. With gene therapy on a DMD background, the relative proportions of dystrophin-positive and dystrophin-negative myocytes vary widely in the heart, often on the basis of drug or virus dose or any modifications to the delivery aimed at enhancing cardiac uptake [161,162,164]. As these developing therapies move into clinical trials and become available to DMD patients, it becomes increasingly important to determine how much dystrophin expression is sufficient to rescue the heart in order to establish dosing. DMD carrier hearts represent a useful preclinical model to evaluate whether approximately 50% dystrophin-positive myocardium will be sufficient to reduce susceptibility to injury in treated dystrophic hearts.

Observations in patients with DMD suggest that episodes of elevated cardiac stress and injury may underlie the progressive nature of DMD cardiomyopathy, indicated by transient periods of angina and elevated serum cardiac troponins in the contexts of surgery or other cardiac stress. We have previously shown that the β-adrenergic receptor agonist isoproterenol (Iso) may represent an appropriate model of episodic cardiac injury in dystrophic mice, based on elevations in serum cardiac troponins and lesion localization in the *mdx* mouse heart injured by a high dose of Iso [31]. Previous

work by Yue et al. had used low doses of Iso to investigate the impact of transient cardiac stress in mouse DMD carrier hearts [32]. This study showed extensive protection from cardiac stress-induced injury in DMD carrier hearts compared to dystrophin-null *mdx* female hearts after a brief 12-hour course of three low-dose Iso injections. However, we had been unable to induce a similar degree of cardiac damage to that reported by Yue et al. using the low-dose Iso protocol, and found contrasting results after inducing injury with high-dose Iso. Additionally, we set out to determine if the degree of susceptibility to injury in the DMD carrier hearts would remain relatively similar in the context of a multiple-day repeated cardiac stressor. Here we present the findings that DMD carrier hearts with ~57% dystrophin-positive myocardium display significant vulnerability to Iso-induced myocardial injury and mortality, and that the parental origin of the mutated *DMD* gene determines the degree of protection afforded by partial dystrophin expression.

2. Methods

2.1. Animals

The wild type control strain *C57BL/10SnJ* (C10), the dystrophic strain *C57BL/10ScSn-Dmd^{mdx}/J* (*mdx*), and the heterozygous offspring of their crosses (Carrier) were bred and maintained at the University of Minnesota. To limit genetic drift within this colony, breed stock were purchased from Jackson Laboratories every 5-6 generations. All mice were 4-6 months of age at the time of experiments and were housed in static cages with a 12-hour light-dark cycle. Since only female animals can be heterozygous with respect to X-chromosome genes like *DMD*, all mice used in this study were female. All animal procedures were approved by the University of Minnesota Institutional Animal Care and Use Committee and performed in compliance with all relevant laws and regulations. To enable the detection of epigenetic effects on experimental outcomes, two groups of DMD Carrier mice were generated with either maternal (Carrier^{M}) or paternal (Carrier^{P}) inheritance of the disease-causing *DMD* allele. Carrier^{M} mice were born to *mdx* dams and C10 sires, and Carrier^{P} mice were born to C10 dams and *mdx* sires.

2.2. Low-dose isoproterenol challenge

(-)-Isoproterenol hydrochloride (Iso; Sigma #I6504) was dissolved in saline to a concentration of 0.2 mg/ml and sterile filtered into a foil-wrapped glass vial prior to

injection. The sterile Iso solution was stored at 4˚C for no more than 3 days, and any solution developing discoloration, indicative of degradation, was discarded. Mice received 3 IP bolus injections of 0.35 mg/kg Iso each in volumes of 40-60 µl adjusted for body weight, with 6 hours between the first two injections and 3 hours between the second and the third injection, as previously described by Yue et al. [32]. Mice were sacrificed and hearts were harvested 30 hours after the first Iso injection.

2.3. High-dose isoproterenol challenge

Iso was dissolved in sterile saline to a concentration of 6 mg/ml, and otherwise handled as described in section 2.2. Mice received a single IP bolus injection of 10 mg/kg Iso in volumes of 40-60 µl adjusted for body weight, as previously described [31]. Hearts were harvested 30 hours after the Iso injection.

2.4. Repeated high-dose isoproterenol challenge

Iso was prepared and handled as described in section 2.2. Mice received up to 14 injections of 10 mg/kg isoproterenol over the course of 5 days, delivered as 3 daily IP injections at 8am, 12pm, and 4pm. Hearts from mice that succumbed to the challenge were harvested at the time of discovery, and all survivors were sacrificed at 2pm on the 5th day. Mice that displayed marked and progressive lethargy or morbidity indicative of a decline toward death were euthanized in compliance with the animal use protocol.

2.5. Histopathology

At the time of harvest, hearts were cut in half along the short axis, and the apical halves were embedded in OCT blocks for histology. Heart section slides were prepared as previously described [31], and all tissues were unfixed at the time of staining. The following antibodies and reagents were used for immunofluorescence staining: goat serum for blocking (Jackson ImmunoResearch # 005-000-121, 10%), rabbit dystrophin monoclonal antibody (Abcam #ab218198, 1:300), goat anti-rabbit IgG (H+L) highly cross-adsorbed Alexa Fluor Plus 647 secondary antibody (Invitrogen #A32733, 1:200), Alexa Fluor 555 goat anti-mouse IgG secondary antibody with minimal cross-reactivity (Biolegend # 405324, 1:150), WGA Alexa Fluor 488 conjugate (ThermoFisher # W11261, 5µg/ml), and ProLong Gold antifade mountant with DAPI (ThermoFisher # P36934). The blocking, primary antibody, and secondary antibody incubation steps were

all carried out at room temperature for 1 hour, separated by three 5-minute washes in fresh PBS.

The following reagents were used for Sirius Red Fast Green (SRFG) staining: 1.2% picric acid solution (Ricca #R5860000), Direct Red 80 (Sigma #365548), Fast Green FCF (Sigma #F7252), Formula 83 clearing solvent (CBG Biotech F83), and organic mounting medium (CBG Biotech MM83). Slides were first fixed for 3 hours in snap chilled acetone at -20˚C before staining, then rehydrated in 70% ethanol followed by two changes of tap water. The tissue was then stained for 25 minutes in SRFG dye solution of picric acid, 0.1% Direct Red 80, and 0.1% Fast Green FCF. Staining was followed by 3 washes in tap water, then dehydration in 70% ethanol, 100% ethanol, and Formula 83 before coverslipping.

All imaging was performed using NIS Elements software on a Nikon Eclipse Ni-E upright epifluorescent microscope with a motorized stage. For dystrophin and IgG lesion analysis, whole heart montages were collected as a stack of four fluorescent channels at a resolution of 0.92 μm/pixel. For evaluation of fibrosis, SRFG-stained sections were imaged as brightfield montages at a resolution of 0.85 μm/pixel.

2.6. Histological analysis

Dystrophin was quantified histologically on whole heart montages in Fiji using the threshold function [219]. An Alexa Fluor Plus 647 secondary antibody was chosen for dystrophin staining due to strong fluorophore signal and low background signal in the heart in that wavelength range, providing for an excellent signal-to-noise ratio and facilitating this thresholding approach. (Note: the coloration used in the figures represents the choice of optimal colors for depiction rather than the original wavelengths used for imaging). Dystrophin$^+$ pixel area was divided by total heart section area as measured using the WGA signal. In wild type hearts, this method produced values with a range of 45.4-49.2% with a mean and standard error of 46.9$\pm$0.3%, reflecting strong consistency. All dystrophin measurements from individual hearts were then normalized to this wild type dystrophin mean value to determine the relative percentage of dystrophin expression in each heart compared to wild type hearts. The small number of revertant dystrophin$^+$ myocytes present in all *mdx* hearts enabled the selection of an appropriate threshold for representing positive dystrophin signal in overwhelmingly dystrophin$^-$ images.

IgG^+ injury area was determined using whole heart montages in Fiji by subtracting the WGA channel (staining extracellular matrix) from the IgG channel to better distinguish intra-myocyte IgG signal. The resulting IgG image was then thresholded to measure total lesion area, and normalized to total heart section area. Only hearts from mice that survived until the 30-hour sacrifice timepoint were analyzed for IgG^+ injury area, due to the technical difficulty of quantifying the poorly-defined early injury present in hearts that succumb earlier in the time course.

Fibrosis was analyzed in whole heart montages of SRFG-stained sections using the color threshold function in Fiji. Areas containing Sirius Red-stained collagen were quantified by measuring the pixel area corresponding to a red hue above a minimum saturation threshold. Total heart section area was represented by the full range of hues above the same minimum saturation threshold, and fibrosis was calculated as the Sirius Red area normalized to total heart area. Only hearts from mice that survived the repeated Iso challenge were used for fibrosis quantification following the challenge. Hearts that succumbed earlier in the challenge displayed a complex mix of degenerating myocytes with acute IgG^+ injury and the fibrosis that was in the process of replacing them, and were thus difficult to quantify for total damaged area.

2.7. Statistics

All statistical analyses were performed using Prism 7 (GraphPad Software). Dystrophin and injury levels were compared across groups using one-way ANOVA with Holm-Sidak post-hoc test. Survival after a single high-dose Iso injection was compared using the Chi-square test, and survival over time in the repeated Iso challenge was compared using a log-rank test with the Bonferroni correction to adjust for multiple comparisons.

3. Results

3.1. DMD Carrier heart dystrophin expression does not depend on parental origin of the disease allele.

Two breeding strategies were used to generate DMD Carrier mice, producing maternal ($Carrier^M$) and paternal ($Carrier^P$) female DMD Carriers from *mdx* dams and *mdx* sires, respectively (Fig. 4.1A). Both strategies resulted in the same degree of dystrophin expression in the Carrier hearts, as measured by histological quantification.

Both groups displayed dystrophin^{+} signal in approximately 57% of the area corresponding to full dystrophin expression seen in wild type (WT) hearts, regardless of maternal or paternal origin of the disease-causing allele (56.8±3.7% in Carrier^{P} and 57.6±3.4% in Carrier^{M}; Fig. 4.1B). The pattern of dystrophin expression was confirmed to be mosaic, with large adjacent regions of dystrophin^{+} and dystrophin^{-} cardiomyocytes (Fig. 4.1D), in agreement with previously published work [32]. The range of quantified dystrophin levels in Carrier hearts represents real biological variability, rather than any artifact of histological processing, with the lowest-expressing heart having 40.0% dystrophin and the highest-expressing heart having 78.4% dystrophin relative to WT hearts (Fig. 4.1E). The levels of dystrophin expression was not litter-dependent, as mice expressing high levels of dystrophin and others expressing lower levels were found in the same litter.

The presence or absence of dystrophin expression did not affect heart weights at baseline, as no significant differences were detected in heart weights between WT, *mdx*, and Carrier female mice, although Carrier hearts trended toward being slightly smaller (123.3±1.2 mg vs. 123.3±2.0 mg vs. 118.1±1.8 mg, respectively; p=0.07). The absence of a significant difference was confirmed by normalizing heart weight in mg to tibial length in mm to account for body size (Fig. 4.1C; p=0.21).

3.2. DMD Carrier hearts display intermediate susceptibility to Iso-induced injury that partially depends on parental origin.

Previously, Yue et al. showed that 3 sequential IP injections of the β-adrenergic receptor agonist isoproterenol (Iso), each at a low dose of 0.35 mg/kg and staggered over a 12-hour period before sacrifice, induced injury in approximately 11% of the *mdx* heart area, but only 2% of the Carrier heart area and negligible injury in wild type hearts [32]. Our attempt to replicate this result with the same Iso dosing protocol instead yielded significantly lower myocardial damage in *mdx* and Carrier mice. Three sequential Iso injections at a dose of 0.35 mg/kg each induced injury in less than 1% of the hearts in each group, with the *mdx* injury approximately 2-fold greater than injury in both wild type and Carrier hearts (Fig. 4.2A). The injured IgG^{+} myocytes in Carrier hearts were largely devoid of dystrophin (Fig. 4.2 B and D), but this was also true in wild type hearts, suggesting that cardiomyocyte injury likely precipitates the dystrophin loss as a consequence of proteolysis [31].

In an effort to recapitulate the higher level of injury in *mdx* hearts presented by Yue et al., a protocol based on a single bolus IP injection of high-dose (10 mg/kg) Iso was used to induce cardiac injury [31]. This dose revealed 10-fold higher injury in *mdx* hearts compared to WT hearts, and an intermediate susceptibility to injury in DMD Carrier hearts (Fig. 4.2C). Surprisingly, 21% (4 of 19) of DMD Carrier mice born to *mdx* dams and WT sires ($Carrier^{M}$) displayed spontaneous mortality after the single Iso injection, while Carriers derived from *mdx* sires and WT dams ($Carrier^{P}$) all survived until sacrifice, and only 1 of 24 *mdx* females died (Fig. 4.2C).

Surviving Carrier mice displayed damaged myocardial area that was significantly higher than in WT hearts and significantly lower than in *mdx* hearts, indicating intermediate susceptibility to a single bout of injury (Fig. 4.2C). As before, the majority of injured IgG^{+} cardiomyocytes lacked dystrophin, although the rare injured myocyte could be found with some dystrophin expression (Fig. 4.2D).

3.3. DMD Carriers are highly susceptible to repeated bouts of high-dose Iso, but display divergent survival.

To determine if hearts with 50% dystrophin expression would continue to show partial protection in the face of repeated bouts of adrenergic stress with high-dose Iso, WT, Carrier, and *mdx* mice received 14 doses of 10mg/kg Iso over a span of 5 days before sacrifice (Fig. 4.3A). As in the case of a single bolus Iso injection, parental origin of the null *DMD* allele had a significant influence on survival. Among $Carrier^{M}$ mice, 31% succumbed to the repeated Iso challenge, reflecting nearly identical mortality as *mdx* mice (38%). However, all $Carrier^{P}$ mice and WT mice survived the challenge (Fig. 4.3B).

Survivors of the challenge were analyzed for cardiac fibrosis area to reflect the amount of myocardium lost during the challenge. Carrier mice were found to have equally high levels of cardiac damage as *mdx* mice, regardless of maternal or paternal origin of the disease-causing allele (Fig. 4.3C). Carrier hearts showed similar distribution of replacement fibrosis as dystrophic hearts, with large lesions scattered randomly throughout the myocardium, including subepicardial regions, in contrast to the endocardial localization of WT heart lesions (Fig. 4.3D).

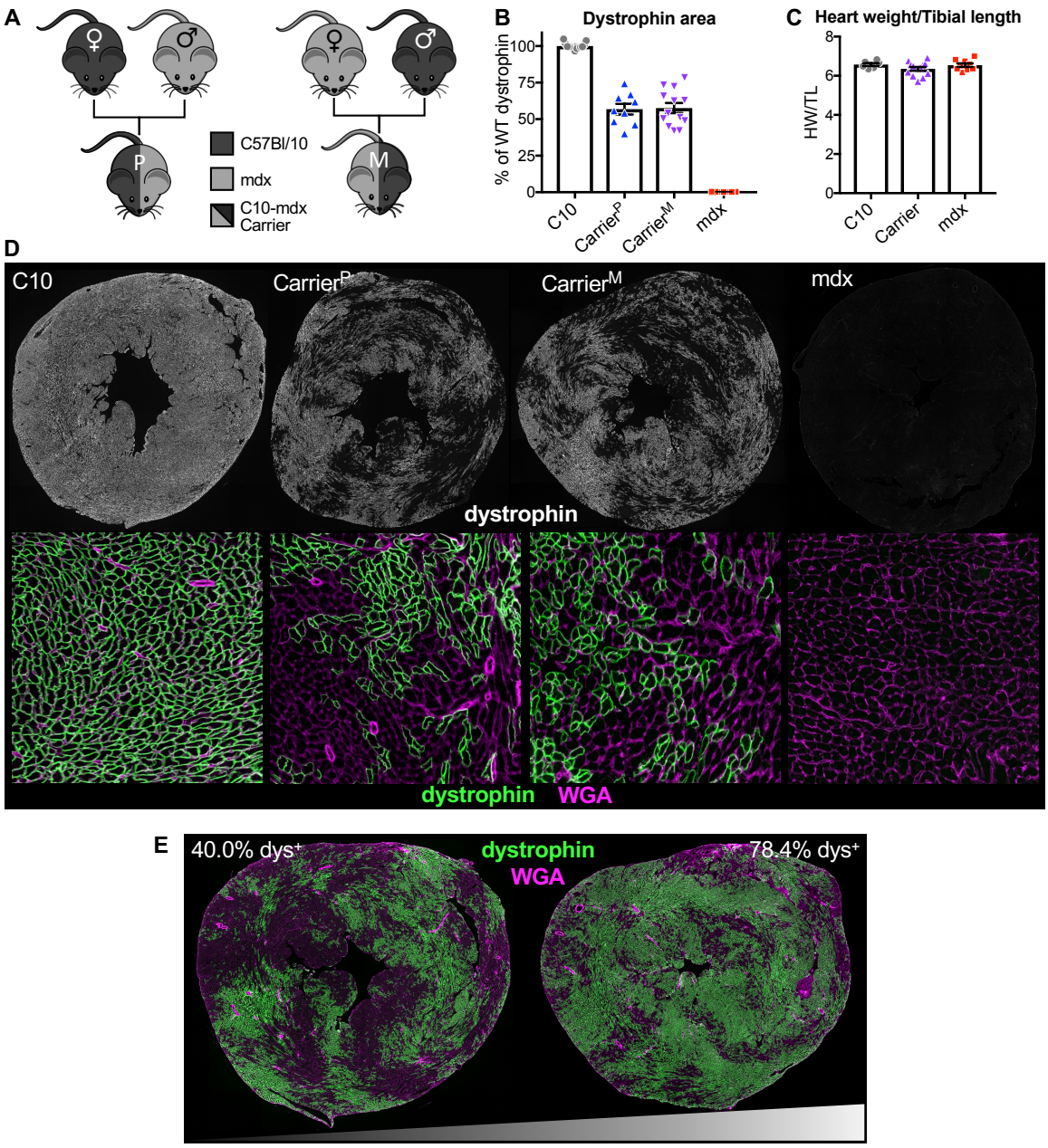

Figure 4.1: DMD Carrier hearts display mosaic dystrophin expression throughout the myocardium.

(A) Heterozygous DMD Carrier mice were generated from two different crosses. Paternal Carrier (Carrier^{P}) mice were bred from *mdx* fathers and wild type (C57Bl/10) mothers, maternal Carrier (Carrier^{M}) mice were derived from *mdx* mothers and wild type fathers. **(B)** Histological quantification of dystrophin^{+} signal in Carrier hearts normalized to dystrophin^{+} signal in wild type (C10) hearts. Both types of Carriers express dystrophin

in ~57% of the heart area (n=7-13 per group). **(C)** Heart weights were not different between C10, Carrier, and *mdx* mice at baseline when normalized to tibial length to control for body size (n=6-14 per group; p=0.21). **(D)** Representative images of dystrophin distribution in C10, Carrier, and *mdx* hearts. Magnified images show the mosaic distribution of dystrophin^{+} and dystrophin^{-} myocytes in Carrier hearts. Magnified image scale = 0.5×0.5 mm. **(E)** Representative images of biological variability in dystrophin expression in carrier hearts, ranging from 40.0-78.4%.

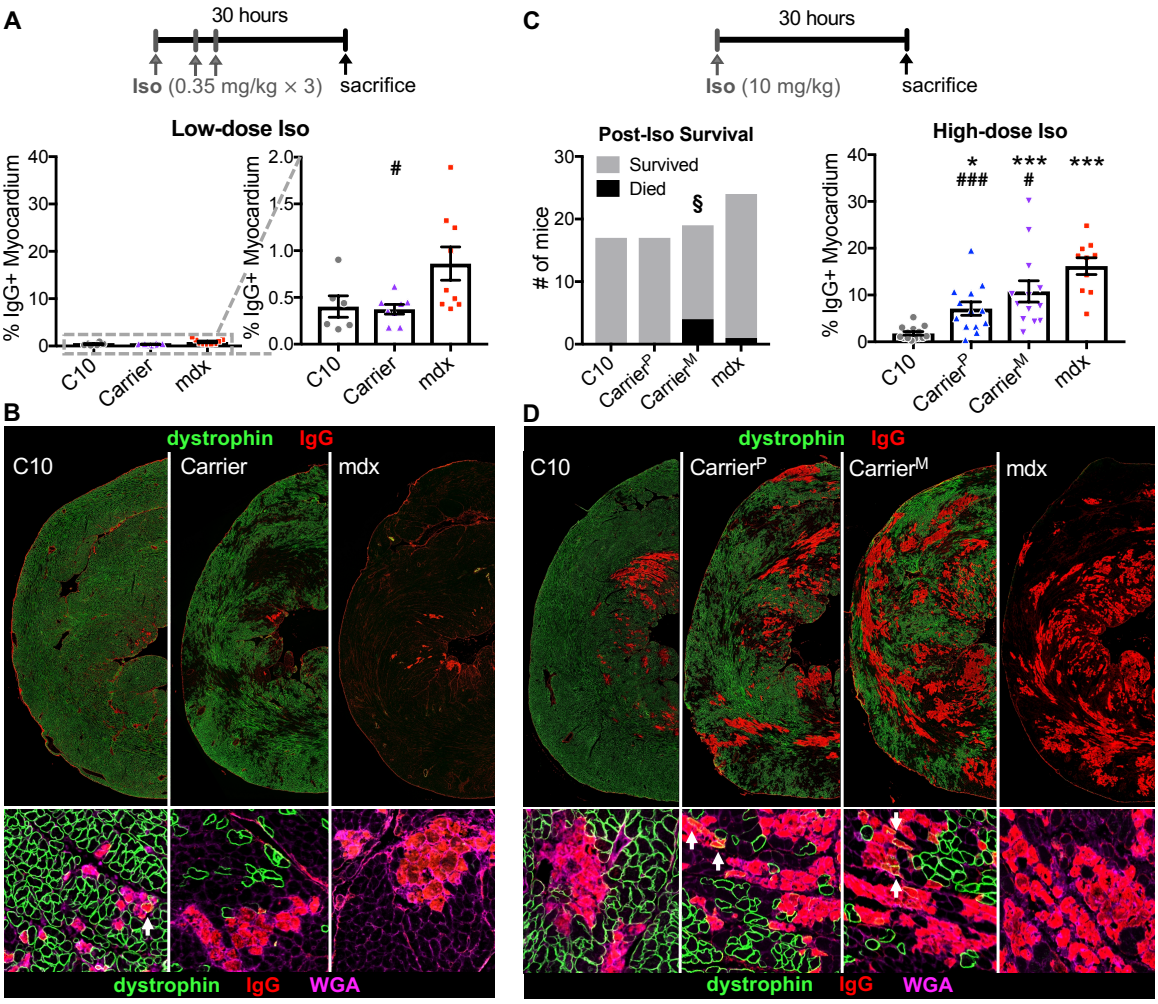

Figure 4.2: DMD Carrier susceptibility to cardiac injury is significant and partially dependent on allelic parental origin.

(A) Three injections of low-dose Iso (0.35 mg/kg each) induced slight injury in C10, Carrier, and *mdx* hearts 30 hours after the first Iso injection, with 2-fold higher injury area in *mdx* hearts (n = 6-9 per group; # p=0.04 vs. *mdx*). **(B)** Representative images of hearts 30 hours after starting a course of 3 low-dose Iso injections, showing slight IgG^+ (red) cardiomyocyte injury. Most injured cardiomyocytes are lacking dystrophin (green), including in wild type hearts; white arrows indicate injured myocytes displaying dystrophin signal. **(C)** A single injection of high-dose Iso (10 mg/kg) caused widespread lesions in Carrier and *mdx* hearts, and mortality in 21% of $Carrier^M$ mice (n=17-24 per group; § p=0.027). Among survivors, both groups of Carriers displayed significantly higher injury than C10 hearts, and $Carrier^P$ hearts displayed significantly lower injury than *mdx* (n=10-14 per group; * p=0.04 vs. C10; *** p<0.001 vs. C10; # p=0.04 vs. *mdx*;

p<0.001 vs *mdx*). **(D)** Representative images of dystrophin distribution in wild type, Carrier, and *mdx* hearts. Magnified images demonstrate the mosaic distribution of dystrophin^{+} and dystrophin^{-} cardiomyocytes in Carrier hearts. Magnified image scale = 0.3×0.3 mm.

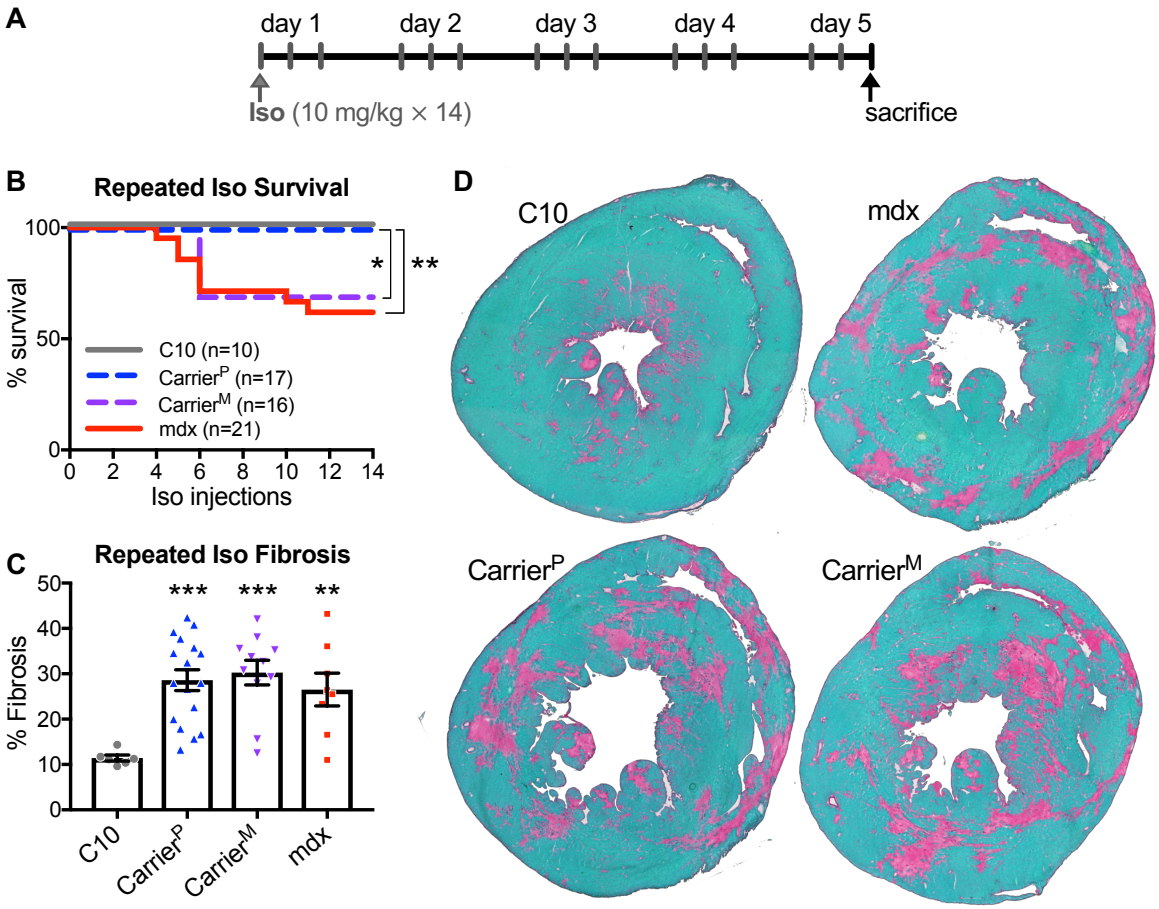

Figure 4.3: DMD Carriers are highly susceptibility to cardiac injury with repeated bouts of injurious stimulation.

(A) The repeated Iso challenge is comprised of 14 injections of high-dose (10 mg/kg) Iso over the span of 5 days. **(B)** All of the C10 and Carrier^{P} mice survived the repeated Iso challenge, but 31% of Carrier^{M} and 38% of *mdx* mice died during the challenge (* p=0.01; ** p=0.005). **(C)** Among survivors, repeated high-dose Iso caused similarly extensive replacement fibrosis in the hearts of Carrier and *mdx* mice, which was significantly higher than C10 injury (n=6-17 per group; ** p=0.01; *** p<0.001). **(D)** Representative images of fibrosis in wild type (C10), Carrier, and *mdx* hearts after repeated injury with high-dose Iso. Fibrosis is red, and intact myocardium is green.

4. Discussion

DMD has been described in the literature for nearly 200 years as a devastating, progressive disease that wastes away skeletal muscle and causes heart disease. In the intervening decades, clinical advances that include symptomatic respiratory therapies and scoliosis correction have markedly extended lifespans, but only modest strides have been made in treating DMD cardiomyopathy [1,25]. A new wave of emerging gene-targeted therapies holds the promise of potentially correcting the underlying defect in DMD by restoring dystrophin expression, but the efficacy of these approaches in treating the heart remains unknown. A major obstacle to maximizing the cardiac benefits of these corrective strategies lies in differences in tissue transduction between the heart and skeletal muscle that can result in hindered cardiac efficiency. In preclinical studies of antisense-mediated exon skipping, CRISPR-Cas9 gene editing, and micro-dystrophin gene delivery have resulted in incomplete cardiac dystrophin restoration, leaving a mosaic pattern of dystrophin-positive and dystrophin-negative myocardium [161,162,164]. A similar distribution of dystrophin is seen in the hearts of DMD carriers who have one normal allele and one null allele of the X-chromosomal *DMD* gene, due to random X-inactivation throughout the myocardium.

In the present study, we have used the mouse model of DMD carriers to determine whether dystrophin expression in approximately half of the heart can protect the remaining myocardium in the context of single or repeated bouts of workload-induced cardiac stress. We reported that Carrier mice display intermediate susceptibility to a single bout of high-dose Iso-induced injury relative to wild type and dystrophin-null hearts, but they sustain the same degree of injury as dystrophic hearts with repeated injurious Iso stimulation. Importantly, the comparison between Carriers derived from two different breeding schemes revealed the surprising finding that mortality following Iso varies in relation to the parent from whom the dystrophin-null allele is inherited. Specifically, although all Carriers derived from *mdx* fathers and wild type mothers survived the Iso-induced stress, Carrier mice from *mdx* mothers and wild type fathers showed 21% mortality after a single dose and 31% mortality after repeated doses of Iso, despite similar dystrophin expression.

Many of the findings presented here do not align with those reported by Yue et al. in 2004, including the susceptibility to injury observed in carrier mouse hearts and the divergent phenotypes of carriers from the two different breeding strategies [32]. Many of

these differences may be related to the isoproterenol dose, which is the largest deviation in experimental details between previous and current work. In our hands, the low dose of Iso (0.35 mg/kg) previously used in the 2004 study was inadequate to cause more than 1-2% injury in *mdx* hearts, thus we turned to the high dose of Iso (10 mg/kg) that our previous work is based on to recapitulate widespread injury in dystrophic hearts. It is unclear what factors underlie the large differences in susceptibility observed in the two studies. While the mice in the present study were 1-3 months older, this is unlikely to account for their increased resilience. Another possible explanation may lie in the use of Evans Blue dye by Yue et al. in contrast to IgG staining used in the current study. Although both measures reflect cardiomyocyte permeability to serum proteins, Evans Blue dye was injected 12 hours ahead in the earlier work, and may have exerted mild cytotoxic effects that were subsequently amplified by Iso-induced stress. A multitude of other unknown factors could also contribute to the overall effect of Iso in conscious animals, including injection timing relative to light/dark cycles, single or group housing, handling during the study, and other environmental influences.

The critical implication of these results for DMD therapies is that the degree of protection from mortality in partially dystrophin-expressing hearts likely depends on additional factors besides dystrophin levels. Although average dystrophin levels were nearly identical in the hearts of both groups of this Carrier mouse model, their response to high cardiac workload appears to be altered through a mechanism that significantly affects their vulnerability and survival. This mechanism is beyond the scope of this work, but it may be related to epigenetic differences causing divergent expression of genes involved in cardiac resilience, or it may stem from different *in utero* environments belonging to healthy and dystrophic mothers. The differences in vulnerability may also involve a more complex behavioral basis, like differential interactions between healthy and dystrophic mothers with their heterozygous offspring, leading to differences in psychosocial stresses. This suggests that in human patients, a variety of factors could influence the degree of therapeutic correction that is sufficient to prevent lethal heart failure, potentially including polymorphisms in other genes, maternal and paternal epigenetic imprinting, and even environmental or dietary factors.

Phenotypic diversity stemming from complex factors besides dystrophin is readily evident in human DMD patients and DMD carriers. Marked phenotypic variability with respect to the degree of cardiac and respiratory disease severity has been documented

in multiple sets of brothers diagnosed with the same DMD-causing mutation, without clear evidence of what may cause the divergence [260]. Furthermore, the cardiac and respiratory phenotypes in any given patient may progress independently of each other, and with trajectories that are not predictable based on the disease-causing mutation, in a phenomenon referred to as phenotypic discordance [261]. Likewise, human carriers of DMD have been documented to have variable skeletal muscle and cardiac phenotypes that were not overtly linked to their underlying mutation [262,263]. In fact, the reported incidence of cardiomyopathic symptoms in DMD carriers ranges from <10% to nearly 50%, reflecting the high variability of the carrier cardiac phenotype [20,262]. Regardless of the variability in symptomology, current guidelines recommend routine monitoring of carrier cardiac function, reflecting the understanding that DMD carriers are at high risk for developing cardiomyopathy [6,20,264]. Together with the preclinical findings presented here, these observations in human patients underscore the notion that the therapeutic efficacy of partial dystrophin restoration in the heart is difficult to predict.

Current evidence points to the strong possibility that the restoration of dystrophin in roughly half of in the heart may be sufficient to steer the course of the disease away from heart failure in some patients, but not in others. Further preclinical and clinical research will need to be directed at determining the factors that contribute the overall outcomes in partially dystrophin-replete hearts. Additionally, the hearts of human patients undergoing gene-targeted therapies should continue to be carefully monitored using the latest available guidelines to evaluate the potential need for additional therapeutic interventions with pharmacological therapies like angiotensin receptor blockers or ACE inhibitors.

CHAPTER 5

LOSARTAN PROTECTS MALE HEARTS AND ELIMINATES SEX DIFFERENCES IN CARDIAC INJURY IN SARCOGLYCAN-NULL MOUSE MODEL

Tatyana A. Meyers[1], Jackie A. Heitzman[1], Dewayne Townsend[1,2,3]

[1] Department of Integrative Biology and Physiology, University of Minnesota Medical School, Minneapolis, MN, USA

[2] Paul and Sheila Wellstone Muscular Dystrophy Center, University of Minnesota Medical School, Minneapolis, MN, USA

[3] Lillehei Heart Institute, University of Minnesota Medical School, Minneapolis, MN, USA

J.A.H. provided essential support with animal handling, drug delivery, tissue harvesting, colony management, and protocol adherence.

D.T. designed and performed the in vivo hemodynamic studies (Figure 2).

Summary

Muscular dystrophies are a genetically diverse group of muscle wasting diseases. Sarcoglycanopathies belong to the category of autosomal recessive Limb-girdle muscular dystrophies (LGMD), with many clinical cases featuring early onset, progressive degeneration of skeletal muscles, and significant cardiomyopathy. The sarcoglycan complex is a heterotetrameric member of the dystrophin glycoprotein complex, which is critical in maintaining myocyte membrane integrity. The loss of the sarcoglycans induces high membrane permeability, leading to myocyte death, fibrosis, and cardiomyopathy. Individual mutations in four different sarcoglycan genes have been documented to give rise to LGMD with a Duchenne-like disease course and severity. Among the sarcoglycanopathies, the absence of β-sarcoglycan is associated with particularly early onset and high rates of cardiac involvement.

The β-sarcoglycan-null mouse ($\beta sg^{-/-}$), a model of LGMD2E, displays a progressive cardiac phenotype that can be exacerbated by stressing the heart. The β-adrenergic receptor agonist isoproterenol (Iso, 10 mg/kg) was used to induce cardiac stress and injury in $\beta sg^{-/-}$ mice. A single dose of Iso caused early cardiac injury and fibrosis in 10-24% of the heart area in $\beta sg^{-/-}$ mice. Surprisingly, male $\beta sg^{-/-}$ hearts displayed 2.1-fold higher cardiomyocyte injury and 2.2-fold higher fibrosis compared to female hearts. Chronic and acute treatments with the angiotensin receptor blocker losartan markedly reduced cardiac damage and hypertrophy in male $\beta sg^{-/-}$ hearts, but had no significant effect in female hearts. Due to the sex-dependence of this protective effect, losartan treatment of $\beta sg^{-/-}$ mice resulted in the elimination of sex differences in Iso-induced cardiac injury.

Here we report a striking sex difference in susceptibility to cardiac injury in mice lacking the sarcoglycan complex, and demonstrate that angiotensin receptor blockade reduces cardiac damage in male hearts, abolishing the sex difference. These findings suggest that angiotensin receptor signaling contributes to exacerbation of cardiac injury in these dystrophic hearts in a sex-dependent manner.

1. Introduction

Muscular dystrophies are a genetically heterogeneous group of progressive muscle wasting diseases with variable cardiac involvement. Limb-girdle muscular dystrophy (LGMD) is a large and diverse category of muscular dystrophies, with LGMD type 2 representing the subgroup with an autosomal recessive mode of inheritance. Several of the diseases from this group feature clinically significant cardiomyopathy [265]. Among these, the sarcoglycanopathies are particularly remarkable for presenting with a degree of muscle deterioration and heart disease similar in severity to Duchenne muscular dystrophy (DMD) [266,267].

The four primary sarcoglycanopathies are LGMD2C, 2D, 2E, and 2F, all arising from mutations resulting in the absence of one or more proteins that constitute the heterotetrameric sarcoglycan complex [268]. The sarcoglycans are important members of the larger dystrophin-glycoprotein complex (DGC), which plays a critical role in maintaining sarcolemmal integrity by serving as the node between the intracellular stabilizing protein dystrophin and the extracellular anchoring protein laminin [193,269]. Although the transmembrane sarcoglycan complex does not interact directly with either dystrophin or laminin, the loss of this complex can have grave consequences for the skeletal muscle and heart tissue. The loss of α-sarcoglycan may leave the rest of the sarcoglycan complex intact, explaining the observation that the associated pathology is often milder [269,270]. However, the absence of β-, δ-, or γ-sarcoglycan can deplete the whole sarcoglycan complex, precipitating childhood onset of pathological effects that may include muscle weakness, myocyte necrosis, fibrosis, loss of ambulation, heart failure, and premature death from cardiorespiratory insufficiency [266,271,272]. The loss of β-sarcoglycan appears to be the most devastating, as indicated by the age of onset, severity of the disease, and proportion of cardiac involvement [265,270,271]. Because some patients completely lack one or more of the sarcoglycans but others retain partial expression of the mutated protein, the phenotypic range of sarcoglycanopathies is large, perhaps analogous to that of Duchenne and Becker muscular dystrophies combined [271,272]. Sarcoglycanopathies have been estimated to have a prevalence of roughly 1 in 180,000, and account for up to 68% of patients with the more aggressive childhood-onset autosomal recessive LGMD, but only ~10% of the milder adult-onset cases [270,273].

The β-sarcoglycan-null mouse ($\beta sg^{-/-}$) is a preclinical model of LGMD2E that displays progressive muscle degeneration and cardiac fibrosis [274–276]. Earlier work characterizing this mouse model demonstrated total loss of the sarcoglycan complex and the associated protein sarcospan with retention of other DGC components, in parallel with similar observations in human patient biopsies [275,277,278]. The cardiac phenotype of the $\beta sg^{-/-}$ mouse can be accelerated by increasing stress on the heart to induce acute myocardial injury and its conversion to fibrosis. The β-adrenergic receptor agonist isoproterenol (Iso) has been successfully used for this purpose by our group and several others, triggering increases in cardiac contractility and heart rate that produce scattered clusters of injured cardiomyocytes [31,32,77]. These areas of myocardial injury, detectable acutely by imaging cardiomyocyte uptake of endogenous serum proteins (IgG or Evans blue dye-bound albumin), are subsequently replaced within a few days by fibrotic lesions [31]. In earlier work, we have shown that the hearts of *mdx* mice, a popular model of DMD, are significantly susceptible to acute Iso-induced injury, but this susceptibility is markedly reduced by treatment with the angiotensin II type 1 receptor (AT_1R) blocker losartan [31]. Because the phenotypes of DMD and LGMD2E display many similarities in both human patients and mouse models, we set out to determine whether this therapeutic effect may be recapitulated in the absence of β-sarcoglycan.

In the present study, we aimed to assess the susceptibility of $\beta sg^{-/-}$ hearts to acute Iso-induced injury, evaluate the conversion of these myocardial wounds to the fibrotic scar, and determine whether global blockade of AT_1R may ameliorate these processes. Here we report a sex-dependent beneficial effect of losartan on acute injury and fibrosis reduction in male $\beta sg^{-/-}$ mouse hearts but not female hearts, underscoring the surprising discovery that cardiac vulnerability and the benefits of AT_1R blockade diverge by sex in this mouse model.

2. Methods

2.1. Animals

β-sarcoglycan-null ($\beta sg^{-/-}$) mice were bred at the University of Minnesota from breeding pairs obtained from the Jackson Laboratory. Mice were 4-6 months of age during all isoproterenol studies. Because LGMD2E is an autosomal disease, both male and female mice were used for these studies. All animal procedures were approved by

the University of Minnesota Institutional Animal Care and Use Committee and performed in compliance with all relevant laws and regulations.

2.2. VCD Study

The degree of ovarian hormone influence on cardiac injury was investigated by inducing chemical ovarian senescence in a group of female mice using vinylcyclohexene dioxide (VCD) [279–281]. The VCD was purchased from Synquest Laboratories (#2209-1-08) and prepared to a concentration of 64 ng/ml in sesame oil, as described elsewhere [280]. Starting at 1-2 months of age, the mice received daily injections of 160 mg/kg VCD or sesame oil vehicle, in volumes of 35-60 µl adjusted for body weight, for 15 days. Mice entered the studies and were sacrificed 40-70 days from the end of their VCD injection course. A significant reduction in uterine weights after VCD treatment compared to vehicle-treated littermates and untreated female mice confirmed that VCD had the intended effect of diminishing ovarian hormone production (75.4±4.3 mg control vs. 52.9±2.6 mg with VCD; $p<0.001$). All VCD-treated mice remained healthy throughout the study.

2.3. Isoproterenol Studies

(-)-Isoproterenol hydrochloride (Iso; Sigma #I6504) was prepared and delivered as previous described, as a single IP injection of 10 mg/kg per mouse [31]. Hearts were harvested at timepoints of 30 hours and 1 month after the injection.

2.4. Acute Losartan Studies

A group of $\beta sg^{-/-}$ mice was assigned to receive acute treatment with losartan starting 1 hour before the Iso injection, as previous described [31]. Briefly, a sterile losartan solution was prepared from a crushed generic losartan tablet dissolved in saline, and delivered as four intermittent IP injections totaling 160 mg/kg over the course of the 30-hour timeframe. The injections began 1 hour before Iso and ended 7 hours before the 30-hour heart harvest, without interrupting the dark cycle. Dosing was based on the half-lives of losartan and its major active metabolite (EXP3174), and intended to minimize the troughs in drug serum levels between the loading dose and the time of sacrifice with minimal disruptions to the mice.

2.5. Pretreatment Losartan Studies

To investigate further protective effects that may arise after pretreatment, an additional group of $\beta sg^{-/-}$ mice was assigned to drink losartan dissolved in water for 2 weeks prior to Iso-induced injury. Losartan water was prepared from a crushed generic tablet and given at a concentration of 600 mg/L in 2.5% dextrose, with an average consumed dose of 80 mg/kg daily. Losartan-containing water was replaced 3 times per week, and each mouse was weighed before and after the pretreatment.

The physical discomfort experienced by mice following Iso administration can interrupt their water intake for 1-2 days, so the mode of drug delivery was switched from the drinking water to IP injections for a period of 30 hours after Iso to maintain therapeutic drug levels. On the 15^{th} day after the start of pretreatment, mice received fresh tap water and a single a single 10mg/kg Iso injection. For the next 30 hours, the pretreated mice received booster injections of losartan as described in section 2.3 above and elsewhere previously [31]. A subset of $\beta sg^{-/-}$ mice was sacrificed for the heart harvest 30 hours after the Iso injection. The rest were placed back on the same losartan treatment in the drinking water for 1 month after the Iso injection, and then sacrificed for the heart harvest.

2.6. Histopathology

Only the hearts of mice that survived to their 30-hour and 1-month timepoints were used for quantification of injury area for each timepoint, as we have shown cardiac injury to undergo changes in appearance and total area during this time. The mortality rate in any given sex and treatment group was no greater than 10%, thus this is not expected to significantly skew the results.

Histopathology studies were carried out as previously described, using 7 μm slices of unfixed frozen hearts [31]. The following reagents were used for IF staining: goat serum for blocking (Jackson ImmunoResearch # 005-000-121, 10%), goat anti-mouse IgG (H+L) secondary antibody (Invitrogen #R37121, 1:200), WGA AlexaFluor conjugate (ThermoFisher, 5μg/ml), and ProLong Gold Antifade Mountant with DAPI (ThermoFisher). After blocking, staining was performed as a single step at room temperature for 1 hour, flanked by three 5-minute washes in PBS.

The following reagents were used for Sirius Red Fast Green (SRFG) staining: 1.2% picric acid solution (Ricca #R5860000), Direct Red 80 (Sigma #365548), Fast

Green FCF (Sigma #F7252), Formula 83 clearing solvent (CBG Biotech F83), and organic mounting medium (CBG Biotech MM83). Slides were fixed for 3 hours in chilled acetone at -20˚C before staining, then rehydrated in 70% ethanol followed by two changes of tap water. The rehydrated slides were stained for 25 minutes in rocking SRFG dye solution of picric acid, 0.1% Direct Red 80, and 0.1% Fast Green FCF. The slides were then rinsed in 3 changes of tap water, and dehydrated in 70% ethanol, 100% ethanol, and Formula 83 before applying organic mounting medium and coverslips.

2.7. Microscopy and Image Analysis

All imaging was performed in NIS Elements software on a Nikon Eclipse Ni-E upright epifluorescent microscope with a motorized stage. Whole heart montages of acute injury were collected as a stack of three fluorescent channels at a resolution of 0.92 µm/pixel.

IgG-positive injury area was determined using Fiji by subtracting the WGA channel (staining extracellular matrix) from the IgG channel to better distinguish intra-myocyte IgG signal [219]. This injury area was then quantified by thresholding the resulting IgG image for total lesion area, and normalizing it to total heart section area. SRFG-stained sections were collected as brightfield whole heart montages at a resolution of 0.85 µm/pixel. Fibrosis was analyzed in these images using the color threshold function in Fiji. Areas containing Sirius Red-stained collagen were measured by counting the pixel area corresponding to a red hue above a minimum saturation threshold. Total heart area was represented by the number of pixels with any hue above the minimum saturation threshold, and fibrosis was calculated as the Sirius Red area normalized to total heart area.

2.8. In Vivo Hemodynamic Assay

Left ventricular catheterization was performed as described previously [200,202,282]. Briefly, mice were induced and maintained at a surgical plane of anesthesia with isoflurane. Temperature was maintained at 37°C throughout the procedure. A bilateral thoracotomy was performed to expose the apex of the heart. The pericardium was removed, and a 1.4 Fr pressure-volume catheter was inserted into the left ventricle via an apical stab incision created using a 25g needle. An intravenous catheter was placed in the external jugular vein and 10% albumin-supplemented saline

was infused to a final volume of 5 µl/g body weight. This infusion was delivered during a 10-minute equilibration period. At the end of this equilibration period, baseline hemodynamics parameters were collected. Dobutamine was then infused (42µg/kg/min) to assess cardiac reserve. After 5 minutes of dobutamine infusion, hemodynamic parameters were collected again.

2.9. Statistics

All statistical analyses were performed using Prism 7 (GraphPad Software). Comparisons between $\beta sg^{-/-}$ males, $\beta sg^{-/-}$ females, and VCD-treated $\beta sg^{-/-}$ females were made using one-way ANOVA with Sidak post-hoc test. Hemodynamic parameters were compared using two-way ANOVA for repeated measures. All other comparisons were made using regular two-way ANOVA with Sidak post-hoc test. All graphs display the mean with standard error.

3. Results

3.1. The amount of Iso-induced injury in $\beta sg^{-/-}$ hearts depends on sex but not on ovarian hormones.

A single injection of isoproterenol (Iso) induced extensive and scattered injury in $\beta sg^{-/-}$ male and female hearts harvested 30 hours after the injection. Interestingly, the cardiac injury area was 2.1-fold greater in male than female $\beta sg^{-/-}$ hearts, and the depletion of ovarian hormones with VCD did not alter female susceptibility to Iso-induced cardiac injury (Fig. 5.1A).

Quantification of fibrosis in hearts harvested 1 month after Iso-induced injury revealed a similar 2.2-fold sex difference between male and female cardiac fibrosis. Again, the degree of Iso-induced fibrosis was nearly identical in all female $\beta sg^{-/-}$ mice, regardless of VCD treatment (Fig. 5.1B). Notably, some $\beta sg^{-/-}$ male hearts displayed ventricular dilation at the time of sacrifice 1 month after Iso (Fig. 5.1C), reflecting the dilated cardiomyopathy that has been documented in LGMD2E patients.

In vivo cardiac catheterization in male and female $\beta sg^{-/-}$ mice revealed that the sex differences in cardiac injury are not a reflection of different cardiac performance at baseline or under adrenergic stimulation. The short-lived β_1-adrenergic receptor agonist dobutamine, infused to evaluate the responsiveness of $\beta sg^{-/-}$ hearts to catecholamine stimulation, induced similar increases in heart rate, ejection fraction, and contractility in

βsg$^{-/-}$ hearts of both sexes, and neither sex showed a change in lusitropy with adrenergic stimulation (Fig. 5.2).

3.2. Losartan reduces early injury in βsg$^{-/-}$ male hearts and eliminates the sex difference.

Broadly, βsg$^{-/-}$ mice treated with the angiotensin receptor blocker (ARB) losartan displayed reductions in cardiac susceptibility to injury, and the losartan treatment benefits were not significantly different between acute treatment started 1 hour before Iso and chronic pretreatment given for 2 weeks before Iso (Fig. 5.3 A-C).
When compared to βsg$^{-/-}$ mice that had only received Iso, the combined group of losartan-treated βsg$^{-/-}$ males from both treatment regimens displayed a striking 64% reduction in early cardiomyocyte injury present 30 hours after the Iso injection. In contrast, cardiac injury in female βsg$^{-/-}$ hearts treated with losartan trended toward a modest reduction of approximately 40% that did not reach statistical significance ($p=0.12$, Fig. 5.3D). Importantly, the protective effect of losartan on early cardiac injury was significantly greater in βsg$^{-/-}$ males and erased the sex difference in cardiac injury (interaction $p=0.002$, Fig. 5.3D).

3.3. Chronic losartan treatment after injury selectively benefits male βsg$^{-/-}$ hearts.

Within the group that continued to receive losartan in the drinking water for 1 month after Iso-induced injury, the treatment only ameliorated cardiac remodeling in male βsg$^{-/-}$ hearts, without a significant effect in female hearts (Fig 5.4). Heart weights normalized to body weight demonstrated that, on average, male βsg$^{-/-}$ hearts were hypertrophied 1 month after Iso-induced injury, and losartan prevented this increase in heart size ($p<0.001$; Fig. 5.4B). In contrast, female heart weights did not increase significantly 1 month after Iso-induced cardiac injury, and the trend toward a modest reduction in heart weight with losartan did not reach statistical significance ($p=0.09$; interaction $p=0.05$; Fig. 5.4B).

Quantification of cardiac fibrosis showed that βsg$^{-/-}$ male hearts chronically treated with losartan had a 46% reduction in Iso-induced cardiac fibrosis, but female cardiac fibrosis was nearly identical with and without losartan (interaction $p=0.01$; Fig. 5.4C). As with acute injury, these discordant effects resulted in the elimination of sex differences in cardiac remodeling after Iso-induced injury in losartan-treated βsg$^{-/-}$ hearts.

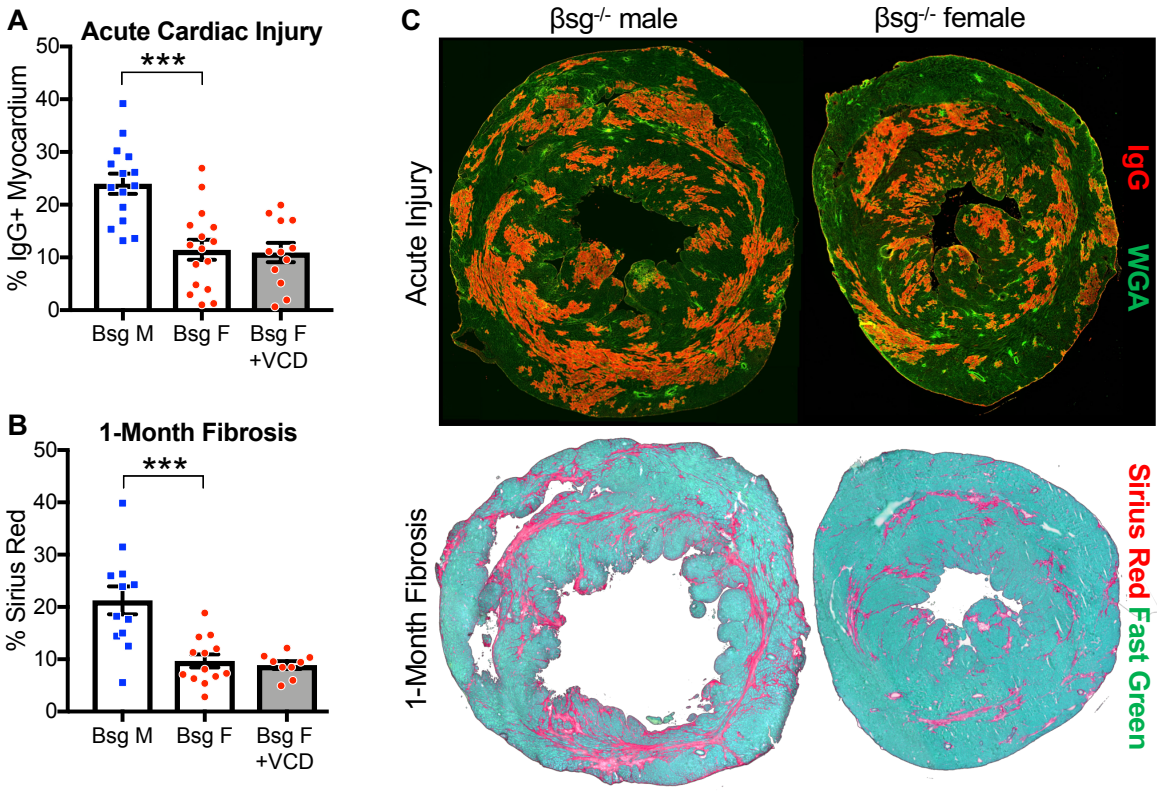

Figure 5.1: βsg$^{-/-}$ hearts show significant vulnerability to Iso-induced injury that varies by sex.

(A) Iso-induced early myocardial injury area, reflected in cardiomyocyte uptake of endogenous mouse IgG, was 2.2-fold larger in male than female βsg$^{-/-}$ hearts. Female cardiac injury was not altered by VCD treatment, which causes early ovarian senescence (n=12-16 per group; *** p<0.001). **(B)** 1 month after Iso-induced injury, cardiac fibrosis was 2.2-fold higher in male βsg$^{-/-}$ hearts than female hearts, and female cardiac fibrosis was unaffected by VCD treatment (n=9-13 per group; *** p<0.001). **(C)** Representative images of cardiac injury distribution in βsg$^{-/-}$ male and female hearts after one injection of Iso. Images of early myocardial injury (top) and cardiac fibrosis (bottom) both show lesions in red and total heart area in green.

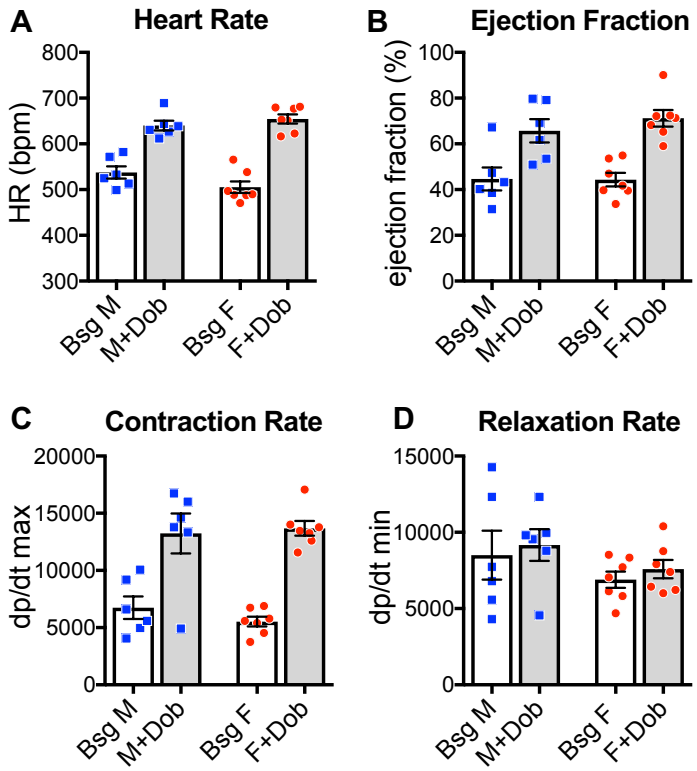

Figure 5.2: βsg$^{-/-}$ hearts of both sexes show similar performance at rest and with adrenergic stimulation.

Cardiac functional parameters were measured in vivo in anesthetized mice at rest and under adrenergic stimulation with dobutamine. These parameters show that βsg$^{-/-}$ male and female hearts have similar cardiac function and adrenergic responsiveness, as demonstrated by heart rate (A), ejection fraction (B), maximal rate of contraction (C), and maximal rate of relaxation (D). All parameters except for the relaxation rate (D) showed a significant main effect of stimulation ($p<0.001$), and none of the parameters showed a main effect of sex or a significant interaction by two-way ANOVA (n=6-7 per group).

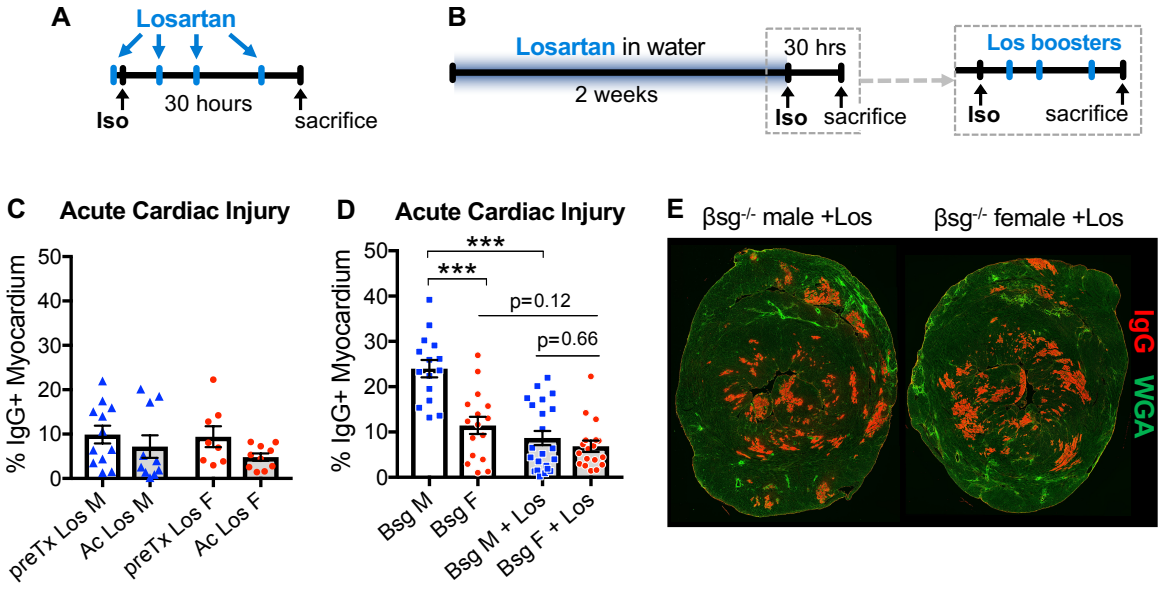

Figure 5.3: Losartan reduces early injury triggered by Iso in βsg$^{-/-}$ hearts and eliminates the sex difference.

(A) Acute losartan treatment was initiated by injection 1 hour before Iso, and was maintained with booster injections until the 30-hour sacrifice. **(B)** Chronic losartan pretreatment began 2 weeks before the Iso injection in the drinking water, and was maintained after Iso with booster injections until sacrifice. **(C)** The amount of Iso-induced early cardiac injury in losartan-treated mice was not altered significantly based on the length of the losartan treatment course ($p>0.05$ for sex, treatment type, and interaction; n=8-12 per group). **(D)** The combined group of male βsg$^{-/-}$ mice treated with losartan showed 64% lower early cardiac injury compared to male hearts without losartan. The combined group of female βsg$^{-/-}$ mice treated with losartan trended toward a modest reduction in early cardiac injury that was not statistically significant. The sex-dependence of losartan's effect on cardiac damage resulted in the loss of the sex difference in losartan-treated mice (n=15-22; *** $p<0.001$; interaction $p=0.002$). The untreated βsg$^{-/-}$ male and female injury data are reproduced from Fig. 1A. **(E)** Representative images of cardiac injury in βsg$^{-/-}$ male and female hearts treated with losartan after one injection of Iso, with myocardial damage shown in red and the total heart area shown in green.

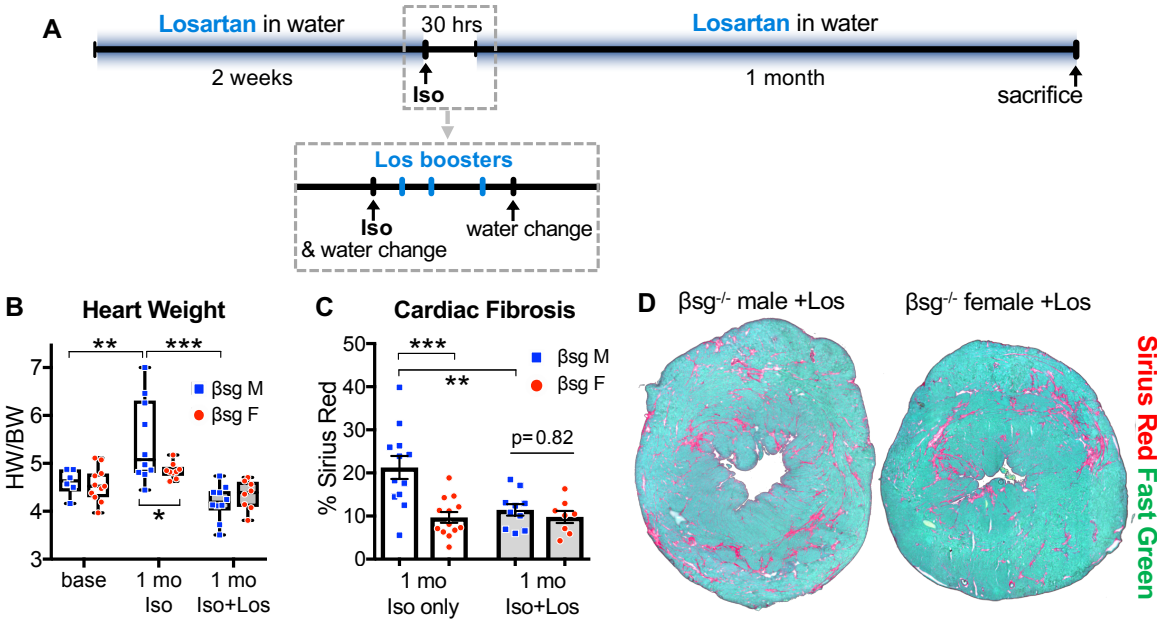

Figure 5.4: Chronic losartan treatment reduces cardiac fibrosis and normalizes heart weight in male βsg$^{-/-}$ mice.

(A) The effects of losartan on cardiac remodeling after injury were assessed in mice pretreated with losartan for 2 weeks before Iso, and maintained on losartan treatment in the water for 1 month after Iso. During the 30-hour period immediately after Iso, the mice received plain tap water and injected losartan boosters to ensure maintenance of therapeutic levels (inset). **(B)** Male βsg$^{-/-}$ hearts were significantly enlarged 1 month after Iso-induced injury, and chronic losartan treatment normalized heart weights in male βsg$^{-/-}$ mice. Female hearts did not change in size significantly after Iso administration, with or without losartan (n=6-11 per group; * p=0.02, ** p=0.003, *** p<0.001; interaction p=0.05). **(C)** 1 month after Iso-induced injury, losartan treatment caused 46% lower cardiac fibrosis in male βsg$^{-/-}$ hearts, compared to untreated mice. No detectable effect on cardiac fibrosis was observed in female hearts (n=8-13 per group; ** p=0.001, *** p<0.001; interaction p=0.01). The untreated βsg$^{-/-}$ male and female fibrosis data are reproduced from Fig. 1B. **(D)** Representative images of cardiac fibrosis 1 month after one injection of Iso in βsg$^{-/-}$ male and female hearts treated with losartan. Fibrosis is shown in red and the total heart area shown in green.

4. Discussion

The severity of the cardiomyopathy noted in many patients and preclinical models with sarcoglycanopathies underscores the importance of identifying cardiac-directed therapies that may help these vulnerable hearts. In recent work, we identified AT_1R blockade as a potential treatment strategy for preventing the accumulation of early myocardial injury in the mouse model of DMD, which shares many features with LGMD2E [31,271]. In the present study, we aimed to evaluate the potential benefits of treatment with the ARB losartan for preventing workload-induced injury in β-sarcoglycan-null mouse hearts. While the protective effects of ARB treatment were partially substantiated in this work, they are confounded by a striking sex difference manifesting as enhanced cardiac resilience in dystrophic female mice. Specifically, male $\beta sg^{-/-}$ hearts were roughly twice as susceptible as female hearts to early cardiomyocyte injury and the fibrosis that replaces those cardiomyocytes, and losartan treatment served to eliminate the sex differences through disproportionate protection in male hearts. These results suggest that any degree of protection that is afforded to male $\beta sg^{-/-}$ hearts by AT_1R blockade may already be present in female $\beta sg^{-/-}$ hearts without additional treatments.

The marked rarity of LGMD2E, combined with the phenotypic variability stemming from incomplete loss of β-sarcoglycan in some of the patients, significantly complicates the evaluation of any potential sex differences in the cardiac phenotype of human LGMD2E patients. One recent study set out to evaluate the phenotypic characteristics of the largest cohort of LGMDE2 patients yet, and included 16 male and 16 female patients, with a severe phenotype observed in 7 and 8 of each group, respectively [271]. However, this classification was based on loss of ambulation, and the observations related to cardiomyopathy were not reported in relation to biological sex, precluding any conclusions about cardiac sex-based differences. The large intra-group variability in cardiac injury in the present study required sizeable cohorts of genetically-identical mice to detect the sex difference, despite its large effect size, thus the question of a sex difference in human sarcoglycan-null hearts may not be readily answerable.

It is possible that the sex difference in cardiac resilience reported in this study only exists in mice, and may not reflect similar underlying differences in human patients. If this were the case, it highlights the question of the physiological differences that exist between female humans and mice that enable the female mice to be markedly protected despite the absence of the sarcoglycan complex. Interestingly, the existence of this

protective mechanism in female mice does not depend on ovarian hormones, suggesting that it may represent a potential basis for therapeutics that could be used to protect the hearts of male and female sarcoglycanopathy patients. In clinical practice and preclinical work, female protection from the more aggressive features of various acquired cardiovascular diseases has been consistently documented, including in contexts of myocardial injury, heart failure, and hypertension [283–290]. Although estrogen has been linked to many of these protective effects, some known instances of female resilience and protection do not depend on estrogen, and estrogen-independent protective mechanisms may represent promising targets for therapeutic development for all sexes [284,287,291,292]

Previous reports have detailed numerous sex differences in the renin-angiotensin system, most notably with respect to angiotensin receptors and responses to angiotensin II [293–296]. Importantly, the overall trend in the literature suggests that female physiology may be skewed in favor of protective features of the angiotensin system. However, until recently, it has been a common practice to only include males in preclinical animal studies, potentially due to the assumption that female reproductive cycling introduces excessive variability, or perhaps due to observing a confounding sex difference [297]. In previous work, activation of AT_1R with angiotensin II has been extensively documented to induce many pathological effects in the cardiovascular system and elsewhere [80,83,84,231,232], although it is less clear how many of these conclusions were based on studies of males. The finding that AT_1R blockade nullified the existing sex difference in cardiac susceptibility in these mice, combined with reports of pathological processes activated by AT_1R signaling, suggests that less injurious angiotensin signaling could underlie some aspects of female resilience.

Although sex differences complicate the interpretation of losartan's benefits in the present study, the protective effect of AT_1R blockade on early Iso-induced myocardial injury has been confirmed in male $\beta sg^{-/-}$ mice. Furthermore, we have shown here that this protection persists chronically with ongoing treatment, resulting in amelioration of cardiac remodeling and fibrosis that occur after myocardial damage. These observations should be used to inform the course of treatment of LGMD2E in clinical settings, with a possible goal of starting treatment with ARBs as early as reasonable to intervene in the early disease processes in the heart. The first gene therapy aiming to completely replace the absent β-sarcoglycan gene by an AAV-delivered vector has recently moved into a

clinical trial with promising preliminary results, but its cardiac efficiency has not yet been assessed in human patients [276,298]. There is a risk that the restoration of the cardiac sarcoglycan complex may be incomplete in patient hearts after gene therapy, which may occur as a consequence of efforts to identify the lowest effective AAV dose for achieving sufficient skeletal muscle correction. In this case, patients with partial sarcoglycan restoration may remain subject to underlying disease processes that could jeopardize their hearts in the absence of additional therapeutic interventions, analogously to LGMD2E patients who have been shown to develop cardiomyopathy even in the context of partial endogenous β-sarcoglycan expression and mild skeletal muscle disease [271,272]. Future work should aim to shed light on any potential sex differences in the cardiac phenotype of sarcoglycanopathy patients, and continue to investigate the protective capacity of AT_1R blockade in their hearts.

CHAPTER 6
CONCLUSIONS AND FUTURE DIRECTIONS

This dissertation represents a body of work driven by the pursuit of insights into the dysfunctional processes underlying dystrophic cardiomyopathy and the interventions that may limit these processes. These studies were carried out with the understanding that small mammalian models of complex progressive diseases represent a compromise between the desire for clear mechanistic answers and the importance of physiological relevance to human disease. This compromise means that many of the conclusions and future directions arising from this work should be tested at additional tiers of complexity. More reductionist systems, such as ex vivo hearts and isolated cardiomyocytes, may allow for clearer characterization of cellular features, processes, and causal relationships with less potential for compensatory confounding effects. Conversely, only careful clinical research will be able to assess parallels between these models and human patients to determine whether the findings reported here are applicable to the ultimate goal of treating disease in human patients.

1. Conclusions

The work described here has centered on the exploration of cardiac vulnerability in mouse models of muscular dystrophies, with the goal of identifying relationships or interventions that can help shape the management of these diseases in human patients. Because the most severe muscular dystrophies are diseases of childhood and early adulthood, the use of young adult mice enabled the study of cardiac disease without concerns about aging as a confounding factor, but it presented the problem of only modest cardiac involvement in these mice. For this reason, this work has relied on the induction of cardiac stress with the β-adrenergic receptor agonist isoproterenol to produce the kind of myocardial injury that may accumulate intermittently in human patient hearts during bouts of high cardiac stress. This adrenergic stress model is thought to be relevant to perioperative cardiac stresses in dystrophic patients, with procedures requiring anesthesia and resulting in bouts of elevated cardiac stress being a regular part of treatment [6,216]. Additionally, periods of chest pain accompanied by serum cardia troponin elevations have been documented in DMD patients, in parallel with effects of isoproterenol documented in our earlier work [30,31,252]

One major finding arising from this injury model is the robust capacity of angiotensin receptor blockers to limit the extent of cardiomyocyte injury when given in advance of the injurious stimulus. ARBs like losartan, along with ACE inhibitors, have been understood to benefit failing and injured hearts by modifying transcriptional profiles that drive adverse cardiac remodeling. The effects of angiotensin II signaling through AT_1R include the transcriptional activation of pro-fibrotic gene programs that contribute to myocyte hypertrophy, myocyte death, fibrosis, and functional decline. The more immediate, signaling-based effects of AT_1R activation are less often addressed, but the results described here suggest that acute AT_1R signaling may represent an important mechanism underlying myocardial injury in the dystrophic heart. In males of two different genetic models of muscular dystrophy, the reduction in Iso-induced cardiomyocyte injury was similarly robust if they were treated with losartan for two weeks or only 1 hour before isoproterenol. This suggests that the effects of transcriptional changes are not needed for this mechanism of protection at the time of injury, and it may instead depend predominantly on blocking rapid signal transduction downstream of AT_1R. NADPH oxidase is a potential candidate for mediating this effect, as the activation of AT_1R signaling has been linked to ROS production via NADPH oxidase 2 [80,83,84]. Neither an acute or chronic treatment course with an ACE inhibitor had an effect on early cardiac injury, indicating that the inhibition of angiotensin's pathological contribution to injury is more effective with direct receptor blockade. Two primary implications can be derived from this finding for further investigation. The first is the potentially causal role for reactive oxygen species produced by NADPH oxidase, a downstream effector of AT_1R signaling, in the expansion of dystrophic myocardial injury. The second is the possibility that dystrophic heart disease in human patients may be effectively delayed by the use ARBs, in place of the more popular ACE inhibitors, at a sufficiently young age to precede initial cardiac damage.

Another major conclusion stemming from this work is the discovery of significant cardiac vulnerability and even Iso-induced mortality in female DMD carrier mice. Based on earlier preclinical work with partial cardiac transduction of micro-dystrophin therapies, combined with a previous study showing a lack of cardiac disease indicators in DMD carrier mice, the extent of Iso-induced injury in dystrophin-mosaic carrier hearts was surprising. Even more surprising was the observation that survival after isoproterenol was highly divergent between the carrier mice bred from *mdx* males and those bred from

mdx females. The mechanisms that may underlie this difference based on parental genotypes are likely very complex and represent an interesting target for future studies. However, the observation that hearts with similar levels of dystrophin expression may show discordant vulnerability reveals a new layer of complexity in addressing the question of how much genetic correction or replacement is sufficient in the dystrophin-null heart. A number of gene-targeted therapies in development and in trials for DMD aim to restore skeletal muscle and cardiac dystrophin expression, including antisense oligonucleotide exon skipping, AAV micro-dystrophin therapies, and CRISPR/Cas9 gene editing. However, preclinical work has shown that these approaches may produce a mosaic pattern of transduction in the heart, with clusters of cardiomyocytes that lack dystrophin adjacent to those expressing it [161,164,180,183,257]. This resulting pattern is comparable to mosaic DMD carrier hearts, and human carriers of DMD have been documented to display a varied incidence of cardiac symptoms (<10% to nearly 50%) that were not overtly linked to their underlying mutation [20,262,263]. Based on these observations, the finding that mosaic expression of dystrophin in ~50% of the heart may be insufficient to rescue the myocardium merits careful investigation.

A third major conclusion of this work is the possibility that sex-based alterations in physiological processes that underlie dystrophic heart injury may partially overlap with the benefits of AT_1R blockade. In dystrophic mice lacking the sarcoglycan complex, male hearts displayed over 2-fold higher Iso-induced cardiomyocyte injury and subsequent fibrosis compared to female heart. However, ARB treatment selectively benefitted the male mice without any significant protection in dystrophic female mice, abolishing the sex differences in early injury, fibrosis, and hypertrophy in sarcoglycan-null hearts. In light of previously reported sex differences in the renin-angiotensin system in humans and animal models, this finding supports the possibility of an endogenous mechanism that may mitigate angiotensin's effects in female mouse hearts in the absence of ARB treatment.

A central theme in this collection of work has been the exacerbation of existing cardiac vulnerability in dystrophic mouse hearts using isoproterenol, a drug that activates endogenous β-adrenergic receptors. This adrenergic stimulation produces a response akin to "fight-or-flight" by approximating a robust upsurge in sympathetic nervous system activation, which drives sharp increases in cardiac contractility and heart rate. The increased workload on the myocardium is presumed to be the predominant

cause of the cardiac damage presented here. However, many other factors could contribute to the injury processes and mortality that follow isoproterenol administration, including influences from the vascular, renal, immune, and central nervous systems.

2. Future Directions

Future work aiming to build upon the results reported here should continue to probe the cellular processes that drive myocardial injury after Iso stimulation and investigate how these conclusions are relevant to human dystrophic patients.

The study of the mechanistic effects of AT_1R blockade in ex vivo working hearts, cardiac papillary muscle preparations, or isolated cardiomyocytes would enable the detection of reactive oxygen species production by dystrophic myocardium, as well as any functional changes that may accompany ARB treatment. Furthermore, the comparison of ARB effects on ROS production in whole hearts compared to cardiomyocytes may shed light on the potential role of non-myocyte cardiac cells. The pursuit of similar experiments in hearts from male and female sarcoglycan-null mice would shed light on any differences in ROS accumulation that may exist without ARB blockade, and reveal whether ARB treatment equalizes any such differences in male and female hearts. Furthermore, efforts to recapitulate the benefits of losartan by inhibiting NADPH oxidase or increasing antioxidant defenses could support or refute the hypothesis that NADPH oxidase-mediated ROS production drives the deleterious effects of angiotensin that are blocked by losartan. This work would help define the link between AT_1R and cardiomyocyte injury, determining whether ROS is the mediator of non-transcriptional AT_1R effects that exacerbate myocardial injury.

Investigation of the clinical relevance of this ARB-mediated cardiac injury prevention should begin in patients with DMD or genetically-diagnosed sarcoglycanopathies before 10 years of age, with ARB treatment in place of ACE inhibitor treatment. Clinical studies have shown similar efficacy of both drug classes in treating heart failure in general and DMD cardiomyopathy in particular, and ARBs are also better-tolerated than ACE inhibitors, resulting in minimal risk to patients. The comparison of patients treated with ARBs from a young age to those treated with ACE inhibitors or other non-ARB treatments can shed light on any significant differences in the degree of benefits afforded by the different treatment options.

To address cardiac vulnerability and the influence of non-dystrophin factors in DMD carrier hearts, RNAseq comparing hearts from wild type, dystrophic, and carrier mice could be used to generate hypotheses in preclinical work. Differences in a variety of epigenetic influences between maternal and paternal DMD carriers should become evident in assessing the transcriptome of their hearts. This approach could reveal the differentially-expressed genes that modify cardiac vulnerability in hearts with mosaic dystrophin expression, potentially contributing to the development and implementation of cardiac gene-targeted therapies in DMD. Furthermore, human DMD carriers should continue to be monitored and characterized in clinical work to improve understanding of the phenotype of partial dystrophin expression.

Most importantly, future work must aim to continue improving approaches for evaluating cardiac health and function in dystrophic hearts, and utilizing those approaches to improve understanding of the cardiac phenotype in carriers of DMD and patients with Becker muscular dystrophy. The landscape of DMD cardiomyopathy is on the precipice of significant changes, as gene-targeted therapies aim to restore truncated dystrophin expression that may have discordant efficiency in the heart and skeletal muscle. The treatment of dystrophic patients with AAV-delivered replacement genes has shown very promising early results in human trials. Limitations of this approach have historically included immunogenicity, pre-existing neutralizing immunity, and the challenges of producing sufficient amounts of virus for human dosing. However, recent work has made progress in addressing these limitations, and earlier dosing of human patients at a young age will require less virus than the dosing of older children and adolescents patients. Because of the encouraging trajectory of AAV gene therapy, it seems inevitable that it will play a major role in shaping the future of muscular dystrophies. With the possibility of sustained ambulation and physical activity in dystrophic patients comes an increased need to ensure that the heart can keep up. The hearts of wheelchair-bound patients are subject to a very different set of demands than the hearts of patients who may remain ambulatory for the duration of their adult lives, thus future efforts must be directed at optimizing the cardiac efficacy of gene therapies along with the pursuit of correcting skeletal muscle.

REFERENCES

1. Eagle, M.; Baudouin, S. V; Chandler, C.; Giddings, D.R.; Bullock, R.; Bushby, K. Survival in Duchenne muscular dystrophy: improvements in life expectancy since 1967 and the impact of home nocturnal ventilation. *Neuromuscul. Disord.* **2002**, *12*, 926–929.
2. Rafael-Fortney, J.A.; Chadwick, J.A.; Raman, S. V. Duchenne muscular dystrophy mice and men: Can understanding a genetic cardiomyopathy inform treatment of other myocardial diseases? *Circ. Res.* **2016**, *118*, 1059–1061.
3. Nigro, G.; Comi, L.I.; Politano, L.; Bain, R.J.I. The incidence and evolution of cardiomyopathy in Duchenne muscular dystrophy. *Int. J. Cardiol.* **1990**, *26*, 271–277.
4. Spurney, C.F.; Shimizu, R.; Morgenroth, L.P.; Kolski, H.; Gordish-Dressman, H.; Clemens, P.R.; Cregan, M.; Goude, E.; Glick, M.; Johnson, L.; et al. CINRG Duchenne Natural History Study demonstrates insufficient diagnosis and treatment of cardiomyopathy in Duchenne muscular dystrophy. *Muscle and Nerve* **2014**, *50*, 250–256.
5. McNally, E.M.; Kaltman, J.R.; Benson, D.W.; Canter, C.E.; Cripe, L.H.; Duan, D.; Finder, J.D.; Hoffman, E.P.; Judge, D.P.; Kertesz, N.; et al. Contemporary cardiac issues in Duchenne muscular dystrophy. *Circulation* **2015**, *131*, 1590–1598.
6. Birnkrant, D.J.; Bushby, K.; Bann, C.M.; Alman, B.A.; Apkon, S.D.; Blackwell, A.; Case, L.E.; Cripe, L.H.; Hadjiyannakis, S.; Olson, A.K.; et al. Diagnosis and management of Duchenne muscular dystrophy, part 2: respiratory, cardiac, bone health, and orthopaedic management. *Lancet Neurol.* **2018**, *17*, 347–361.
7. Kamdar, F.; Garry, D.J. Dystrophin-Deficient Cardiomyopathy. *J. Am. Coll. Cardiol.* **2016**, *67*, 2533–2546.
8. Bladen, C.L.; Salgado, D.; Monges, S.; Foncuberta, M.E.; Kekou, K.; Kosma, K.; Dawkins, H.; Lamont, L.; Roy, A.J.; Chamova, T.; et al. The TREAT-NMD DMD Global Database: analysis of more than 7,000 Duchenne muscular dystrophy mutations. *Hum. Mutat.* **2015**, *36*, 395–402.
9. Flanigan, K.M. Duchenne and Becker Muscular Dystrophies. In *Swaiman's Pediatric Neurology*; Elsevier Inc., 2017; pp. e2482–e2492.
10. Mendell, J.R.; Shilling, C.; Leslie, N.D.; Flanigan, K.M.; Gastier-foster, J.; Kneile, K.; Dunn, D.M.; Duval, B.; Aoyagi, A.; Hamil, C.; et al. Evidence-Based Path to Newborn Screening for Duchenne Muscular Dystrophy. *Ann. Neurol.* **2012**, *71*, 304–313.
11. Mah, J.K.; Korngut, L.; Dykeman, J.; Day, L.; Pringsheim, T.; Jette, N. A systematic review and meta-analysis on the epidemiology of Duchenne and Becker muscular dystrophy. *Neuromuscul. Disord.* **2014**, *24*, 482–491.
12. Guiraud, S.; Aartsma-Rus, A.; Vieira, N.M.; Davies, K.E.; van Ommen, G.-J.B.; Kunkel, L.M. The Pathogenesis and Therapy of Muscular Dystrophies. *Annu. Rev. Genomics Hum. Genet.* **2015**, *16*, 281–308.
13. Nicolas, A.; Raguènès-Nicol, C.; Yaou, R. Ben; Hir, S.A. Le; Chéron, A.; Vié, V.; Claustres, M.; Leturcq, F.; Delalande, O.; Hubert, J.F.; et al. Becker muscular dystrophy severity is linked to the structure of dystrophin. *Hum. Mol. Genet.* **2015**, *24*, 1267–1279.
14. Tyler, K.L. Origins and early descriptions of "Duchenne muscular dystrophy." *Muscle and Nerve* **2003**, *28*, 402–422.
15. Torriani, M.; Townsend, E.; Thomas, B.J.; Bredella, M.A.; Ghomi, R.H.; Tseng, B.S. Lower leg muscle involvement in Duchenne muscular dystrophy: An MR

imaging and spectroscopy study. *Skeletal Radiol.* **2012**, *41*, 437–445.
16. Birnkrant, D.J.; Bushby, K.; Bann, C.M.; Apkon, S.D.; Blackwell, A.; Colvin, M.K.; Cripe, L.H.; Herron, A.R.; Kennedy, A.; Kinnett, K.; et al. Diagnosis and management of Duchenne muscular dystrophy, part 3 : primary care, emergency management, psychosocial care, and transitions of care across the lifespan. *Lancet Neurol.* **2018**, *17*, 445–455.
17. Banihani, R.; Smile, S.; Yoon, G.; Dupuis, A.; Mosleh, M.; Snider, A.; McAdam, L. Cognitive and neurobehavioral profile in boys with duchenne muscular dystrophy. *J. Child Neurol.* **2015**, *30*, 1472–1482.
18. Tandon, A.; Villa, C.R.; Hor, K.N.; Jefferies, J.L.; Gao, Z.; Towbin, J.A.; Wong, B.L.; Mazur, W.; Fleck, R.J.; Sticka, J.J.; et al. Myocardial fibrosis burden predicts left ventricular ejection fraction and is associated with age and steroid treatment duration in Duchenne muscular dystrophy. *J. Am. Heart Assoc.* **2015**, *4*, 1–8.
19. Hor, K.N.; Wansapura, J.; Markham, L.W.; Mazur, W.; Cripe, L.H.; Fleck, R.; Benson, D.W.; Gottliebson, W.M. Circumferential Strain Analysis Identifies Strata of Cardiomyopathy in Duchenne Muscular Dystrophy. A Cardiac Magnetic Resonance Tagging Study. *J. Am. Coll. Cardiol.* **2009**, *53*, 1204–1210.
20. Hor, K.N.; Mah, M.L.; Johnston, P.; Cripe, T.P.; Cripe, L.H. Advances in the diagnosis and management of cardiomyopathy in Duchenne muscular dystrophy. *Neuromuscul. Disord.* **2018**, *28*, 711–716.
21. Matsumura, T.; Saito, T.; Fujimura, H.; Shinno, S. Cardiac troponin I for accurate evaluation of cardiac status in myopathic patients. *Brain Dev.* **2007**, *29*, 496–501.
22. Ergul, Y.; Ekici, B.; Nisli, K.; Tatli, B.; Binboga, F.; Acar, G.; Ozmen, M.; Omeroglu, R.E. Evaluation of the North Star Ambulatory Assessment scale and cardiac abnormalities in ambulant boys with Duchenne muscular dystrophy. *J. Paediatr. Child Health* **2012**, *48*, 610–616.
23. Ramaciotti, C.; Iannaccone, S.T.; Scott, W.A. Myocardial cell damage in Duchenne muscular dystrophy. *Pediatr. Cardiol.* **2003**, *24*, 503–506.
24. Cheeran, D.; Khan, S.; Khera, R.; Bhatt, A.; Garg, S.; Grodin, J.L.; Morlend, R.; Araj, F.G.; Amin, A.A.; Thibodeau, J.T.; et al. Predictors of death in adults with Duchenne muscular dystrophy-associated cardiomyopathy. *J. Am. Heart Assoc.* **2017**, *6*, 1–12.
25. Eagle, M.; Bourke, J.; Bullock, R.; Gibson, M.; Mehta, J.; Giddings, D.; Straub, V.; Bushby, K. Managing Duchenne muscular dystrophy - The additive effect of spinal surgery and home nocturnal ventilation in improving survival. *Neuromuscul. Disord.* **2007**, *17*, 470–475.
26. Rybakova, I.N.; Patel, J.R.; Ervasti, J.M. The dystrophin complex forms a mechanically strong link between the sarcolemma and costameric actin. *J. Cell Biol.* **2000**, *150*, 1209–1214.
27. Ervasti, J.M. Dystrophin, its interactions with other proteins, and implications for muscular dystrophy. *Biochim. Biophys. Acta - Mol. Basis Dis.* **2007**, *1772*, 108–117.
28. Sharpe, K.M.; Premsukh, M.D.; Townsend, D. Alterations of dystrophin-associated glycoproteins in the heart lacking dystrophin or dystrophin and utrophin. *J. Muscle Res. Cell Motil.* **2013**, *34*, 395–405.
29. Townsend, D.; Blankinship, M.J.; Allen, J.M.; Gregorevic, P.; Chamberlain, J.S.; Metzger, J.M. Systemic administration of micro-dystrophin restores cardiac geometry and prevents dobutamine-induced cardiac pump failure. *Mol. Ther.* **2007**, *15*, 1086–1092.
30. Hor, K.N.; Johnston, P.; Kinnett, K.; Mah, M.L.; Stiver, C.; Markham, L.W.; Cripe,

L.H. Progression of Duchenne Cardiomyopathy Presenting with Chest Pain and Troponin Elevation. *J. Neuromuscul. Dis.* **2017**, *4*, 307–314.
31. Meyers, T.A.; Heitzman, J.A.; Krebsbach, A.; Aufdembrink, L.M.; Hughes, R.; Bartolomucci, A.; Townsend, D. Acute AT1R blockade prevents isoproterenol-induced injury in mdx hearts. *J. Mol. Cell. Cardiol.* **2019**, *128*, 51–61.
32. Yue, Y.; Skimming, J.W.; Liu, M.; Strawn, T.; Duan, D. Full-length dystrophin expression in half of the heart cells ameliorates β-isoproterenol-induced cardiomyopathy in mdx mice. *Hum. Mol. Genet.* **2004**, *13*, 1669–1675.
33. Olthoff, J.T.; Lindsay, A.; Abo-Zahrah, R.; Baltgalvis, K.A.; Patrinostro, X.; Belanto, J.J.; Yu, D.-Y.; Perrin, B.J.; Garry, D.J.; Rodney, G.G.; et al. Loss of peroxiredoxin-2 exacerbates eccentric contraction-induced force loss in dystrophin-deficient muscle. *Nat. Commun.* **2018**, *9*, 5104.
34. Han, R.; Bansal, D.; Miyake, K.; Muniz, V.P.; Weiss, R.M.; McNeil, P.L.; Campbell, K.P. Dysferlin-mediated membrane repair protects the heart from stress-induced left ventricular injury. *J. Clin. Invest.* **2007**, *117*, 1805–1813.
35. Cai, C.; Masumiya, H.; Weisleder, N.; Matsuda, N.; Nishi, M.; Hwang, M.; Ko, J.K.; Lin, P.; Thornton, A.; Zhao, X.; et al. MG53 nucleates assembly of cell membrane repair machinery. *Nat. Cell Biol.* **2009**, *11*, 56–64.
36. Zhang, C.; Chen, B.; Wang, Y.; Guo, A.; Tang, Y.; Khataei, T.; Shi, Y.; Kutschke, W.J.; Zimmerman, K.; Weiss, R.M.; et al. MG53 is dispensable for T-tubule maturation but critical for maintaining T-tubule integrity following cardiac stress. *J. Mol. Cell. Cardiol.* **2017**, *112*, 123–130.
37. Vanhoutte, D.; Schips, T.G.; Kwong, J.Q.; Davis, J.; Tjondrokoesoemo, A.; Brody, M.J.; Sargent, M.A.; Kanisicak, O.; Yi, H.; Gao, Q.Q.; et al. Thrombospondin expression in myofibers stabilizes muscle membranes. *Elife* **2016**, *5*, 1–33.
38. Brody, M.J.; Vanhoutte, D.; Schips, T.G.; Boyer, J.G.; Bakshi, C. V.; Sargent, M.A.; York, A.J.; Molkentin, J.D. Defective Flux of Thrombospondin-4 through the Secretory Pathway Impairs Cardiomyocyte Membrane Stability and Causes Cardiomyopathy. *Mol. Cell. Biol.* **2018**, *38*, 1–14.
39. Harris, E.; Bladen, C.L.; Mayhew, A.; James, M.; Bettinson, K.; Moore, U.; Smith, F.E.; Rufibach, L.; Cnaan, A.; Goebel, D.X.B.; et al. The clinical outcome study for dysferlinopathy: An international multicenter study. *Neurol. Genet.* **2016**, *2*, e89.
40. He, B.; Tang, R.H.; Weisleder, N.; Xiao, B.; Yuan, Z.; Cai, C.; Zhu, H.; Lin, P.; Qiao, C.; Li, J.; et al. Enhancing muscle membrane repair by gene delivery of MG53 ameliorates muscular dystrophy and heart failure inδ-sarcoglycan-deficient hamsters. *Mol. Ther.* **2012**, *20*, 727–735.
41. Weisleder, N.; Takizawa, N.; Lin, P.; Wang, X.; Cao, C.; Zhang, Y.; Tan, T.; Ferrante, C.; Zhu, H.; Chen, P.J.; et al. Recombinant MG53 protein modulates therapeutic cell membrane repair in treatment of muscular dystrophy. *Sci. Transl. Med.* **2012**, *4*, 139ra85.
42. Houang, E.M.; Bates, F.S.; Sham, Y.Y.; Metzger, J.M. All-Atom Molecular Dynamics-Based Analysis of Membrane-Stabilizing Copolymer Interactions with Lipid Bilayers Probed under Constant Surface Tensions. *J. Phys. Chem. B* **2017**, *121*, 10657–10664.
43. Houang, E.M.; Sham, Y.Y.; Bates, F.S.; Metzger, J.M. Muscle membrane integrity in Duchenne muscular dystrophy: Recent advances in copolymer-based muscle membrane stabilizers. *Skelet. Muscle* **2018**, *8*, 1–19.
44. Townsend, D.; Turner, I.; Yasuda, S.; Martindale, J.; Davis, J.; Shillingford, M.; Kornegay, J.N.; Metzger, J.M. Chronic administration of membrane sealant prevents severe cardiac injury and ventricular dilatation in dystrophic dogs. *J. Clin.*

Invest. **2010**, *120*, 1140–1150.
45. Yasuda, S.; Townsend, D.; Michele, D.E.; Favre, E.G.; Day, S.M.; Metzger, J.M. Dystrophic heart failure blocked by membrane sealant poloxamer. *Nature* **2005**, *436*, 1025–1029.
46. Houang, E.M.; Haman, K.J.; Filareto, A.; Perlingeiro, R.C.; Bates, F.S.; Lowe, D.A.; Metzger, J.M. Membrane-stabilizing copolymers confer marked protection to dystrophic skeletal muscle in vivo. *Mol. Ther. - Methods Clin. Dev.* **2015**, *2*, 15042.
47. Townsend, D.; Yasuda, S.; Metzger, J. Cardiomyopathy of Duchenne muscular dystrophy: pathogenesis and prospect of membrane sealants as a new therapeutic approach. *Expert Rev. Cardiovasc. Ther.* **2007**, *5*, 99–109.
48. Ryan, T.; Phrixus Pharmaceuticals Inc. NCT03558958: Safety and Efficacy of P-188 NF in DMD Patients. 2018.
49. Vallejo-Illarramendi, A.; Toral-Ojeda, I.; Aldanondo, G.; López de Munain, A. Dysregulation of calcium homeostasis in muscular dystrophies. *Expert Rev. Mol. Med.* **2014**, *16*, e16.
50. Williams, I.A.; Allen, D.G. Intracellular calcium handling in ventricular myocytes from mdx mice. *Am. J. Physiol. Circ. Physiol.* **2007**, *292*, H846–H855.
51. Johnstone, V.P.A.; Viola, H.M.; Hool, L.C. Dystrophic cardiomyopathy—potential role of calcium in pathogenesis, treatment and novel therapies. *Genes (Basel).* **2017**, *8*.
52. Allen, D.G.; Whitehead, N.P. Duchenne muscular dystrophy - What causes the increased membrane permeability in skeletal muscle? *Int. J. Biochem. Cell Biol.* **2010**, *43*, 290–294.
53. Lorin, C.; Vögeli, I.; Niggli, E. Dystrophic cardiomyopathy: Role of TRPV2 channels in stretch-induced cell damage. *Cardiovasc. Res.* **2015**, *106*, 153–162.
54. Allen, D.G.; Whitehead, N.P.; Yeung, E.W. Mechanisms of stretch-induced muscle damage in normal and dystrophic muscle: Role of ionic changes. *J. Physiol.* **2005**, *567*, 723–735.
55. Koenig, X.; Rubi, L.; Obermair, G.J.; Cervenka, R.; Dang, X.B.; Lukacs, P.; Kummer, S.; Bittner, R.E.; Kubista, H.; Todt, H.; et al. Enhanced currents through L-type calcium channels in cardiomyocytes disturb the electrophysiology of the dystrophic heart. *Am. J. Physiol. Heart Circ. Physiol.* **2014**, *306*, H564–H573.
56. Viola, H.M.; Davies, S.M.K.; Filipovska, A.; Hool, L.C. L-type Ca 2+ channel contributes to alterations in mitochondrial calcium handling in the mdx ventricular myocyte. *Am. J. Physiol. Circ. Physiol.* **2013**, *304*, H767–H775.
57. Sadeghi, A.; Doyle, A.D.; Johnson, B.D. Regulation of the cardiac L-type Ca2+ channel by the actin-binding proteins alpha-actinin and dystrophin. *Am. J. Physiol. Cell Physiol.* **2002**, *282*, C1502-11.
58. Andersson, D.C.; Marks, A.R. Fixing ryanodine receptor Ca2+ leak – A novel therapeutic strategy for contractile failure in heart and skeletal muscle. *Drug Discov. Today Dis. Mech.* **2010**, *7*, e151–e157.
59. Fauconnier, J.; Thireau, J.; Reiken, S.; Cassan, C.; Richard, S.; Matecki, S.; Marks, A.R.; Lacampagne, A. Leaky RyR2 trigger ventricular arrhythmias in Duchenne muscular dystrophy. *Proc. Natl. Acad. Sci.* **2010**, *107*, 1559–1564.
60. Bellinger, A.M.; Reiken, S.; Carlson, C.; Mongillo, M.; Liu, X.; Rothman, L.; Matecki, S.; Lacampagne, A.; Marks, A.R. Hypernitrosylated ryanodine receptor calcium release channels are leaky in dystrophic muscle. *Nat. Med.* **2009**, *15*, 325–330.
61. Sarma, S.; Li, N.; van Oort, R.J.; Reynolds, C.; Skapura, D.G.; Wehrens, X.H.T.

Genetic inhibition of PKA phosphorylation of RyR2 prevents dystrophic cardiomyopathy. *Proc. Natl. Acad. Sci.* **2010**, *107*, 13165–13170.
62. Wang, Q.; Wang, W.; Wang, G.; Rodney, G.G.; Wehrens, X.H.T. Crosstalk between RyR2 oxidation and phosphorylation contributes to cardiac dysfunction in mice with Duchenne muscular dystrophy. *J. Mol. Cell. Cardiol.* **2015**, *89*, 177–184.
63. Voit, A.; Patel, V.; Pachon, R.; Shah, V.; Bakhutma, M.; Kohlbrenner, E.; McArdle, J.J.; Dell'Italia, L.J.; Mendell, J.R.; Xie, L.H.; et al. Reducing sarcolipin expression mitigates Duchenne muscular dystrophy and associated cardiomyopathy in mice. *Nat. Commun.* **2017**, *8*, 1068.
64. Rohman, M.S.; Emoto, N.; Takeshima, Y.; Yokoyama, M.; Matsuo, M. Decreased mAKAP, ryanodine receptor, and SERCA2a gene expression in mdx hearts. *Biochem. Biophys. Res. Commun.* **2003**, *310*, 228–235.
65. Shin, J.; Tajrishi, M.M.; Ogura, Y.; Kumar, A. Wasting mechanisms in muscular dystrophy. *Int. J. Biochem. Cell Biol.* **2013**, *45*, 2266–2279.
66. Zatz, M.; Starling, A. Calpains and Disease. *N. Engl. J. Med.* **2005**, *352*, 2413–2423.
67. Letavernier, E.; Zafrani, L.; Perez, J.; Letavernier, B.; Haymann, J.P.; Baud, L. The role of calpains in myocardial remodelling and heart failure. *Cardiovasc. Res.* **2012**, *96*, 38–45.
68. Freitas, A.C.S.; Figueiredo, M.J.; Campos, E.C.; Soave, D.F.; Ramos, S.G.; Tanowitz, H.B.; Celes, M.R.N. Activation of both the calpain and ubiquitin-proteasome systems contributes to septic cardiomyopathy through dystrophin loss/disruption and mTOR inhibition. *PLoS One* **2016**, *11*, 1–14.
69. Shoshan-Barmatz, V.; De, S.; Meir, A. The Mitochondrial Voltage-Dependent Anion Channel 1, Ca2+ Transport, Apoptosis, and Their Regulation. *Front. Oncol.* **2017**, *7*, 1–12.
70. Glancy, B.; Balaban, R.S. Role of mitochondrial Ca 2+ in the regulation of cellular energetics. *Biochemistry* **2012**, *51*, 2959–7293.
71. Lemasters, J.J.; Theruvath, T.P.; Zhong, Z.; Nieminen, A.L. Mitochondrial calcium and the permeability transition in cell death. *Biochim. Biophys. Acta - Bioenerg.* **2009**, *1787*, 1395–1401.
72. Kyrychenko, V.; Poláková, E.; Janíček, R.; Shirokova, N. Mitochondrial dysfunctions during progression of dystrophic cardiomyopathy. *Cell Calcium* **2015**, *58*, 186–195.
73. Millay, D.P.; Sargent, M.A.; Osinska, H.; Baines, C.P.; Barton, E.R.; Vuagniaux, G.; Sweeney, H.L.; Robbins, J.; Molkentin, J.D. Genetic and pharmacologic inhibition of mitochondrial-dependent necrosis attenuates muscular dystrophy. *Nat. Med.* **2008**, *14*, 442–447.
74. Gonzalez, D.R.; Treuer, A. V; Lamirault, G.; Mayo, V.; Cao, Y.; Dulce, R.A.; Hare, J.M. NADPH oxidase-2 inhibition restores contractility and intracellular calcium handling and reduces arrhythmogenicity in dystrophic cardiomyopathy. *Am. J. Physiol. - Hear. Circ. Physiol.* **2014**, *307*, H710–H721.
75. Prosser, B.L.; Ward, C.W.; Lederer, W.J. X-ROS signaling: Rapid mechano-chemo transduction in heart. *Science* **2011**, *333*, 1440–1445.
76. Loehr, J.A.; Wang, S.; Cully, T.R.; Pal, R.; Larina, I. V; Larin, K. V; Rodney, G.G. NADPH oxidase mediates microtubule alterations and diaphragm dysfunction in dystrophic mice. *Elife* **2018**, *7*, 1–19.
77. Strakova, J.; Dean, J.D.; Sharpe, K.M.; Meyers, T.A.; Odom, G.L.; Townsend, D. Dystrobrevin increases dystrophin's binding to the dystrophin-glycoprotein complex and provides protection during cardiac stress. *J. Mol. Cell. Cardiol.* **2014**,

76, 106–115.
78. Belanto, J.J.; Olthoff, J.T.; Mader, T.L.; Chamberlain, C.M.; Nelson, D.M.; McCourt, P.M.; Talsness, D.M.; Gundersen, G.G.; Lowe, D.A.; Ervasti, J.M. Independent variability of microtubule perturbations associated with dystrophinopathy. *Hum. Mol. Genet.* **2016**, *25*, 4951–4961.
79. Matecki, S.; Fauconnier, J.; Lacampagne, A. Reactive Oxygen Species and Muscular Dystrophy. *Syst. Biol. Free Radicals Antioxidants* **2014**, 3055–3072.
80. Dikalov, S.I.; Nazarewicz, R.R. Angiotensin II-Induced Production of Mitochondrial Reactive Oxygen Species: Potential Mechanisms and Relevance for Cardiovascular Disease. *Antioxid. Redox Signal.* **2013**, *19*, 1085–1094.
81. Allen, D.G.; Whitehead, N.P.; Froehner, S.C. Absence of Dystrophin Disrupts Skeletal Muscle Signaling: Roles of Ca2+, Reactive Oxygen Species, and Nitric Oxide in the Development of Muscular Dystrophy. *Physiol. Rev.* **2015**, *96*, 253–305.
82. Prosser, B.L.; Khairallah, R.J.; Ziman, A.P.; Ward, C.W.; Lederer, W.J. X-ROS signaling in the heart and skeletal muscle: Stretch-dependent local ROS regulates [Ca2+]i. *J. Mol. Cell. Cardiol.* **2013**, *58*, 172–181.
83. Münzel, T.; Gori, T.; Keaney, J.F.; Maack, C.; Daiber, A. Pathophysiological role of oxidative stress in systolic and diastolic heart failure and its therapeutic implications. *Eur. Heart J.* **2015**, *36*, 2555–2564.
84. Choi, H.; Leto, T.L.; Hunyady, L.; Catt, K.J.; Yun, S.B.; Sue, G.R. Mechanism of angiotensin II-induced superoxide production in cells reconstituted with angiotensin type 1 receptor and the components of NADPH oxidase. *J. Biol. Chem.* **2008**, *283*, 255–267.
85. Spurney, C.F.; Sali, A.; Guerron, A.D.; Iantorno, M.; Yu, Q.; Gordish-Dressman, H.; Rayavarapu, S.; Van Der Meulen, J.; Hoffman, E.P.; Nagaraju, K. Losartan decreases cardiac muscle fibrosis and improves cardiac function in dystrophin-deficient mdx mice. *J. Cardiovasc. Pharmacol. Ther.* **2011**, *16*, 87–95.
86. Lee, E.-M.; Kim, D.-Y.; Kim, A.-Y.; Lee, E.-J.; Kim, S.-H.; Lee, M.-M.; Sung, S.-E.; Park, J.-K.; Jeong, K.-S. Chronic effects of losartan on the muscles and the serologic profiles of mdx mice. *Life Sci.* **2015**, *143*, 35–42.
87. Brenman, J.E.; Chao, D.S.; Xia, H.; Aldape, K.; Bredt, D.S. Nitric oxide synthase complexed with dystrophin and absent from skeletal muscle sarcolemma in Duchenne muscular dystrophy. *Cell* **1995**, *82*, 743–752.
88. Martin, E.A.; Barresi, R.; Byrne, B.J.; Tsimerinov, E.I.; Scott, B.L.; Walker, A.E.; Gurudevan, S. V.; Anene, F.; Elashoff, R.M.; Thomas, G.D.; et al. Tadalafil alleviates muscle ischemia in patients with becker muscular dystrophy. *Sci. Transl. Med.* **2012**, *4*, 162ra155.
89. Thomas, G.D.; Sander, M.; Lau, K.S.; Huang, P.L.; Stull, J.T.; Victor, R.G. Impaired metabolic modulation of alpha-adrenergic vasoconstriction in dystrophin-deficient skeletal muscle. *Proc. Natl. Acad. Sci.* **1998**, *95*, 15090–15095.
90. Johnson, E.K.; Zhang, L.; Adams, M.E.; Phillips, A.; Freitas, M.A.; Froehner, S.C.; Green-Church, K.B.; Montanaro, F. Proteomic analysis reveals new cardiac-specific dystrophin-associated proteins. *PLoS One* **2012**, *7*, e43515.
91. Bia, B.L.; Cassidy, P.J.; Young, M.E.; Rafael-Fortney, J.A.; Leighton, B.; Davies, K.E.; Radda, G.K.; Clarke, K. Decreased myocardial nNOS, increased iNOS and abnormal ECGs in mouse models of duchenne muscular dystrophy. *J. Mol. Cell. Cardiol.* **1999**, *31*, 1857–1862.
92. Ramachandran, J.; Schneider, J.S.; Crassous, P.-A.; Zheng, R.; Gonzalez, J.P.; Xie, L.-H.; Beuve, A.; Fraidenraich, D.; Peluffo, R.D. Nitric oxide signalling

pathway in Duchenne muscular dystrophy mice: up-regulation of L-arginine transporters. *Biochem. J.* **2012**, *449*, 133–142.
93. Garbincius, J.F.; Michele, D.E. Dystrophin–glycoprotein complex regulates muscle nitric oxide production through mechanoregulation of AMPK signaling. *Proc. Natl. Acad. Sci.* **2015**, *112*, 13663–13668.
94. Balligand, J.L.; Ungureanu-Longrois, D.; Simmons, W.W.; Pimental, D.; Malinski, T.A.; Kapturczak, M.; Taha, Z.; Lowenstein, C.J.; Davidoff, A.J.; Kelly, R.A.; et al. Cytokine-inducible nitric oxide synthase (iNOS) expression in cardiac myocytes. Characterization and regulation of iNOS expression and detection of iNOS activity in single cardiac myocytes in vitro. *J. Biol. Chem.* **1994**, *269*, 27580–27588.
95. Altamirano, F.; López, J.R.; Henríquez, C.; Molinski, T.; Allen, P.D.; Jaimovich, E. Increased resting intracellular calcium modulates NF-κB-dependent inducible nitric-oxide synthase gene expression in dystrophic mdx skeletal myotubes. *J. Biol. Chem.* **2012**, *287*, 20876–20887.
96. Kanai, A.J.; Pearce, L.L.; Clemens, P.R.; Birder, L.A.; VanBibber, M.M.; Choi, S.-Y.; de Groat, W.C.; Peterson, J. Identification of a neuronal nitric oxide synthase in isolated cardiac mitochondria using electrochemical detection. *Proc. Natl. Acad. Sci.* **2002**, *98*, 14126–14131.
97. Massion, P.B.; Feron, O.; Dessy, C.; Balligand, J.-L. Nitric oxide and cardiac function: ten years after, and continuing. *Circ. Res.* **2003**, *93*, 388–398.
98. Adamo, C.M.; Dai, D.-F.F.; Percival, J.M.; Minami, E.; Willis, M.S.; Patrucco, E.; Froehner, S.C.; Beavo, J.A. Sildenafil reverses cardiac dysfunction in the mdx mouse model of Duchenne muscular dystrophy. *Proc. Natl. Acad. Sci.* **2010**, *107*, 19079–19083.
99. Khairallah, M.; Khairallah, R.J.; Young, M.E.; Allen, B.G.; Gillis, M.A.; Danialou, G.; Deschepper, C.F.; Petrof, B.J.; Des Rosiers, C. Sildenafil and cardiomyocyte-specific cGMP signaling prevent cardiomyopathic changes associated with dystrophin deficiency. *Proc. Natl. Acad. Sci.* **2008**, *105*, 7028–7033.
100. Sander, M.; Chavoshan, B.; Harris, S.A.; Iannaccone, S.T.; Stull, J.T.; Thomas, G.D.; Victor, R.G. Functional muscle ischemia in neuronal nitric oxide synthase-deficient skeletal muscle of children with Duchenne muscular dystrophy. *Proc. Natl. Acad. Sci.* **2000**, *97*, 13818–13823.
101. Leung, D.G.; Herzka, D.A.; Thompson, W.R.; He, B.; Bibat, G.; Tennekoon, G.; Russell, S.D.; Schuleri, K.H.; Lardo, A.C.; Kass, D.A.; et al. Sildenafil does not improve cardiomyopathy in Duchenne/Becker muscular dystrophy. *Ann. Neurol.* **2014**, *76*, 541–549.
102. Chung, H.S.; Kim, G.E.; Holewinski, R.J.; Venkatraman, V.; Zhu, G.; Bedja, D.; Kass, D.A.; Van Eyk, J.E. Transient receptor potential channel 6 regulates abnormal cardiac S-nitrosylation in Duchenne muscular dystrophy. *Proc. Natl. Acad. Sci.* **2017**, *114*, E10763–E10771.
103. Lai, Y.; Zhao, J.; Yue, Y.; Wasala, N.B.; Duan, D. Partial restoration of cardiac function with ΔPDZ nNOS in aged mdx model of Duchenne cardiomyopathy. *Hum. Mol. Genet.* **2014**, *23*, 3189–3199.
104. Wehling-Henricks, M.; Jordan, M.C.; Roos, K.P.; Deng, B.; Tidball, J.G. Cardiomyopathy in dystrophin-deficient hearts is prevented by expression of a neuronal nitric oxide synthase transgene in the myocardium. *Hum. Mol. Genet.* **2005**, *14*, 1921–1933.
105. Wehling-Henricks, M.; Tidball, J.G. Neuronal nitric oxide synthase-rescue of dystrophin/utrophin double knockout mice does not require nNOS localization to the cell membrane. *PLoS One* **2011**, *6*, e25071.

106. Hor, K.N.; Taylor, M.D.; Al-Khalidi, H.R.; Cripe, L.H.; Raman, S. V; Jefferies, J.L.; O'Donnell, R.; Benson, D.W.; Mazur, W. Prevalence and distribution of late gadolinium enhancement in a large population of patients with Duchenne muscular dystrophy: Effect of age and left ventricular systolic function. *J. Cardiovasc. Magn. Reson.* **2013**, *15*, 1–9.
107. Kong, P.; Christia, P.; Frangogiannis, N.G. The pathogenesis of cardiac fibrosis. *Cell. Mol. Life Sci.* **2014**, *71*, 549–574.
108. Porter, K.E.; Turner, N.A. Cardiac fibroblasts: At the heart of myocardial remodeling. *Pharmacol. Ther.* **2009**, *123*, 255–278.
109. Heras-Bautista, C.O.; Mikhael, N.; Lam, J.; Shinde, V.; Katsen-Globa, A.; Dieluweit, S.; Molcanyi, M.; Uvarov, V.; Jütten, P.; Sahito, R.G.A.; et al. Cardiomyocytes facing fibrotic conditions re-express extracellular matrix transcripts. *Acta Biomater.* **2019**, *89*, 180–192.
110. Ma, Y.; Mouton, A.J.; Lindsey, M.L. Cardiac macrophage biology in the steady-state heart, the aging heart, and following myocardial infarction. *Transl. Res.* **2018**, *191*, 15–28.
111. Chadwick, J.A.; Swager, S.A.; Lowe, J.; Welc, S.S.; Tidball, J.G.; Gomez-Sanchez, C.E.; Gomez-Sanchez, E.P.; Rafael-Fortney, J.A. Myeloid cells are capable of synthesizing aldosterone to exacerbate damage in muscular dystrophy. *Hum. Mol. Genet.* **2016**, *25*, 5167–5177.
112. Rafael-Fortney, J.A.; Chimanji, N.S.; Schill, K.E.; Martin, C.D.; Murray, J.D.; Ganguly, R.; Stangland, J.E.; Tran, T.; Xu, Y.; Canan, B.D.; et al. Early treatment with lisinopril and spironolactone preserves cardiac and skeletal muscle in Duchenne muscular dystrophy mice. *Circulation* **2011**, *124*, 582–588.
113. Rodriguez, E.K.; Hunter, W.C.; Royce, M.J.; Leppo, M.K.; Douglas, A.S.; Weisman, H.F. A method to reconstruct myocardial sarcomere lengths and orientations at transmural sites in beating canine hearts. *Am. J. Physiol. Circ. Physiol.* **2017**, *263*, H293–H306.
114. Dasgupta, C.; Zhang, L. Angiotensin II receptors and drug discovery in cardiovascular disease. *Drug Discov. Today* **2011**, *16*, 22–34.
115. Iwanami, J.; Mogi, M.; Iwai, M.; Horiuchi, M. Inhibition of the renin–angiotensin system and target organ protection. *Hypertens. Res.* **2009**, *32*, 229–237.
116. Kawai, T.; Forrester, S.J.; O'Brien, S.; Baggett, A.; Rizzo, V.; Eguchi, S. AT1 receptor signaling pathways in the cardiovascular system. *Pharmacol. Res.* **2017**, *125*, 4–13.
117. Duboc, D.; Meune, C.; Lerebours, G.; Devaux, J.Y.; Vaksmann, G.; Bécane, H.M. Effect of perindopril on the onset and progression of left ventricular dysfunction in Duchenne muscular dystrophy. *J. Am. Coll. Cardiol.* **2005**, *45*, 855–857.
118. Duboc, D.; Meune, C.; Pierre, B.; Wahbi, K.; Eymard, B.; Toutain, A.; Berard, C.; Vaksmann, G.; Weber, S.; Bécane, H.M. Perindopril preventive treatment on mortality in Duchenne muscular dystrophy: 10 years' follow-up. *Am. Heart J.* **2007**, *154*, 596–602.
119. Eichhorn, E.; Domanski, M.; Krause-Steinrauf, H.; Anderson, J. A trial of the beta-blocker bucindolol in patients with advanced chronic heart failure. *ACC Curr. J. Rev.* **2001**, *344*, 1659–1667.
120. Meyers, T.A.; Heitzman, J.A.; Townsend, D. Acute myocardial injury in mdx hearts ameliorated by ARB but not ACE inhibitor treatment. *Submitted* **2019**.
121. Bangalore, S.; Fakheri, R.; Toklu, B.; Ogedegbe, G.; Weintraub, H.; Messerli, F.H. Angiotensin-Converting Enzyme Inhibitors or Angiotensin Receptor Blockers in Patients Without Heart Failure? Insights from 254,301 Patients from Randomized

Trials. *Mayo Clin. Proc.* **2016**, *91*, 51–60.
122. Pitt, B.; Poole-Wilson, P.A.; Segal, R.; Martinez, F.A.; Dickstein, K.; Camm, A.J.; Konstam, M.A.; Riegger, G.; Klinger, G.H.; Neaton, J.; et al. Effect of losartan compared with captopril on mortality in patients with symptomatic heart failure: randomised trial - the Losartan Heart Failure Survival Study ELITE II. *Lancet* **2000**, *355*, 1582–1587.
123. Allen, H.D.; Flanigan, K.M.; Thrush, P.T.; Viollet-Callendret, L.; Dvorchik, I.; Yin, H.; Canter, C.E.; Connolly, A.M.; Parrish, M.; McDonald, C.M.; et al. A Randomized, Double-Blind Trial of Lisinopril and Losartan for the Treatment of Cardiomyopathy in Duchenne Muscular Dystrophy. *PLoS Curr. Muscular Dystrophy* **2013**, *5*.
124. Hollenberg, N.K.; Fisher, N.D.L.; Price, D.A. Pathways for angiotensin II generation in intact human tissue: Evidence from comparative pharmacological interruption of the renin system. *Hypertension* **1998**, *32*, 387–392.
125. Uehara, Y.; Miura, S.; Yahiro, E.; Saku, K. Non-ACE Pathway-induced Angiotensin II Production. *Curr. Pharm. Des.* **2013**, *19*, 3054–3059.
126. Basu, R.; Poglitsch, M.; Yogasundaram, H.; Thomas, J.; Rowe, B.H.; Oudit, G.Y. Roles of Angiotensin Peptides and Recombinant Human ACE2 in Heart Failure. *J. Am. Coll. Cardiol.* **2017**, *69*, 805–819.
127. Zou, Y.; Akazawa, H.; Qin, Y.; Sano, M.; Takano, H.; Minamino, T.; Makita, N.; Iwanaga, K.; Zhu, W.; Kudoh, S.; et al. Mechanical stress activates angiotensin II type 1 receptor without the involvement of angiotensin II. *Nat. Cell Biol.* **2004**, *6*, 499–506.
128. Takezako, T.; Unal, H.; Karnik, S.S.; Node, K. Structure-Function Basis of Attenuated Inverse Agonism of Angiotensin II Type 1 Receptor Blockers for Active-State Angiotensin II Type 1 Receptors. *Mol. Pharmacol.* **2015**, *88*, 488–501.
129. Chow, B.S.M.; Allen, T.J. Angiotensin II type 2 receptor (AT2R) in renal and cardiovascular disease. *Clin. Sci.* **2016**, *130*, 1307–1326.
130. Pavo, N.; Goliasch, G.; Wurm, R.; Novak, J.; Strunk, G.; Gyöngyösi, M.; Poglitsch, M.; Säemann, M.D.; Hülsmann, M. Low- and high-renin heart failure phenotypes with clinical implications. *Clin. Chem.* **2018**, *64*, 597–608.
131. Viollet, L.; Thrush, P.T.; Flanigan, K.M.; Mendell, J.R.; Allen, H.D. Effects of angiotensin-converting enzyme inhibitors and/or beta blockers on the cardiomyopathy in Duchenne muscular dystrophy. *Am. J. Cardiol.* **2012**, *110*, 98–102.
132. Wagner, S.; Maier, L.S.; Bers, D.M. Role of Sodium and Calcium Dysregulation in Tachyarrhythmias in Sudden Cardiac Death. *Circ. Res.* **2015**, *16*, 1956–1970.
133. Triposkiadis, F.; Karayannis, G.; Giamouzis, G.; Skoularigis, J.; Louridas, G.; Butler, J. The Sympathetic Nervous System in Heart Failure. Physiology, Pathophysiology, and Clinical Implications. *J. Am. Coll. Cardiol.* **2009**, *54*, 1747–1762.
134. Kajimoto, H.; Ishigaki, K.; Okumura, K.; Tomimatsu, H.; Nakazawa, M.; Saito, K.; Osawa, M.; Nakanishi, T. Beta-Blocker Therapy for Cardiac Dysfunction in Patients With Muscular Dystrophy. *Circ. J.* **2006**, *70*, 991–994.
135. Matsumura, T.; Tamura, T.; Kuru, S.; Kikuchi, Y.; Kawai, M. Carvedilol can Prevent Cardiac Events in Duchenne Muscular Dystrophy. *Intern. Med.* **2010**, *49*, 1357–1363.
136. Raman, S. V.; Hor, K.N.; Mazur, W.; Halnon, N.J.; Kissel, J.T.; He, X.; Tran, T.; Smart, S.; McCarthy, B.; Taylor, M.D.; et al. Eplerenone for early cardiomyopathy

in Duchenne muscular dystrophy: a randomised, double-blind, placebo-controlled trial. *Lancet. Neurol.* **2015**, *14*, 153–161.
137. Heier, C.R.; Yu, Q.; Fiorillo, A.A.; Tully, C.B.; Tucker, A.; Mazala, D.A.; Uaesoontrachoon, K.; Srinivassane, S.; Damsker, J.M.; Hoffman, E.P.; et al. Vamorolone targets dual nuclear receptors to treat inflammation and dystrophic cardiomyopathy. *Life Sci. Alliance* **2019**, *2*, e201800186.
138. Janssen, P.M.L.; Murray, J.D.; Schill, K.E.; Rastogi, N.; Schultz, E.J.; Tran, T.; Raman, S. V.; Rafael-Fortney, J.A. Prednisolone attenuates improvement of cardiac and skeletal contractile function and histopathology by lisinopril and spironolactone in the mdx mouse model of duchenne muscular dystrophy. *PLoS One* **2014**, *9*, e88360.
139. Raman, S. V.; Hor, K.N.; Mazur, W.; He, X.; Kissel, J.T.; Smart, S.; McCarthy, B.; Roble, S.L.; Cripe, L.H. Eplerenone for early cardiomyopathy in Duchenne muscular dystrophy: results of a two-year open-label extension trial. *Orphanet J. Rare Dis.* **2017**, *12*, 1–5.
140. Griggs, R.C.; Herr, B.E.; Reha, A.; Elfring, G.; Atkinson, L.; Cwik, V.; Mccoll, E.; Tawil, R.; Pandya, S.; Mcdermott, M.P.; et al. Corticosteroids in Duchenne muscular dystrophy: Major variations in practice. *Muscle and Nerve* **2013**, *48*, 27–31.
141. Hoffman, E.P.; Reeves, E.; Damsker, J.; Nagaraju, K.; McCall, J.M.; Connor, E.M.; Bushby, K. Novel Approaches to Corticosteroid Treatment in Duchenne Muscular Dystrophy. *Phys. Med. Rehabil. Clin. N. Am.* **2012**, *23*, 821–828.
142. Bauer, R.; Straub, V.; Blain, A.; Bushby, K.; MacGowan, G.A. Contrasting effects of steroids and angiotensin-converting-enzyme inhibitors in a mouse model of dystrophin-deficient cardiomyopathy. *Eur. J. Heart Fail.* **2009**, *11*, 463–471.
143. Schram, G.; Fournier, A.; Leduc, H.; Dahdah, N.; Therien, J.; Vanasse, M.; Khairy, P. All-cause mortality and cardiovascular outcomes with prophylactic steroid therapy in Duchenne muscular dystrophy. *J. Am. Coll. Cardiol.* **2013**, *61*, 948–954.
144. Markham, L.W.; Spicer, R.L.; Khoury, P.R.; Wong, B.L.; Mathews, K.D.; Cripe, L.H. Steroid therapy and cardiac function in duchenne muscular dystrophy. *Pediatr. Cardiol.* **2005**, *26*, 768–771.
145. Barber, B.J.; Andrews, J.G.; Lu, Z.; West, N.A.; Meaney, F.J.; Price, E.T.; Gray, A.; Sheehan, D.W.; Pandya, S.; Yang, M.; et al. Oral corticosteroids and onset of cardiomyopathy in Duchenne muscular dystrophy. *J. Pediatr.* **2013**, *163*, 1080-1084.e1.
146. Silversides, C.K.; Webb, G.D.; Harris, V.A.; Biggar, D.W. Effects of deflazacort on left ventricular function in patients with Duchenne muscular dystrophy. *Am. J. Cardiol.* **2003**, *91*, 769–772.
147. Raman, S. V.; Cripe, L.H. Glucocorticoid Therapy for Duchenne Cardiomyopathy: A Hobson's Choice? *J. Am. Heart Assoc.* **2015**, *4*, 1–3.
148. Spurney, C.F. Cardiomyopathy of Duchenne muscular dystrophy: current understanding and future directions. *Muscle Nerve* **2011**, *44*, 8–19.
149. Heier, C.R.; Damsker, J.M.; Yu, Q.; Dillingham, B.C.; Huynh, T.; Van der Meulen, J.H.; Sali, A.; Miller, B.K.; Phadke, A.; Scheffer, L.; et al. VBP15, a novel anti-inflammatory and membrane-stabilizer, improves muscular dystrophy without side effects. *EMBO Mol. Med.* **2013**, *5*, 1569–1585.
150. Rodrigues, M.; Echigoya, Y.; Fukada, S.; Yokota, T. Current Translational Research and Murine Models For Duchenne Muscular Dystrophy. *J. Neuromuscul. Dis.* **2016**, *3*, 29–48.

151. Berko, B.A.; Swift, M. X-Linked dilated cardiomyopathy. *N. Engl. J. Med.* **1985**, *316*, 1186–1191.
152. Ferlini, A.; Sewry, C.; Melis, M.A.; Mateddu, A.; Muntoni, F. X-linked dilated cardiomyopathy and the dystrophin gene. *Neuromuscul. Disord.* **1999**, *9*, 339–346.
153. Nakamura, A. X-linked dilated cardiomyopathy: A cardiospecific phenotype of dystrophinopathy. *Pharmaceuticals* **2015**, *8*, 303–320.
154. Kaspar, R.W.; Allen, H.D.; Ray, W.C.; Alvarez, C.E.; Kissel, J.T.; Pestronk, A.; Weiss, R.B.; Flanigan, K.M.; Mendell, J.R.; Montanaro, F. Analysis of dystrophin deletion mutations predicts age of cardiomyopathy onset in becker muscular dystrophy. *Circ. Cardiovasc. Genet.* **2009**, *2*, 544–551.
155. Namgoong, J.H.; Bertoni, C. Clinical potential of ataluren in the treatment of Duchenne muscular dystrophy. *Degener. Neurol. Neuromuscul. Dis.* **2016**, *6*, 37–48.
156. Welch, E.M.; Barton, E.R.; Zhuo, J.; Tomizawa, Y.; Friesen, W.J.; Trifillis, P.; Paushkin, S.; Patel, M.; Trotta, C.R.; Hwang, S.; et al. PTC124 targets genetic disorders caused by nonsense mutations. *Nature* **2007**, *447*, 87–91.
157. Ebrahimi-Fakhari, D.; Dillmann, U.; Flotats-Bastardas, M.; Poryo, M.; Abdul-Khaliq, H.; Shamdeen, M.G.; Mischo, B.; Zemlin, M.; Meyer, S. Off-Label Use of Ataluren in Four Non-ambulatory Patients With Nonsense Mutation Duchenne Muscular Dystrophy: Effects on Cardiac and Pulmonary Function and Muscle Strength. *Front. Pediatr.* **2018**, *6*, 316.
158. Lu, Q.L.; Rabinowitz, A.; Chen, Y.C.; Yokota, T.; Yin, H.; Alter, J.; Jadoon, A.; Bou-Gharios, G.; Partridge, T. Systemic delivery of antisense oligoribonucleotide restores dystrophin expression in body-wide skeletal muscles. *Proc. Natl. Acad. Sci.* **2005**, *102*, 198–203.
159. Yokota, T.; Lu, Q.L.; Partridge, T.; Kobayashi, M.; Nakamura, A.; Takeda, S.; Hoffman, E. Efficacy of systemic morpholino exon-skipping in duchenne dystrophy dogs. *Ann. Neurol.* **2009**, *65*, 667–676.
160. Nguyen, Q.; Yokota, T. Antisense oligonucleotides for the treatment of cardiomyopathy in Duchenne muscular dystrophy. *Am. J. Transl. Res.* **2019**, *11*, 1202–1218.
161. Wu, B.; Lu, P.; Benrashid, E.; Malik, S.; Ashar, J.; Doran, T.J.; Lu, Q.L. Dose-dependent restoration of dystrophin expression in cardiac muscle of dystrophic mice by systemically delivered morpholino. *Gene Ther.* **2010**, *17*, 132–140.
162. Yin, H.; Moulton, H.M.; Seow, Y.; Boyd, C.; Boutilier, J.; Iverson, P.; Wood, M.J.A. Cell-penetrating peptide-conjugated antisense oligonucleotides restore systemic muscle and cardiac dystrophin expression and function. *Hum. Mol. Genet.* **2008**, *17*, 3909–3918.
163. Betts, C.; Saleh, A.F.; Arzumanov, A.A.; Hammond, S.M.; Godfrey, C.; Coursindel, T.; Gait, M.J.; Wood, M.J. Pip6-PMO, A New Generation of Peptide-oligonucleotide Conjugates With Improved Cardiac Exon Skipping Activity for DMD Treatment. *Mol. Ther. Nucleic Acids* **2012**, *1*, e38.
164. Echigoya, Y.; Nakamura, A.; Nagata, T.; Urasawa, N.; Lim, K.R.Q.; Trieu, N.; Panesar, D.; Kuraoka, M.; Moulton, H.M.; Saito, T.; et al. Effects of systemic multiexon skipping with peptide-conjugated morpholinos in the heart of a dog model of Duchenne muscular dystrophy. *Proc. Natl. Acad. Sci. U. S. A.* **2017**, *114*, 4213–4218.
165. Mendell, J.R.; Goemans, N.; Lowes, L.P.; Alfano, L.N.; Berry, K.; Shao, J.; Kaye, E.M.; Mercuri, E. Longitudinal effect of eteplirsen versus historical control on

ambulation in Duchenne muscular dystrophy. *Ann. Neurol.* **2016**, *79*, 257–271.
166. Echevarría, L.; Aupy, P.; Goyenvalle, A. Exon-skipping advances for Duchenne muscular dystrophy. *Hum. Mol. Genet.* **2018**, *27*, R163–R172.
167. McNally, E.M.; Wyatt, E.J. Mutation-based therapy for duchenne muscular dystrophy: Antisense treatment arrives in the clinic. *Circulation* **2017**, *136*, 979–981.
168. Chamberlain, J.R.; Chamberlain, J.S. Progress toward Gene Therapy for Duchenne Muscular Dystrophy. *Mol. Ther.* **2017**, *25*, 1125–1131.
169. Duan, D. Systemic AAV Micro-dystrophin Gene Therapy for Duchenne Muscular Dystrophy. *Mol. Ther.* **2018**, *26*, 2337–2356.
170. Shin, J.H.; Nitahara-Kasahara, Y.; Hayashita-Kinoh, H.; Ohshima-Hosoyama, S.; Kinoshita, K.; Chiyo, T.; Okada, H.; Okada, T.; Takeda, S. Improvement of cardiac fibrosis in dystrophic mice by rAAV9-mediated microdystrophin transduction. *Gene Ther.* **2011**, *18*, 910–919.
171. Gregorevic, P.; Allen, J.M.; Minami, E.; Blankinship, M.J.; Haraguchi, M.; Meuse, L.; Finn, E.; Adams, M.E.; Froehner, S.C.; Murry, C.E.; et al. rAAV6-microdystrophin preserves muscle function and extends lifespan in severely dystrophic mice. *Nat. Med.* **2006**, *12*, 787–789.
172. Wang, B.; Li, J.; Fu, F.H.; Chen, C.; Zhu, X.; Zhou, L.; Jiang, X.; Xiao, X. Construction and analysis of compact muscle-specific promoters for AAV vectors. *Gene Ther.* **2008**, *15*, 1489–1499.
173. Salva, M.Z.; Himeda, C.L.; Tai, P.W.L.; Nishiuchi, E.; Gregorevic, P.; Allen, J.M.; Finn, E.E.; Nguyen, Q.G.; Blankinship, M.J.; Meuse, L.; et al. Design of tissue-specific regulatory cassettes for high-level rAAV-mediated expression in skeletal and cardiac muscle. *Mol. Ther.* **2007**, *15*, 320–329.
174. Hakim, C.H.; Wasala, N.B.; Pan, X.; Kodippili, K.; Yue, Y.; Zhang, K.; Yao, G.; Haffner, B.; Duan, S.X.; Ramos, J.; et al. A Five-Repeat Micro-Dystrophin Gene Ameliorated Dystrophic Phenotype in the Severe DBA/2J-mdx Model of Duchenne Muscular Dystrophy. *Mol. Ther. - Methods Clin. Dev.* **2017**, *6*, 216–230.
175. Louis Jeune, V.; Joergensen, J.A.; Hajjar, R.J.; Weber, T. Pre-existing Anti–Adeno-Associated Virus Antibodies as a Challenge in AAV Gene Therapy. *Hum. Gene Ther. Methods* **2013**, *24*, 59–67.
176. Chicoine, L.G.; Montgomery, C.L.; Bremer, W.G.; Shontz, K.M.; Griffin, D.A.; Heller, K.N.; Lewis, S.; Malik, V.; Grose, W.E.; Shilling, C.J.; et al. Plasmapheresis eliminates the negative impact of AAV antibodies on microdystrophin gene expression following vascular delivery. *Mol. Ther.* **2014**, *22*, 338–347.
177. Min, Y.-L.; Bassel-Duby, R.; Olson, E.N. CRISPR Correction of Duchenne Muscular Dystrophy. *Annu. Rev. Med.* **2018**, *70*, 239–255.
178. Lim, K.R.Q.; Yoon, C.; Yokota, T. Applications of CRISPR/Cas9 for the treatment of Duchenne muscular dystrophy. *J. Pers. Med.* **2018**, *8*, E38.
179. Nelson, C.E.; Hakim, C.H.; Ousterout, D.G.; Thakore, P.I.; Moreb, E.A.; Castellanos Rivera, R.M.; Madhavan, S.; Pan, X.; Ran, F.A.; Yan, W.X.; et al. In vivo genome editing improves muscle function in a mouse model of Duchenne muscular dystrophy. *Science* **2016**, *351*, 403–407.
180. Amoasii, L.; Li, H.; Sanchez-Ortiz, E.; Caballero, D.; Harron, R.; Massey, C.; Shelton, J.; Piercy, R.; Olson, E.N. Gene editing restores dystrophin expression in a canine model of Duchenne muscular dystrophy. *Science* **2018**, *362*, 86–91.
181. Amoasii, L.; Long, C.; Li, H.; Mireault, A.A.; Shelton, J.M.; Sanchez-Ortiz, E.; McAnally, J.R.; Bhattacharyya, S.; Schmidt, F.; Grimm, D.; et al. Single-cut

genome editing restores dystrophin expression in a new mouse model of muscular dystrophy. *Sci. Transl. Med.* **2017**, *9*, 1–11.
182. Bengtsson, N.E.; Hall, J.K.; Odom, G.L.; Phelps, M.P.; Andrus, C.R.; Hawkins, R.D.; Hauschka, S.D.; Chamberlain, J.R.J.S.J.R.; Chamberlain, J.R.J.S.J.R. Muscle-specific CRISPR/Cas9 dystrophin gene editing ameliorates pathophysiology in a mouse model for Duchenne muscular dystrophy. *Nat. Commun.* **2017**, *8*, 1–9.
183. Hakim, C.H.; Wasala, N.B.; Nelson, C.E.; Wasala, L.P.; Yue, Y.; Louderman, J.A.; Lessa, T.B.; Dai, A.; Zhang, K.; Jenkins, G.J.; et al. AAV CRISPR editing rescues cardiac and muscle function for 18 months in dystrophic mice. *JCI Insight* **2018**, *3*, 1–13.
184. Xu, L.; Lau, Y.S.; Gao, Y.; Li, H.; Han, R. Life-Long AAV-Mediated CRISPR Genome Editing in Dystrophic Heart Improves Cardiomyopathy without Causing Serious Lesions in mdx Mice. *Mol. Ther.* **2019**, *27*, 1–8.
185. Nelson, C.E.; Wu, Y.; Gemberling, M.P.; Oliver, M.L.; Waller, M.A.; Bohning, J.D.; Robinson-Hamm, J.N.; Bulaklak, K.; Castellanos Rivera, R.M.; Collier, J.H.; et al. Long-term evaluation of AAV-CRISPR genome editing for Duchenne muscular dystrophy. *Nat. Med.* **2019**, *25*, 427–432.
186. Long, C.; Amoasii, L.; Mireault, A.A.; McAnally, J.R.; Li, H.; Sanchez-Ortiz, E.; Bhattacharyya, S.; Shelton, J.M.; Bassel-Duby, R.; Olson, E.N. Postnatal genome editing partially restores dystrophin expression in a mouse model of muscular dystrophy. *Science* **2016**, *351*, 400–403.
187. Fu, Y.; Foden, J.A.; Khayter, C.; Maeder, M.L.; Reyon, D.; Joung, J.K.; Sander, J.D. High-frequency off-target mutagenesis induced by CRISPR-Cas nucleases in human cells. *Nat. Biotechnol.* **2013**, *31*, 822–826.
188. Kleinstiver, B.P.; Pattanayak, V.; Prew, M.S.; Tsai, S.Q.; Nguyen, N.T.; Zheng, Z.; Joung, J.K. High-fidelity CRISPR-Cas9 nucleases with no detectable genome-wide off-target effects. *Nature* **2016**, *529*, 490–495.
189. Muntoni, F. Cardiomyopathy in muscular dystrophies. *Curr. Opin. Neurol.* **2003**, *16*, 577–583.
190. Hoffman, E.P.; Brown, R.H.; Kunkel, L.M. Dystrophin: the protein product of the Duchene muscular dystrophy locus. *Cell* **1987**, *51*, 919–928.
191. Hoffman, E.P.; Kunkel, L.M. Dystrophin abnormalities in Duchenne/Becker muscular dystrophy. *Neuron* **1989**, *2*, 1019–1029.
192. Campbell, K.P.; Ervasti, J.M. Dystrophin and the membrane skeleton. *Curr. Opin. Cell Biol.* **1993**, *5*, 82–87.
193. Ervasti, J.M.; Sonnemann, K.J. Biology of the Striated Muscle Dystrophin-Glycoprotein Complex. *Int. Rev. Cytol.* **2008**, *265*, 191–225.
194. Wagner, K.R. Approaching a New Age in Duchenne Muscular Dystrophy Treatment. *Neurotherapeutics* **2008**, *5*, 583–591.
195. Chamberlain, J.S.; Metzger, J.; Reyes, M.; Townsend, D.; Faulkner, J.A. Dystrophin-deficient mdx mice display a reduced life span and are susceptible to spontaneous rhabdomyosarcoma. *FASEB J.* **2007**, *21*, 2195–2204.
196. Birnkrant, D.J.; Bushby, K.; Bann, C.M.; Apkon, S.D.; Blackwell, A.; Brumbaugh, D.; Case, L.E.; Clemens, P.R.; Hadjiyannakis, S.; Pandya, S.; et al. Diagnosis and management of Duchenne muscular dystrophy, part 1 : diagnosis, and neuromuscular, rehabilitation, endocrine, and gastrointestinal and nutritional management. *Lancet Neurol.* **2018**, *17*, 251–267.
197. Bulfield, G.; Siller, W.G.; Wight, P.A.; Moore, K.J. X chromosome-linked muscular dystrophy (mdx) in the mouse. *Proc. Natl. Acad. Sci.* **1984**, *81*, 1189–1192.

198. Ryder-Cook, A.S.; Sicinski, P.; Thomas, K.; Davies, K.E.; Worton, R.G.; Barnard, E.A.; Darlison, M.G.; Barnard, P.J. Localization of the mdx mutation within the mouse dystrophin gene. *EMBO J.* **1988**, *7*, 3017–3021.
199. McGreevy, J.W.; Hakim, C.H.; McIntosh, M.A.; Duan, D. Animal models of Duchenne muscular dystrophy: from basic mechanisms to gene therapy. *Dis. Model. Mech.* **2015**, *8*, 195–213.
200. Meyers, T.A.; Townsend, D. Early right ventricular fibrosis and reduction in biventricular cardiac reserve in the dystrophin-deficient mdx heart. *Am. J. Physiol. - Hear. Circ. Physiol.* **2015**, *308*, H303–H315.
201. Spurney, C.F.; Guerron, A.D.; Yu, Q.; Sali, A.; van der Meulen, J.H.; Hoffman, E.P.; Nagaraju, K. Membrane sealant Poloxamer P188 protects against isoproterenol induced cardiomyopathy in dystrophin deficient mice. *BMC Cardiovasc. Disord.* **2011**, *11*, 20.
202. Townsend, D.; Yasuda, S.; McNally, E.M.; Metzger, J.M. Distinct pathophysiological mechanisms of cardiomyopathy in hearts lacking dystrophin or the sarcoglycan complex. *FASEB J.* **2011**, *25*, 3106–3114.
203. Heydemann, A.; Ceco, E.; Lim, J.E.; Hadhazy, M.; Ryder, P.; Moran, J.L.; Beier, D.R.; Palmer, A.A.; McNally, E.M. Latent TGF-β – binding protein 4 modifies muscular dystrophy in mice. *J. Clin. Invest.* **2009**, *119*, 3703–3712.
204. Lorts, A.; Schwanekamp, J.A.; Baudino, T.A.; McNally, E.M.; Molkentin, J.D. Deletion of periostin reduces muscular dystrophy and fibrosis in mice by modulating the transforming growth factor-β pathway. *Proc. Natl. Acad. Sci.* **2012**, *109*, 10978–10983.
205. Cohn, R.D.; Erp, C. Van; Habashi, J.P.; Soleimani, A.A.; Klein, E.C.; Lisi, M.T.; Gamradt, M.; Rhys, C.M.; Holm, T.M.; Loeys, B.L.; et al. Angiotensin II type 1 receptor blockade attenuates TGF- b – induced failure of muscle regeneration in multiple myopathic states. **2007**, *13*, 204–211.
206. Tidball, J.G.; Wehling-Henricks, M. The role of free radicals in the pathophysiology of muscular dystrophy. *J. Appl. Physiol.* **2007**, *102*, 1677–1686.
207. Williams, I.A.; Allen, D.G. The role of reactive oxygen species in the hearts of dystrophin-deficient mdx mice. *Am. J. Physiol. - Hear. Circ. Physiol.* **2007**, *293*, H1969–H1977.
208. Whitehead, N.P.; Pham, C.; Gervasio, O.L.; Allen, D.G. N-Acetylcysteine ameliorates skeletal muscle pathophysiology in mdx mice. *J. Physiol.* **2008**, *586*, 2003–2014.
209. Russo, V.; Papa, A.A.; Williams, E.A.; Rago, A.; Palladino, A.; Politano, L.; Nigro, G. ACE inhibition to slow progression of myocardial fibrosis in muscular dystrophies. *Trends Cardiovasc. Med.* **2018**, *28*, 330–337.
210. de Senzi Moraes Pinto, R.; Ferretti, R.; Moraes, L.H.R.; Neto, H.S.; Marques, M.J.; Minatel, E. N-Acetylcysteine treatment reduces TNF-α levels and myonecrosis in diaphragm muscle of mdx mice. *Clin. Nutr.* **2013**, *32*, 472–475.
211. Guiraud, S.; Davies, K.E. Pharmacological advances for treatment in Duchenne muscular dystrophy. *Curr. Opin. Pharmacol.* **2017**, *34*, 36–48.
212. Markham, L.W.; Michelfelder, E.C.; Border, W.L.; Khoury, P.R.; Spicer, R.L.; Wong, B.L.; Benson, D.W.; Cripe, L.H. Abnormalities of Diastolic Function Precede Dilated Cardiomyopathy Associated with Duchenne Muscular Dystrophy. *J. Am. Soc. Echocardiogr.* **2006**, *19*, 865–871.
213. McNally, E.M. New Approaches in the Therapy of Cardiomyopathy in Muscular Dystrophy. *Annu. Rev. Med.* **2007**, *58*, 75–88.
214. Kirchmann, C.; Kececioglu, D.; Korinthenberg, R.; Dittrich, S. Echocardiographic

and electrocardiographic findings of cardiomyopathy in Duchenne and Becker-Kiener muscular dystrophies. *Pediatr. Cardiol.* **2005**, *26*, 66–72.
215. Tuttle, R.R.; Mills, J. Dobutamine: Development of a new catecholamine to selectively increase cardiac contractility. *Circ. Res.* **1975**, *36*, 185–196.
216. Schmidt, G.N.; Burmeister, M.-A.; Lilje, C.; Wappler, F.; Bischoff, P. Acute heart failure during spinal surgery in a boy with Duchenne muscular dystrophy. *Br. J. Anaesth.* **2003**, *90*, 800–804.
217. Tamaki, T.; Nishiyama, A.; Kimura, S.; Aki, Y.; Yoshizumi, M.; Houchi, H.; Morita, K.; Abe, Y. EXP3174: The Major Active Metabolite of Losartan. *Cardiovasc. Drug Rev.* **1997**, *15*, 122–136.
218. Lo, M.W.; Goldberg, M.R.; McCrea, J.B.; Lu, H.; Furtek, C.I.; Bjornsson, T.D. Pharmacokinetics of losartan, an angiotensin II receptor antagonist, and its active metabolite EXP3174 in humans. *Clin. Pharmacol. Ther.* **1995**, *58*, 641–649.
219. Schindelin, J.; Arganda-Carreras, I.; Frise, E.; Kaynig, V.; Longair, M.; Pietzsch, T.; Preibisch, S.; Rueden, C.; Saalfeld, S.; Schmid, B.; et al. Fiji: an open-source platform for biological-image analysis. *Nat. Methods* **2012**, *9*, 676–682.
220. R Core Team R: A Language and Environment for Statistical Computing 2014.
221. Junqueira, L.C.U.; Bignolas, G.; Brentani, R.R. Picrosirius staining plus polarization microscopy, a specific method for collagen detection in tissue sections. *Histochem. J.* **1979**, *11*, 447–455.
222. Lattouf, R.; Younes, R.; Lutomski, D.; Naaman, N.; Godeau, G.; Senni, K.; Changotade, S. Picrosirius Red Staining: A Useful Tool to Appraise Collagen Networks in Normal and Pathological Tissues. *J. Histochem. Cytochem.* **2014**, *62*, 751–758.
223. Rich, L.; Whittaker, P. Collagen and Picrosirius red staining : a polarized light assessment of fibrillar hue and spatial distribution. *Brazilian J. Morphol. Sci.* **2005**, *22*, 97–104.
224. Junqueira, L.C.U.; Montes, G.S.; Sanchez, E.M. The influence of tissue section thickness on the study of collagen by the Picrosirius-polarization method. *Histochemistry* **1982**, *74*, 153–156.
225. Dayan, D.; Hiss, Y.; Hirshberg, A.; Bubis, J.J.; Wolman, M. Are the polarization colors of Picrosirius red-stained collagen determined only by the diameter of the fibers? *Histochemistry* **1989**, *93*, 27–29.
226. Hermiston, M.L.; Xu, Z.; Weiss, A. CD45: A Critical Regulator of Signaling Thresholds in Immune Cells. *Annu. Rev. Immunol.* **2003**, *21*, 107–37.
227. Patties, I.; Haagen, J.; Dörr, W.; Hildebrandt, G.; Glasow, A. Late inflammatory and thrombotic changes in irradiated hearts of C57BL/6 wild-type and atherosclerosis-prone ApoE-deficient mice. *Strahlentherapie und Onkol.* **2015**, *191*, 172–179.
228. Barros, M.H.M.; Hauck, F.; Dreyer, J.H.; Kempkes, B.; Niedobitek, G. Macrophage polarisation: An immunohistochemical approach for identifying M1 and M2 macrophages. *PLoS One* **2013**, *8*, e80908.
229. Raggi, F.; Pelassa, S.; Pierobon, D.; Penco, F.; Gattorno, M.; Novelli, F.; Eva, A.; Varesio, L.; Giovarelli, M.; Bosco, M.C. Regulation of human Macrophage M1-M2 Polarization Balance by hypoxia and the Triggering receptor expressed on Myeloid cells-1. *Front. Immunol.* **2017**, *8*, 1097.
230. Genin, M.; Clement, F.; Fattaccioli, A.; Raes, M.; Michiels, C. M1 and M2 macrophages derived from THP-1 cells differentially modulate the response of cancer cells to etoposide. *BMC Cancer* **2015**, *15*, 1–14.
231. Kharraz, Y.; Guerra, J.; Pessina, P.; Serrano, A.L.; Munoz-Canoves, P.

Understanding the process of fibrosis in Duchenne muscular dystrophy. *Biomed Res. Int.* **2014**, *2014*, 1–11.
232. Rosenkranz, S. TGF-β1 and angiotensin networking in cardiac remodeling. *Cardiovasc. Res.* **2004**, *63*, 423–432.
233. Munger, M.A. Use of Angiotensin receptor blockers in cardiovascular protection: Current evidence and future directions. *Pharm. Ther.* **2011**, *36*, 22–40.
234. Sukumaran, V.; Watanabe, K.; Veeraveedu, P.T.; Thandavarayan, R.A.; Gurusamy, N.; Ma, M.; Yamaguchi, K.; Suzuki, K.; Kodama, M.; Aizawa, Y. Telmisartan, an angiotensin-II receptor blocker ameliorates cardiac remodeling in rats with dilated cardiomyopathy. *Hypertens. Res.* **2010**, *33*, 695–702.
235. Khan, R.; Sheppard, R. Fibrosis in heart disease: Understanding the role of transforming growth factor-β1 in cardiomyopathy, valvular disease and arrhythmia. *Immunology* **2006**, *118*, 10–24.
236. Heydemann, A.; Huber, J.M.; Kakkar, R.; Wheeler, M.T.; McNally, E.M. Functional nitric oxide synthase mislocalization in cardiomyopathy. *J. Mol. Cell. Cardiol.* **2004**, *36*, 213–223.
237. Flanigan, K.M.; Ceco, E.; Lamar, K.-M.; Kaminoh, Y.; Dunn, D.M.; Mendell, J.R.; King, W.M.; Pestronk, A.; Florence, J.M.; Mathews, K.D.; et al. LTBP4 genotype predicts age of ambulatory loss in duchenne muscular dystrophy. *Ann. Neurol.* **2013**, *73*, 481–488.
238. Cozzoli, A.; Liantonio, A.; Conte, E.; Cannone, M.; Massari, A.M.; Giustino, A.; Scaramuzzi, A.; Pierno, S.; Mantuano, P.; Capogrosso, R.F.; et al. Angiotensin II modulates mouse skeletal muscle resting conductance to chloride and potassium ions and calcium homeostasis via the AT1 receptor and NADPH oxidase. *Am. J. Physiol. - Cell Physiol.* **2014**, *307*, C634–C647.
239. Bedard, K.; Krause, K.-H. The NOX family of ROS-generating NADPH oxidases: physiology and pathophysiology. *Physiol. Rev.* **2007**, *87*, 245–313.
240. Ismail, H.M.; Scapozza, L.; Ruegg, U.T.; Dorchies, O.M. Diapocynin, a dimer of the NADPH oxidase inhibitor apocynin, reduces ROS production and prevents force loss in eccentrically contracting dystrophic muscle. *PLoS One* **2014**, *9*, e110708.
241. Yang, J.; Zhang, X.; Yu, X.; Tang, W.; Gan, H. Renin-Angiotensin system activation accelerates atherosclerosis in experimental renal failure by promoting endoplasmic reticulum stress-related inflammation. *Int. J. Mol. Med.* **2017**, *39*, 613–621.
242. Yao, Y.; Li, Y.; Zeng, X.; Ye, Z.; Li, X.; Zhang, L. Losartan Alleviates Renal Fibrosis and Inhibits Endothelial-to-Mesenchymal Transition (EMT) Under High-Fat Diet-Induced Hyperglycemia. *Front. Pharmacol.* **2018**, *9*, 1213.
243. Fujisaka, S.; Usui, I.; Kanatani, Y.; Ikutani, M.; Takasaki, I.; Tsuneyama, K.; Tabuchi, Y.; Bukhari, A.; Yamazaki, Y.; Suzuki, H.; et al. Telmisartan improves insulin resistance and modulates adipose tissue macrophage polarization in high-fat-fed mice. *Endocrinology* **2011**, *152*, 1789–1799.
244. Yamamoto, S.; Yancey, P.G.; Zuo, Y.; Ma, L.-J.; Kaseda, R.; Fogo, A.B.; Ichikawa, I.; Linton, M.F.; Fazio, S.; Kon, V. Macrophage polarization by angiotensin II-type 1 receptor aggravates renal injury-acceleration of atherosclerosis. *Arterioscler. Thromb. Vasc. Biol.* **2011**, *31*, 2856–2864.
245. Westermeier, F.; Bustamante, M.; Pavez, M.; Garcia, L.; Chiong, M.; Ocaranza, M.P.; Lavandero, S. Novel players in cardioprotection: Insulin like growth factor-1, angiotensin-(1-7) and angiotensin-(1-9). *Pharmacol. Res.* **2015**, *101*, 41–55.
246. Chappell, M.C.; Marshall, A.C.; Alzayadneh, E.M.; Shaltout, H.A.; Diz, D.I. Update

on the angiotensin converting enzyme 2-angiotensin (1-7)-Mas receptor axis: fetal programing, sex differences, and intracellular pathways. *Front. Endocrinol. (Lausanne).* **2014**, *4*, 201.
247. Santos, R.A. Angiotensin-(1-7). *Hypertension* **2014**, *63*, 1138–1147.
248. Manolis, A.J.; Marketou, M.E.; Gavras, I.; Gavras, H. Cardioprotective properties of bradykinin: role of the B2 receptor. *Hypertens. Res.* **2010**, *33*, 772–777.
249. Hartman, J.C. The role of bradykinin and nitric oxide in the cardioprotective action of ACE inhibitors. *Ann. Thorac. Surg.* **1995**, *60*, 789–792.
250. Bish, L.T.; Yarchoan, M.; Sleeper, M.M.; Gazzara, J.A.; Morine, K.J.; Acosta, P.; Barton, E.R.; Sweeney, H.L. Chronic Losartan Administration Reduces Mortality and Preserves Cardiac but Not Skeletal Muscle Function in Dystrophic Mice. *PLoS One* **2011**, *6*, e20856.
251. Blain, A.; Greally, E.; Laval, S.H.; Blamire, A.M.; MacGowan, G. a.; Straub, V.W. Absence of Cardiac Benefit with Early Combination ACE Inhibitor and Beta Blocker Treatment in mdx Mice. *J. Cardiovasc. Transl. Res.* **2015**, *8*, 198–207.
252. Thrush, P.T.; Flanigan, K.M.; Mendell, J.R.; Raman, S. V.; Daniels, C.J.; Allen, H.D. Visual Diagnosis: Chest Pain in a Boy With Duchenne Muscular Dystrophy and Cardiomyopathy. *Pediatr. Rev.* **2014**.
253. Lowe, J.; Wodarcyk, A.J.; Floyd, K.T.; Rastogi, N.; Schultz, E.J.; Swager, S. a.; Chadwick, J. a.; Tran, T.; Raman, S. V.; Janssen, P.M.L.; et al. The Angiotensin Converting Enzyme Inhibitor Lisinopril Improves Muscle Histopathology but not Contractile Function in a Mouse Model of Duchenne Muscular Dystrophy. *J. Neuromuscul. Dis.* **2015**, *2*, 257–268.
254. Romero, C.A.; Orias, M.; Weir, M.R. Novel RAAS agonists and antagonists: clinical applications and controversies. *Nat. Rev. Endocrinol.* **2015**, *11*, 242–252.
255. Kostenis, E.; Milligan, G.; Christopoulos, A.; Sanchez-Ferrer, C.F.; Heringer-Walther, S.; Sexton, P.M.; Gembardt, F.; Kellett, E.; Martini, L.; Vanderheyden, P.; et al. G-protein-coupled receptor Mas is a physiological antagonist of the angiotensin II type 1 receptor. *Circulation* **2005**, *111*, 1806–1813.
256. Acuña, M.J.; Pessina, P.; Olguin, H.; Cabrera, D.; Vio, C.P.; Bader, M.; Muñoz-canoves, P.; Santos, R.A.; Cabello-verrugio, C.; Brandan, E. Restoration of muscle strength in dystrophic muscle by angiotensin-1-7 through inhibition of TGF-β signalling. *Hum. Mol. Genet.* **2014**, *23*, 1237–1249.
257. Yue, Y.; Li, Z.; Harper, S.Q.; Davisson, R.L.; Chamberlain, J.S.; Duan, D. Microdystrophin gene therapy of cardiomyopathy restores dystrophin-glycoprotein complex and improves sarcolemma integrity in the mdx mouse heart. *Circulation* **2003**, *108*, 1626–1632.
258. Viggiano, E.; Ergoli, M.; Picillo, E.; Politano, L. Determining the role of skewed X-chromosome inactivation in developing muscle symptoms in carriers of Duchenne muscular dystrophy. *Hum. Genet.* 2016, *135*.
259. Kalantry, S. Recent advances in X-chromosome inactivation. *J. Cell. Physiol.* **2011**, *226*, 1714–1718.
260. Birnkrant, D.J.; Ashwath, M.L.; Noritz, G.H.; Merrill, M.C.; Shah, T.A.; Crowe, C.A.; Bahler, R.C. Cardiac and pulmonary function variability in Duchenne/Becker muscular dystrophy: a n initial report. *J. Child Neurol.* **2010**, *25*, 1110–1115.
261. Jin, J.B.; Carter, J.C.; Sheehan, D.W.; Birnkrant, D.J. Cardiopulmonary phenotypic discordance is common in Duchenne muscular dystrophy. *Pediatr. Pulmonol.* **2019**, *54*, 186–193.
262. Oosterwijk, J.; Majoor-Krakauer, D.; Leschot, N.; Wilde, A.; de Visser, M.; Ippel, P.; van der Wouw, P.; Bakker, E.; Van Essen, A.; Brunner, H.; et al. Signs and

symptoms of Duchenne muscular dystrophy and Becker muscular dystrophy among carriers in the Netherlands: a cohort study. *Lancet* **2002**, *353*, 2116–2119.
263. Florian, A.; Rösch, S.; Bietenbeck, M.; Engelen, M.; Stypmann, J.; Waltenberger, J.; Sechtem, U.; Yilmaz, A. Cardiac involvement in female Duchenne and Becker muscular dystrophy carriers in comparison to their first-degree male relatives: A comparative cardiovascular magnetic resonance study. *Eur. Heart J. Cardiovasc. Imaging* **2016**, *17*, 326–333.
264. Politano, L.; Nigro, V.; Nigro, G.; Petretta, V.R.; Passamano, L.; Papparella, S.; Di Somma, S.; Comi, L.I. Development of cardiomyopathy in female carriers of Duchenne and Becker muscular dystrophies. *J. Am. Med. Assoc.* **1996**, *275*, 1335–1338.
265. Guglieri, M.; Magri, F.; D'Angelo, M.G.; Prelle, A.; Morandi, L.; Rodolico, C.; Cagliani, R.; Mora, M.; Fortunato, F.; Bordoni, A.; et al. Clinical, molecular, and protein correlations in a large sample of genetically diagnosed Italian limb girdle muscular dystrophy patients. *Hum. Mutat.* **2008**, *29*, 258–266.
266. Duggan, D.J.; Gorospe, J.R.; Fanin, M.; Hoffman, E.P.; Angelini, C. Mutations in the sarcoglycan genes in patients with myopathy. *N. Engl. J. Med.* **1997**, *336*, 618–624.
267. Fanin, M.; Melacini, P.; Boito, C.; Pegoraro, E.; Angelini, C. LGMD2E patients risk developing dilated cardiomyopathy. *Neuromuscul. Disord.* **2003**, *13*, 303–309.
268. Nigro, V.; Savarese, M. Genetic basis of limb-girdle muscular dystrophies: The 2014 update. *Acta Myol.* **2014**, *33*, 1–12.
269. Allikian, M.J.; McNally, E.M. Processing and Assembly of the Dystrophin Glycoprotein Complex. *Traffic* **2007**, *8*, 177–183.
270. Fanin, M.; Duggan, D.J.; Mostacciuolo, M.L.; Martinello, F.; Freda, M.P.; Soraru, G.; Trevisan, C.P.; Hoffman, E.P.; Angelini, C. Genetic epidemiology of muscular dystrophies resulting from sarcoglycan gene mutations. *J. Med. Genet.* **1997**, *34*, 973–977.
271. Semplicini, C.; Dahlqvist, J.R.; Stojkovic, T.; Bello, L.; Ambrosio, P.D.; Eymard, B.; Politano, L.; Laforêt, P. Clinical and genetic spectrum in limb-girdle muscular dystrophy type 2E. *Neurology* **2015**, *84*, 1772–81.
272. Barresi, R.; Di Blasi, C.; Negri, T.; Brugnoni, R.; Vitali, A.; Felisari, G.; Salandi, A.; Daniel, S.; Cornelio, F.; Morandi, L.; et al. Disruption of heart sarcoglycan complex and severe cardiomyopathy caused by beta sarcoglycan mutations. *J. Med. Genet.* **2000**, *37*, 102–107.
273. Pegoraro, E.; Hoffman, E.P. Limb-Girdle Muscular Dystrophy Overview. *GeneReviews®* **1993**, 1–27.
274. Durbeej, M.; Cohn, R.D.; Hrstka, R.F.; Moore, S.A.; Allamand, V.; Davidson, B.L.; Williamson, R.A.; Campbell, K.P. Disruption of the beta-sarcoglycan gene reveals pathogenetic complexity of limb-girdle muscular dystrophy type 2E. *Mol. Cell* **2000**, *5*, 141–151.
275. Araishi, K.; Sasaoka, T.; Imamura, M.; Noguchi, S.; Hama, H.; Wakabayashi, E.; Yoshida, M.; Hori, T.; Ozawa, E. Loss of the sarcoglycan complex and sarcospan leads to muscular dystrophy in β-sarcoglycan-deficient mice. *Hum. Mol. Genet.* **1999**, *8*, 1589–1598.
276. Pozsgai, E.R.; Griffin, D.A.; Heller, K.N.; Mendell, J.R.; Rodino-Klapac, L.R. β-Sarcoglycan gene transfer decreases fibrosis and restores force in LGMD2E mice. *Gene Ther.* **2015**, *23*, 57–66.
277. Bonnemann, C.G.; Modi, R.; Noguchi, S.; Mizuno, Y.; Yoshida, M.; Gussoni, E.; McNally, E.M.; Duggan, D.J.; Angelini, C.; Hoffman, E.P. Beta-sarcoglycan (A3b)

mutations cause autosomal recessive muscular dystrophy with loss of the sarcoglycan complex. *Nat Genet* **1995**, *11*, 266–273.
278. Coral-vazquez, R.; Cohn, R.D.; Moore, S. a; Hill, J. a; Weiss, R.M.; Davisson, R.L.; Straub, V.; Barresi, R.; Bansal, D.; Hrstka, R.F.; et al. Disruption of the Sarcoglycan – Sarcospan Complex in Vascular Smooth Muscle : A Novel Mechanism for Cardiomyopathy and Muscular Dystrophy. *Animals* **1999**, *98*, 465–474.
279. Hoyer, P.B.; Devine, P.J.; Hu, X.; Thompson, K.E.; Sipes, I.G. Ovarian Toxicity of 4-Vinylcyclohexene Diepoxide: A Mechanistic Model. *Toxicol. Pathol.* **2001**, *29*, 91–99.
280. Chen, H.; Perez, J.N.; Constantopoulos, E.; McKee, L.; Regan, J.; Hoyer, P.B.; Brooks, H.L.; Konhilas, J. A Method to Study the Impact of Chemically-induced Ovarian Failure on Exercise Capacity and Cardiac Adaptation in Mice. *J. Vis. Exp.* **2014**, 1–8.
281. Greising, S.M.; Carey, R.S.; Blackford, J.E.; Dalton, L.E.; Kosir, A.M.; Lowe, D.A. Estradiol treatment, physical activity, and muscle function in ovarian-senescent mice. *Exp. Gerontol.* **2011**, *46*, 685–93.
282. Townsend, D. Measuring Pressure Volume Loops in the Mouse. *JoVE* **2016**, e53810.
283. Guerra, S.; Leri, A.; Wang, X.; Finato, N.; Loreto, C. Di; Beltrami, C.A.; Kajstura, J.; Anversa, P. Myocyte Death in the Failing Human Heart Is Gender Dependent. *New York* **1999**, 856–866.
284. Fukumoto, T.; Yamashita, N.; Tawa, M.; Ohkita, M.; Matsumura, Y. Sex differences in postischemic cardiac dysfunction and norepinephrine overflow in rat heart: the role of estrogen against myocardial ischemia-reperfusion damage via an NO-mediated mechanism. *J. Cardiovasc. Pharmacol.* **2012**, *60*, 269–75.
285. Cross, H.R.; Murphy, E.; Steenbergen, C. Ca(2+) loading and adrenergic stimulation reveal male/female differences in susceptibility to ischemia-reperfusion injury. *Am. J. Physiol. Heart Circ. Physiol.* **2002**, *283*, H481-9.
286. Chen, Q.; Williams, R.; Healy, C.L.; Wright, C.D.; Wu, S.C.; O'Connell, T.D. An association between gene expression and better survival in female mice following myocardial infarction. *J. Mol. Cell. Cardiol.* **2010**, *49*, 801–11.
287. Ji, H.; Zheng, W.; Wu, X.; Liu, J.; Ecelbarger, C.M.; Watkins, R.; Arnold, A.P.; Sandberg, K. Sex chromosome effects unmasked in angiotensin II-induced hypertension. *Hypertension* **2010**, *55*, 1275–1282.
288. Regitz-Zagrosek, V.; Oertelt-Prigione, S.; Seeland, U.; Hetzer, R. Sex and gender differences in myocardial hypertrophy and heart failure. *Circ. J.* **2010**, *74*, 1265–1273.
289. Martínez-Sellés, M.; Domínguez, M.; Martínez, E.; Fernández, M.A.G.; García, E. Women with left ventricular ejection fraction ≤ 20% have better prognosis than men. *Int. J. Cardiol.* **2007**, *120*, 276–278.
290. Cavasin, M.A.; Tao, Z.; Menon, S.; Yang, X.-P. Gender differences in cardiac function during early remodeling after acute myocardial infarction in mice. *Life Sci.* **2004**, *75*, 2181–2192.
291. Xue, B.; Pamidimukkala, J.; Lubahn, D.B.; Hay, M. Estrogen receptor-alpha mediates estrogen protection from angiotensin II-induced hypertension in conscious female mice. *Am. J. Physiol. Heart Circ. Physiol.* **2007**, *292*, H1770–H1776.
292. Konhilas, J.P.; Leinwand, L. a The effects of biological sex and diet on the development of heart failure. *Circulation* **2007**, *116*, 2747–59.

293. Silva-Antonialli, M.M.; Tostes, R.C.A.; Fernandes, L.; Fior-Chadi, D.R.; Akamine, E.H.; Carvalho, M.H.C.; Fortes, Z.B.; Nigro, D. A lower ratio of AT1/AT2 receptors of angiotensin II is found in female than in male spontaneously hypertensive rats. *Cardiovasc. Res.* **2004**, *62*, 587–593.
294. Xue, Q.; Xiao, D.; Zhang, L. Estrogen Regulates Angiotensin II Receptor Expression Patterns and Protects the Heart from Ischemic Injury in Female Rats 1. **2015**, *93*, 1–9.
295. Sampson, A.K.; Moritz, K.M.; Jones, E.S.; Flower, R.L.; Widdop, R.E.; Denton, K.M. Enhanced angiotensin II type 2 receptor mechanisms mediate decreases in arterial pressure attributable to chronic low-dose angiotensin II in female rats. *Hypertension* **2008**, *52*, 666–671.
296. Sullivan, J.C. Sex and the renin-angiotensin system: inequality between the sexes in response to RAS stimulation and inhibition. *Am. J. Physiol. Regul. Integr. Comp. Physiol.* **2008**, *294*, R1220-6.
297. Maric-Bilkan, C.; Arnold, A.P.; Taylor, D.A.; Dwinell, M.; Howlett, S.E.; Wenger, N.; Reckelhoff, J.F.; Sandberg, K.; Churchill, G.; Levin, E.; et al. Report of the National Heart, Lung, and Blood Institute Working Group on Sex Differences Research in Cardiovascular Disease: Scientific Questions and Challenges. *Hypertension* **2016**, 802–807.
298. Pozsgai, E.R.; Griffin, D.A.; Heller, K.N.; Mendell, J.R.; Rodino-Klapac, L.R. Systemic AAV-Mediated β-Sarcoglycan Delivery Targeting Cardiac and Skeletal Muscle Ameliorates Histological and Functional Deficits in LGMD2E Mice. *Mol. Ther.* **2017**, *25*, 855–869.